FMG based upper limb motion detection methods, performance analysis and control of assistive exoskeletons

Islam, Muhammad Raza Ul

DOI (link to publication from Publisher):
10.54337/aau455016322

Publication date:
2021

Document Version
Publisher's PDF, also known as Version of record

FMG BASED UPPER LIMB MOTION DETECTION METHODS, PERFORMANCE ANALYSIS AND CONTROL OF ASSISTIVE EXOSKELETONS

BY
MUHAMMAD RAZA UL ISLAM

DISSERTATION SUBMITTED 2021

AALBORG UNIVERSITY
DENMARK

FMG based upper limb motion detection methods, performance analysis and control of assistive exoskeletons

Ph.D. Dissertation

by

Muhammad Raza Ul Islam

Department of Materials and Production, Aalborg University
Fibigerstræde 16, 9220, Aalborg, Denmark
E-mail: mraza@mp.aau.dk

Dissertation submitted August 19, 2021

Dissertation submitted: August 19, 2021

PhD supervisor: Professor Shaoping Bai
Aalborg University

PhD committee: Associate Professor Simon Bøgh (chairman)
Aalborg University

Professor Trung Dung Ngo
University of Prince Edward Island

Dr. Jan Frederik Veneman, Product Lead
Hocoma AG

PhD Series: Faculty of Engineering and Science, Aalborg University

Department: Department of Materials and Production

ISSN (online): 2446-1636
ISBN (online): 978-87-7210-871-1

Published by:
Aalborg University Press
Kroghstræde 3
DK – 9220 Aalborg Ø
Phone: +45 99407140
aauf@forlag.aau.dk
forlag.aau.dk

Printed in Denmark by Rosendahls, 2021

Abstract

Exoskeletons are wearable devices designed to assist humans according to their needs. Their applications can be found in rehabilitation, assistance and power augmentation. For assistive powered exoskeletons human motion intention detection is an important element for implementing assistive control strategies. While many methods of motion detection have been developed, however, there still exists many challenges i.e. high robustness, convenience, data repeatability and applicability for implementation on assistive powered exoskeletons. Therefore, new methods that can fulfill these requirements are needed.

The aim of this thesis is to develop novel methods of motion intention detection for control of exoskeletons. The focus of this thesis is to analyze the performance of force myography (FMG) to detect upper limb movements and based on it develop control methods for upper limb assistive exoskeletons.

In this thesis performance of FMG is analyzed by comparing it with sEMG. Motion detection accuracy and data repeatability were compared for detecting forearm motions i.e. forearm flexion, extension, pronation, supination and rest. The study showed the feasibility of FMG when implemented for assistive powered exoskeleton control.

Exoskeleton control with FMG is another focus of this thesis. FMG is first used to control a soft exoskeleton by detecting dynamic hand gestures i.e. rest, opening, closing and grasping. This study addressed the challenges associated with object grasping task i.e. amount of training data, robust detection and assistance level determination. The influence of sensor placement on detection performance was also experimentally analyzed.

Finally, FMG based control method for upper limb exoskeleton, i.e. elbow and shoulder joint, is presented in this thesis. A machine learning based algorithm is developed for determining assistance level during object carrying tasks by estimating the carried payload. The performance of the method is analyzed by testing on healthy subjects. Whereas, the results of physical assistance are verified by comparing the results of load carrying tasks with and without exoskeleton.

This thesis contributes to the state-of-the-art of upper limb motion in-

tention detection using FMG. Studies verify that FMG, being accurate and a convenient method to interpret motion intention, has great potential for application of assistive exoskeletons. A contribution of this thesis is performance analysis of muscle activity detection methods that compares FMG and sEMG in terms of accuracy/repeatability. Another contribution is the novel methods for grasping and load carrying. The proposed techniques are able to reduce system complexity for convenient and robust use in actual environment.

Resumé

Exoskeletter er bærebare enheder, som er designet til at assistere menneskers fysiske behov. Deres anvendelse findes i områder som rehabilitering, assistance og styrkeforøgelse. Identifikation af menneskets ønsker i forbindelse med bevægelser er et vigtig element i implementeringen af styringsstrategier til assistance. Selvom mange metoder til at detektere bevægelser er udviklet, så er der stadig mange udfordringer fx robusthed, brugbarhed, data reproducerbarhed, anvendelse og implementering af assisterende og styrkeforøgende exoskeletter. Grundet disse udfordringer er der stadig behov for udvikling af nye metoder, der kan løse disse problemer.

Formålet med denne afhandling er at udvikle nye metyder til at detektere og registrere bevægelser til styring af exoskeletter. Især vil der være fokus på at analysere ydeevnen af force myography (FMG) til at registrere bevægelser af overkroppen og ud fra dette udvikle metoder til at styre exoskeletter til overkoppen.

I denne afhandling vil ydeevnen af FMG blive analyseret ved at sammenligne den med sEMG. Nøjagtigheden af bevægelsesdetektering og data reproducerbarhed blev sammenlignet ved at sammenligne bevægelser af underarmen, herunder bøjning, forlængelse, pronation, supination og hvile. Studiet viste brugbarheden af FMG til styring af kraftforøgende og assisterende exoskeletter.

Styring af exoskeletter med FMG er også et andet fokus i denne afhandling. FMG er her brugt til at styre et exoskelet ved at genkende dynamiske håndbevægelser, herunder hvile, åbning af hånden, lukning af hånden og gribe bevægelser. Studiet adresserede udfordringer associeret ved opgaver hvori greb af objekter er involveret, herunder mængden af træningsdata, robusthed og estimering er den påkrævede styrkeforøgelse. Vigtigheden af placering af FMG sensorer og dets indflydelse på ydeevnen blev også analyseret.

Til slut blev FMG baseret styringer til exoskeletter til albue- og skulderled præsenteret i denne afhandling. En machine learning baseret algoritme er udviklet til estimering af assistance niveau ved at estimere nyttelasten under opgaver hvori objekter skal bæres. Ydeevnen af denne metode er analyseret

ved eksperimentel test af raske personer. Resultaterne af den fysiske assistance er fundet ved at sammenligne resultaterne fra opgaver hvor objekter er båret med og uden exoskelet.

Denne afhandling bidrager til state of the art idenfor bevægelses detektering og bevægelses registrering af overkroppen ved brug af FMG. Studierne bekræfter at FMG er en nøjagtig og let anvendelig metode til at analysere bevægeles registrering og har et stort potentiale for anvendelse til styring af exoskeletter. Et bidrag af afhandlingen er analyse af ydeevnen til registrering af muskelaktivitet, som sammenligner FMG og sEMG og deres nøjagtighed. Et yderligere bidrag er de nye metoder udviklet til at gribe og bære objekter. Den foreslåede teknik er i stand til at reducere kompleksiteten af systemet og gøre det mere brugbart og robust.

Publications

Parts of the work have been published in peer-reviewed scientific journals and international conferences.

Journal Papers

1. Muhammad Raza Ul Islam, Asim Waris, Ernest Nlandu Kamavuako and Shaoping Bai. "A comparative study of motion detection with FMG and sEMG methods for assistive applications." *Journal of Rehabilitation and Assistive Technologies Engineering*, 7 (2020): 1-11. doi:10.1177/2055668320938588

2. Muhammad Raza Ul Islam and Shaoping Bai. "Effective multi-mode grasping assistance control of a soft hand exoskeleton using force myography." *Frontiers in Robotics and AI*, 7 (2020): 139. doi: 10.3389/frobt.2020.567491

3. Muhammad Raza Ul Islam and Shaoping Bai. "Payload estimation using forcemyography sensors for the control of upper-body exoskeleton in load carrying assistance." *Modeling, Identification and Control*, 40-4 (2019): 189-198. doi:10.4173/mic.2019.4.1

Conference Papers

1. Muhammad Raza Ul Islam and Shaoping Bai. "Intention detection for dexterous human arm motion with FSR sensor bands." in *Proceedings of the Companion of the 2017 ACM/IEEE International Conference on Human-Robot Interaction*, pp. 139-140, March, 2017. doi:10.1145/3029798.3038377

2. Muhammad Raza Ul Islam, Kun Xu and Shaoping Bai. "Position sensing and control with FMG sensors for exoskeleton physical assistance."

in *International Symposium on Wearable Robotics*, pp. 3-7, October, 2018. doi:10.1007/978-3-030-01887-0_1

Patent

1. Shaoping Bai and Muhammad Raza Ul Islam. "A Human intention detection system for motion assistance." IPC No.: B25J 9/16. Patent No.: WO/2018/050191. March 22, 2018, licensed to BioX ApS, Denmark (www.bioxgroup.dk).

Contents

List of Figures

Preface

This thesis is submitted to the Faculty of Engineering and Science, Aalborg University (AAU), with fulfillment of the requirements for the Doctor of Philosophy. The work has been carried out during the period from August 2015 to August 2020, at the Department of Materials and Production (MP), AAU. This work is supervised by Prof. Shaoping Bai.

I would like to express the deepest appreciation to my supervisor Prof. Shaoping Bai. He was always positive and in every difficult situation his advise was to "keep working hard, you will get there eventually". I think this positiveness and because of his invaluable expertise and supervision i am able to achieve this goal.

I would like to thank my friends and colleagues for their companionship through out my studies. I thank also my teachers from Bachelors and Master studies, who guided me and encouraged me to get here and achieve this goal.

I would also like to thank my family, my beautiful Mother, my Uncle/Aunt and Siblings for their immense support and love. They always kept me safe from worries back home and let me focus on my studies. I would also like to thank my Wife. She always supported me, loved me and helped me achieve goals that i couldn't have achieved alone. So thank you all for your prayers and for standing with me all the time.

Finally, my late Father Muhammad Zafar Ul Islam, for him thank you is a very small word. There is no way i can repay for the sacrifices he made. His only ambitions were to educate us and to make our lives better. The things he did for me i can not finish telling in a life time. I wish I could have finished my PhD in his life time. He would have been the happiest person on earth. Father i will work hard and I will try to be the human you wanted me to be. And Thank you Baba Jani for everything.

Muhammad Raza Ul Islam
Aalborg University, August 19, 2021

Chapter 1

Introduction

This research is aimed at developing robust and accurate human motion intention detection methods, which are used to design assistive control strategies for powered exoskeletons. In this work human motion intention is interpreted in terms of motion type and required assistance level. In order to detect motion intention muscle activity reading techniques will be first analyzed for their performances. Afterwards, methods to detect motion intention will be developed. Lastly, based on the developed methods control of upper limb exoskeleton that includes active hand, elbow and shoulder joints, will be implemented and tested.

Furthermore, this PhD is a part of Ambient Assisted Living (AAL), Joint Programme Call 6, funded EU project AXO-SUIT [1]. The goal of this project was to develop a portable full body (upper and lower limb) exoskeleton, Figure 1.1, which is able to assist elderly in their daily activities. In this project 3 universities and 5 companies were collaboratively involved from concept design to the development of final prototype. Aalborg University was the project coordinator, leading the design and development of the upper limb exoskeleton.

1.1 Background

Exoskeleton is an external structural mechanism with joints and links corresponding to those of the human body [2]. It's applications can be found in medical for rehabilitation [3, 4], in manufacturing industry for power augmentation [5] and for people with reduced muscle strength for assistance in daily activities [6].

These devices on basis of actuation can be divided into two types i.e. passive or active exoskeletons. Passive exoskeleton is constructed using mechanical spring and dampers [7]. These exoskeletons are designed to assist in

Figure. 1.1. Full body exoskeleton AXO-SUIT [1]

very specific tasks and can provide a limited amount of assistance. However, active exoskeletons, also called powered exoskeleton comprises of mechanical structure, sensors, actuators and human robot interaction (HRI) systems. In comparison to passive systems these can adapt to various applications and assistive profiles can be modeled according to target applications. However, the proper functioning of these devices needs efficient and effective modeling and control techniques.

For proper functioning HRI is one of the key elements. In exoskeleton systems their control is implemented either by decoding the cognitive processes or by measuring the physical interaction forces that are caused by the motions in result of cognitive processes [8]. Using active exoskeletons for physical assistance of elderly or industrial workers, interpretation of cognitive process is important in order to determine motion intention and to provide assistance as needed.

With the given requirements, methods to interpret motions that are robust and accurate are required. To achieve this goal, human motion intention detection methods to decode cognitive process are studied in this thesis. Several aspects, including detection performance, long term repeatability and assistance level determination, are investigated for using motion detection methods in order to control upper limb exoskeletons.

1.2 Literature Review

1.2.1 Upper limb exoskeletons

In the past couple of decades many exoskeletons have been developed for assistive and rehabilitation applications, which are either passive, active or hybrid, having both active and passive joints [9]. Some examples of such exoskeletons are shown in Figs. 1.2 and 1.3. In this section a brief overview of upper limb exoskeletons and their applications are presented.

EksoVest [10] is a passive exoskeleton designed to assist shoulder movements. Main application of this exoskeleton is to assist overhead tasks e.g. overhead drilling or tooling in automotive industry. Proto-MATE [11] and SkelEx [12] are also passive shoulder exoskeletons that are designed to provide support in overhead tasks. T. Rahman et al. [13] developed a passive elbow exoskeleton called WREX. The exoskeleton uses a linear elastic element to balance gravity in three dimensions.

eWrist [14] is a one DOF powered rehabilitation exoskeleton. It is designed to assist in wrist extension training. SEMGlove [15] is a soft powered hand exoskeleton developed by BioServo technologies. It is designed to assist in grasping task by measuring the contact forces at finger tips. Stuttgart Exo-Jacket [16] is a powered exoskeleton designed to provide assistance in industrial tasks. The exoskeleton has an active elbow and shoulder flexion/extension joints. The exoskeleton also has passive lower-body exoskeleton to ground the forces applied on the upper limb exoskeleton. CADEN-7 [17] is a 7-DOF cable-driven powered upper limb exoskeleton. The exoskeleton allows 3-DOF actuation at shoulder, 1-DOF actuation at elbow and 3-DOF actuation at wrist joint. The exoskeleton can provide the support is both rehabilitation and power amplification applications.

SUEFUL-7 [18] is a wheel chair mounted cable driven 7-DOF exoskeleton. The exoskeleton was aimed for the assistance of weak persons. Another wheel chair mounted 4-DOF upper limb exoskeleton for physical assistance of disabled persons is developed by Gull et al. [19]. CABexo [20] is a cable driven 6-DOF exoskeleton designed by Xiao et al. The exoskeleton was developed for elderly people to provide support in daily living activities. 6-REXOS [21] is a 6-DOF exoskeleton designed for assistance of physically weak people. It is equipped with physical HRI system in order to provide assistance in daily living tasks. MAHI Exo-II [22], developed by French et al., has 4 active DOF and one passive DOF. The exoskeleton was aimed for rehabilitation of stroke and spinal cord injury patients. REHAROB [23] is another rehabilitation exoskeleton with 7 DOF that was designed by Toth et al.

Several other exoskeletons have been developed for rehabilitation purpose i.e. ARAMIS (6-DOF, post stroke rehabilitation) [24], LIMPACT (20-DOF,

(a) (b)

Figure. 1.2. Passive exoskeletons, (a) Proto-MATE [11] and (b) WREX [13].

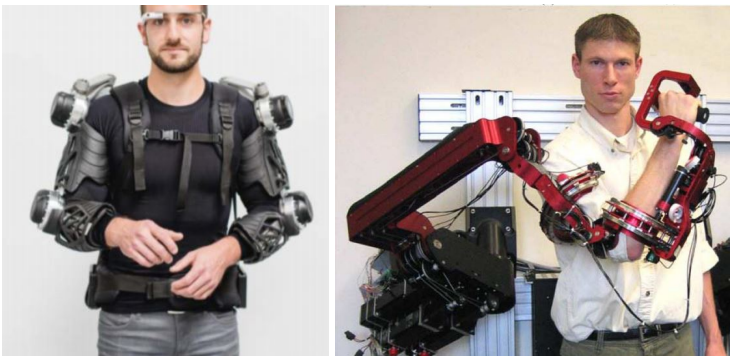

(a) (b)

Figure. 1.3. Active exoskeletons, (a) Stuttgart Exo-Jacket [16] and (b) CADEN-7 [17] .

neurorehabilitation) [25], IntelliArm (9-DOF, neurological impairments) [26], WOTAS (3-DOF, tremor assessment and suppression) [27], NTUH-ARM (7-DOF, post stroke rehabilitation) [28], T-WREX (rehabilitation after chronic stoke) [29], ARMin III (6-DOF, post stroke rehabilitation) [30] and RUPERT IV [31].

1.2.2 Intention detection

Control of exoskeletons for physical assistance depends on accurate detection of motion intention, which is obtained either through physical interaction or cognitive interaction. This section will introduced state of the art techniques that are used to detect motion intention.

Physical Interaction

In physical interaction, desired motion intention is detected by placing force or contact sensors on the exoskeleton. In [32] Huang et al. developed a 3-DOF upper limb power-assist exoskeleton and placed two sensor rings to interpret the intended motion direction. Each sensor ring was embedded with four force sensing resistors (FSR). The FSRs were placed to measure the interaction forces between human, and exoskeleton and interpret the intended motion direction. M. Baklouti et al. [33] proposed a 4-DOF orthosis for rehabilitation purpose. The orthosis also used FSR sensors to measure the interaction forces between human and exoskeleton. Two bracelets were placed on the exoskeleton, one on forearm and one on upper arm, where each bracelet was composed of four FSR sensors.

Nilsson et al. [15] developed a soft hand exoskeleton to assist in grasping tasks. The exoskeleton was also equipped with FSR sensors, placed at the finger tips to identify the physical interaction between finger tip and the object. Depending upon the magnitude of the interaction force, assistive torque was provided by the exoskeleton to grasp the object. FSR sensors for measuring physical interaction forces between human and exoskeleton have also been reported in [34, 35].

Lee et al. [36] used 3-axis load cells to measure physical interaction forces in order to control a upper limb exoskeleton HEXAR. CAREX-7 [37], SUEFUL-7 [18], IntelliArm [26] and EXO-UL7 [38] also used load cells installed at multiple contact points to measure physical interaction forces in order to control exoskeleton motion. Li et al. [39, 40] developed a novel variable stiffness actuator to introduce compliance in exoskeleton movement. Furthermore, by measuring the deflection of input and output link, the joint is also used to measure the interaction forces between human and exoskeleton.

Cognitive Interaction

In cognitive interaction human cognitive processes are measured. There exists several techniques to interpret these process i.e. electroencephalography, electromyography and force myography. Developments using each technique are presented in the forthcoming sections.

- **Electroencephalography** Electroencephalography (EEG) is the method of acquiring brain activity, in form of electrical signals, by placing the electrodes on the skull. The methods has been investigated to detect upper and lower limb movement intentions [41–43]. Wang and Makeig [44] conducted a study on binary single-trial EEG classification i.e. left and right. They placed the electrodes on the complete head and implemented independent component analysis to perform the classification. Bandara et al. [45] used EEG to detect task based motion in-

tention. They implemented neural network (NN) to classify between resting, moving and drinking. Hayashi and Kiguchi [46] proposed EEG based estimation of elbow and shoulder flexion/extension movement. They used 256 EEG channels to gather the brain activity. Afterwards, principle component analysis was implemented to sort out the channels that provide distinguishable results. EEG method has also been proposed in [47] to detect walking direction. The estimation model interpreting human intention uses independent component analysis and multi-class support vector machine (SVM) algorithms to classify the motion type. D. Planelles et al. [48] proposed an SVM classifier to detect gait intention using EEG.

- **Electromyography** Electromyography (EMG) is the method of interpreting the brain activity in form of electrical signals by placing the electrodes on muscle belly. EMG has been widely used to detect arm movements [49–68].

  In [69] Arenas et al. used EMG to detect six hand gestures i.e. finger pointing up, down, left and right, close hand and rest state. Commercially available MYO armband [70] was used to collect EMG data and convolution NN was implemented to classify the gestures. In [71] Abu et al. used EMG to detect hand gestures i.e. open, pronation, supination, cylindrical grasp and rest. MyoWare™ Muscle Sensor (AT-04-001) was used to collect EMG data of brachioradialis and flexor carpi muscles and NN was used to classify the gestures. EMG has also been used to detect reach to grasp and grasping task [72] by placing sixteen EMG channels on upper arm and forearm muscles. Leonardis et al. [73] used EMG to estimate the grasping torque. EMG electrodes were placed at three forearm muscles i.e. extensor digitorum longus, flexor digitorum longus and abductor pollicis brevis and multi-layer NN technique was implemented to estimate the grasping torque.

  Artemiadis and Kyriakopoulos [74] proposed EMG based arm motion, i.e. shoulder adduction/abduction and elbow flexion/extension, detection method in order to control a robotic arm. Ullari et al. [75] proposed EMG based elbow joint torque estimation method. In their method EMG electrodes were placed on the biceps and triceps. They implemented a pneumatic artificial muscles (PAM) based model that used the EMG measurements and elbow joint angle to output the applied joint torque. In [76] Rahman et al. presented an EMG based control of an upper limb exoskeleton to assist elbow and shoulder movement. In their approach, EMG signals were processed to estimate the joint angle, which was further used as reference input to control the exoskeleton movement. In [77] Li et al. proposed an EMG based two stage machine learning network to estimate the corresponding joint torque. In the first

stage linear discriminant analysis (LDA) classifier was implemented to classify the motions type and in the second stage corresponding joint torque was estimated. The joint torque was later used to control the upper limb power assist exoskeleton.

In [78–80] the performance of EMG was investigated by implementing different classification techniques in order to obtain better accuracy and In [81–83] sensor fusion techniques were proposed, by combining IMU and EMG, to improve the gesture detection accuracy.

- **Force myography** In force myography (FMG) muscle activity is detected by measuring muscle contraction intensity. In the last decade this method has been extensively studied for the detection of upper and lower limb movements [84–87, 89–93, 108], in terms of gestures and applied forces.

  Wininger et al. [94] used FMG to predict the grasping force. The goal was achieved by developing a cuff with 14 FSR sensors to be worn at forearm muscles covering mid-to-proximal surface of the forearm. In [95] Sakr et al. used FMG for estimating hand/wrist torque by placing the senor strap, containing 16 FSR sensors, on forearm near elbow joint. In another study [96] the performance of same task was analyzed by comparing SVM and NN techniques. Sakr et al. [97] also investigated the effect of sensor placement and numbers on hand force estimation. Four sensor bands were used, three placed on forearm and one on upper arm. Fifteen combination of sensor bands were analyzed by implementing general regression NN. The sensor placement was also investigated in [98] for gesture classification. In this study eight hand gestures were classified by using three sensor bands placed only on forearm. In [99] performance of FMG was investigated for prosthesis control. In this work 11 grasp types were classified using LDA. Xiao et al. [100] proposed FMG for detection and counting of grasping tasks. Two sensor bands were used, one placed near elbow joint and one placed near wrist. Furthermore, three classification techniques i.e. LDA, SVM and artificial NN, were tested and compared.

  FMG for classification of dynamic gestures, i.e. opening, closing, shaking, rotating, pushing and pulling, was reported in [101]. The study was focused on optimization features extraction in order to improve the classification performance and results showed that optimization do help in improving the classification accuracy. Instead of optimizing the extracted features, Sadrangani et al. [102] tested and analyzed different features, i.e. mean absolute value, root mean square, linear fit, parabolic fit and autoregressive model for improving the accuracy of detecting grasping task. Jiang et al. [103] proposed FMG and leap mo-

tion system for classifying six grasp types. Both systems were tested individually and combined and results showed that the fusion of both systems yield best performance.

Radmand et al. [104] proposed a FMG based high density force sensor grid to measure the muscle activity of forearm muscles. With the developed method they were able to distinguish between eight wrist and hand motions. Ferigo et al. [105] also used high density FMG of forearm muscles for detection of open, rest and 9 grip types.

1.3 Research challenges

In the last section comprehensive state of the art literature survey, related to exoskeleton development and motion intention detection methods, was presented. It is noticed that many developments have been made in the past couple of eras in these areas. The motion intention detection methods have been applied for various applications and their performances are analyzed in terms of muscle activity detection methods, machine learning techniques, sensor fusion, exoskeleton control and many more.

This section will summarize these challenges and will also highlight a few research gaps that will be addressed in this thesis.

1.3.1 Muscle activity detection method

For detecting desired motion intention, reading muscle activity is the primary task. The most commonly used methods for reading muscle activity are EMG [107] and FMG [106] that have shown promising results for the assistive exoskeletons control. Many studies have been performed to compare the performance of these methods. Xiao et al. [108] compared the performance of FMG and sEMG for detecting elbow, forearm and wrist positions using SVM and LDA. Jiang et al. [109] compared FMG and sEMG for detecting 48 hand gestures. Classification was performed using LDA, where in FMG raw FSR data was used as features and in sEMG 13 features were extracted. Ravindra and Castellini [110] compared both techniques for estimating finger forces. The performance was evaluated in terms of estimation accuracy, signal stability, wearability and cost. In [111] FMG and sEMG methods were compared for detecting wrist and hand motions. Signal stability, cluster separability and gesture prediction accuracy were analyzed. Results showed that FMG has better performance, however, fusion of both methods can yield best results. Fusion of multiple modalities is also been investigated in other studies [112, 113], addressing the performances during prosthetic socket shift, user fatigue and muscle activation levels.

1.3.2 Robust motion detection

In the last section literature comparing the performance of FMG and EMG is presented. Each method has been individually investigated for performance improvement from many other aspects. Features selection and optimization [50, 101, 102, 114] were studied to improve the classification performance. Different AI and machine learning algorithms have also been tested for improving the classification accuracy [78–80, 90, 115]. However, the results of features optimization and classifier type have shown dependence on targeted motion and testing conditions.

Many of the experiments reported in literature are performed in controlled environment, which doesn't prove the feasibility of the method applicable in routine life tasks. Hand/wrist motion detection in presence of upper limb movement is one of factors that can affects the pattern recognition performance [116]. However, increasing training dataset and sensor fusion techniques have shown promising results in improving the classification accuracy [105, 117–119].

1.3.3 Long term data repeatability

The purpose of using assistive exoskeletons in industries or at personal space is to provide assistance on daily basis. Motion detection methods governing the control of these exoskeletons require a training phase in which a set of motions are performed for multiple times. Following such routine on daily basis is not feasible and inconvenient. Therefore, besides on day detection accuracy, investigation on robustness of motion detection methods between days is required. Kaufmann et al. [120] analyzed EMG data of hand gestures recorded for 21 days. Five classification techniques i.e. k-nearest- neighbor, LDA, decision trees, artificial NN and SVM, were compared for detecting the gestures and to analyze change in accuracy between days. J. He et al. [121] used 12 days of EMG data for detecting 13 forearm and hand gestures. They analyzed the performance of six time and frequency domain features using LDA. Performance of EMG for long-term pattern recognition is also been investigated in [122, 123]. S. Amsuss et al. [124] proposed a self-correcting pattern method to improve the between day detection performance by implementing two layer detection method. In first layer LDA is implemented to classify a gesture, whereas, artificial NN is implemented in second layer to decide on the correctness of the decision made in first layer. Phinyomark et al. [125] investigated EMG features to improve usability of practical applications of myoelectric control.

1.3.4 cHRI based exoskeleton control for physical assistance

There has been many solutions proposed for the control of assistive exoskeletons that are based on cognitive HRI (cHRI) method. In these methods EMG has been the main source of interpreting the desired motion intention [126–128]. In [129] Luka et al. used muscle activity recorded through EMG as feedback. The information was used in an adaptive feed-forward torque control strategy for elbow exoskeleton in order to minimize human effort in handling unknown load. Luh et al. [130] used EMG to estimate the elbow joint angle by implementing NN technique in order to control a 2-DOF elbow exoskeleton. The method was developed and tested to estimate the joint angle in varying load lifting tasks. Li et al. [131] used EMG to control upper limb exoskeleton for assisting elbow and shoulder flexion/extension movement. In their setup EMG was used to estimate the joint stiffness and adaptive impedance control strategy was implemented to mirror it. Mghames et al. [132] used muscle modeling approach to map EMG readings to muscle force level of biceps and triceps. Afterwards, using muscle forces joint angles were predicted to control a variable stiffness exoskeleton FLExo. Lu et al. [133] used myowear muscle sensor to collect EMG of biceps in order to estimate the elbow joint torque. The estimated joint torque is further used to determine the increment in elbow joint angle and to actuate the elbow exoskeleton motion using PID controller. Khan et al. [134] used muscle circumference sensor, placed on the upper arm and hill muscle model to determine the elbow joint torque. The information was used to implement adaptive impedance control to assist elbow movement through upper limb exoskeleton.

The aforementioned SOA and research challenges shows that human intention detection methods have been analyzed from various perspectives of performances and exoskeleton control. However, there are many research gaps, in terms of daily use performance analysis and usability/convenience in work environment, yet to be investigated. Brief details of the identified gaps and research tasks to address them are as follows:

- **Long term performance comparison**: FMG and sEMG have been the key methods to detect muscle activities. In the reported literature [108–111] performance comparison experiments are conducted for one day only. Day to day performance comparison study has not been reported yet, which is essential for the applications of daily use.
- **FMG based motion detection and assistive exoskeleton control**: The comparison studies [108–111] between FMG and sEMG shows that FMG has better performance than sEMG. However, FMG literature is mainly focused on hand motion detection methods. Furthermore, the methods

developed using FMG are applied for the control of hand prosthesis. FMG has not been explored for the control of upper limb, including hand, elbow and shoulder, assistive exoskeletons.

- **Sensor usability in real work environment**: Usability [135] refers to the ease of using the technology. A couple of challenges of the existing sensing methods w.r.t this aspect are addressed below.

  - The methods of cHRI based upper limb assistive exoskeleton control are mainly based on EMG. In the applied methods [126, 131], assistive torque profile for each joint is determined by placing the sensors at its driving muscles. Thus, In multi DOF exoskeleton, system complexity will increase and also inconvenience in working environment. Therefore, new methods that can reduce sensor requirement are needed in order to improve the usability of motion detection methods and its implementation in the working environment.
  - In machine learning based motion detection methods another challenge in term of sensor usability is the collection of correct and big training datasets. Even after collecting them, performance of detection models can still be affected because of sensor placement after don/doff and change in effort level [120, 122, 123]. Solutions to solve these issues have been reported [121, 124] but they come with expense of extensive user training and classifiers retraining. Therefore, methods that can minimize the training effort without compromising the performance are needed in order to bring motion detection methods more close to work place applications.

1.4 Research questions

In order to address the identified research gaps and to propose solutions to fill those gaps the following research questions are formulated.

- **Rq1:** What muscle activity detection method is suitable for the applications of daily use?
- **Rq2:** How can the usability of FMG based classification/regression methods be improved for detecting upper arm movement intent?
- **Rq3:** How can FMG based motion detection methods be integrated into exoskeletons for intelligent physical assistance in load carrying tasks?

1.5 Objectives and scope of the work

The objective of this PhD is to investigate control methods for upper limb powered exoskeleton in order to provide physical assistance reliably and conveniently on daily basis. Human motion intention is one of the key element to achieve this goal. A proper physical assistance can be provided by knowing the human motion intention. Therefore, in this thesis cHRI method will be studied to determine the desired motion type and required assistance level. The hypothesis is that "FMG can effectively and efficiently detect upper limb motion intention in order to control upper limb exoskeleton for providing physical assistance in load carrying tasks". To this end and in order to address the research questions identified in the previous section, following research activities will be conducted:

- Investigate the performance of different muscle activity sensing methods (**Rq1**).
- Investigate sensor placement and fusion techniques to aid AI methods in motion detection (**Rq2**).
- Develop AI techniques to predict/estimate desired motion intention (**Rq2**).
- Evaluate the performance of motion intention detection techniques by testing it with healthy subjects (**Rq2**).
- Investigate control methods applicable for the assistive exoskeleton robots (**Rq3**).
- Integrate motion intention detection techniques and exoskeleton control strategies (**Rq3**).
- Testing of integrated methods with healthy subjects and analyzing their performances for reducing human effort (**Rq3**).

The overall work scope of this thesis is shown in Fig. 1.4. From Fig. 1.4 it can be seen that "motion intention detection" being the main focus of this thesis is addressed by reporting three papers I, II and III, in chapters 3, 4 and 5, respectively. The figure also encompasses the main tasks, challenges and research questions linked to each study.

1.6 Research Methodology

Research methodology is the necessary process to address the research questions systematically. In this work the research approach is adopted from

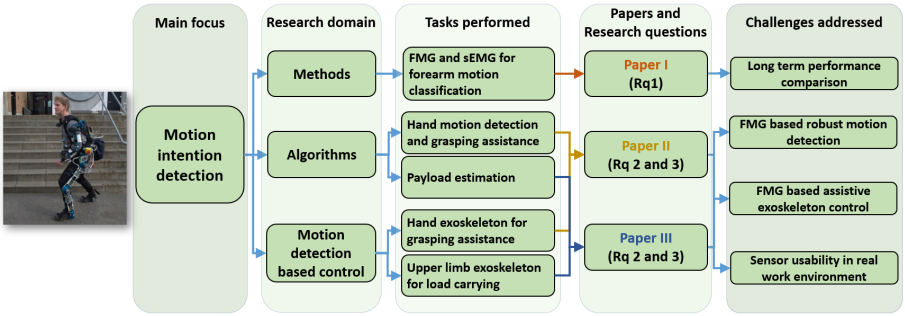

Figure. 1.4. Work scope of the thesis.

Design science research methodology (DSRM) [136]. The methodology offers four entry points to start a research project. One of them is problem-centered initiation that is relevant to this thesis project i.e. the need of assistive exoskeleton for industry and daily use. With the research entry point defined, the research methodology has following steps i.e. identification of problem and motivation followed by an iterative process of defining objectives, designing, experimenting, and evaluating the proposed method/solution. Brief details of how research questions are connected to the aforementioned DSRM steps, applied to this thesis, are given below.

One of the key element for proper working of assistive exoskeleton is human movement intention, detected through muscle activity. In literature review existing strategies were reviewed for measuring muscle activity. **Rq1** focused on problem identification, i.e. daily use, and motivation for the selection of a strategy. With the selected strategy and research gaps identified in state of the art, **Rq2** focused on defining objectives, and designing, experimenting and evaluating the methods to address those research gaps. In **Rq3**, the developed methods were integrated with upper limb exoskeleton control strategies, which were further experimented, evaluated and analyzed for future research directions.

1.7 Outline of thesis

The thesis consists of five chapters, which are as follows

Chapter 1 explains the background and state of the art exoskeleton systems and human motion detection methods. Research challenges of existing human motion detection methods in context of assistive exoskeleton control are also analyzed. Based on the analysis, research questions and objectives of this thesis are also presented.

Chapter 2 introduces FMG method for motion detection. In this chapter,

FMG principle, sensors for performing FMG, signal amplification and design of physical construction of sensor band are explained.

Chapter 3 addresses the performance of muscle activity detection techniques that are sEMG and FMG. The analysis were performed to select a method that is used for the development of assistive control strategies for upper limb exoskeletons.

Chapter 4 describes the application of FMG on hand exoskeleton control. In this chapter an AI technique is developed to detect dynamic hand motions. An assistance level determination method for grasping task is also presented and tested with soft hand exoskeleton.

Chapter 5 describes FMG based payload estimation method and its application on upper limb exoskeleton control. The method is developed to determine the assistive torques to be provided at elbow and shoulder joints. The method is experimentally validated for load carrying tasks.

Chapter 6 concludes this thesis, with a summary and contributions made. Future work is also suggested.

Chapter 2

Motion detection using force myography

This chapter introduces theoretical basis of FMG and its applications. Design principles for constructing a sensor band, amplifier characteristics, data processing methods to determine limb movements are also presented.

2.1 Principle

Limb movements are resulted by the contraction and relaxation of certain muscle groups. As the muscles are contracted or relaxed the tension along the muscle length is increased or decreased, respectively. This change in muscle tension creates a normal force, as illustrated in Fig. 2.1, that is proportional to the muscle contraction intensity. Fig. 2.1 is an example showing the contraction of bicep muscle before and during payload lifting task. Increase in muscle contraction can be observed visually as the payload is lifted and by wrapping a sensor band around upper arm outward normal force **f**, caused by muscle contraction, can be measured. The process of reading this normal force is referred as FMG [137]. Hereafter, the normal force **f** will be referred as muscle contraction-induced (MCI) force.

2.2 Sensing methods

Several sensors have been being proposed to detect MCI forces, which include:

- **Force sensing resistor:** FSR sensor acts as a variable resistor and has an inverse relationship to applied force i.e. higher the applied force

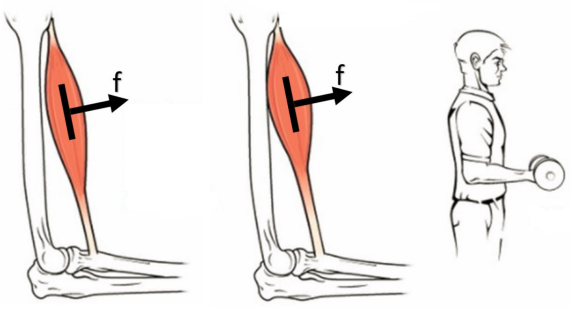

Figure. 2.1. Muscle contraction, (a) without and (b) with payload.

lower is the resistance. Fig. 2.2(a) shows the placement of FSR sensors to read muscle activity. In this configuration FSR sensors can measure MCI forces directly [84, 85].

- **Strain gauge:** Strain gauge sensor [138], Fig. 2.2(b), also measures forces by varying its resistance. However, instead of MCI force, radial forces are measured to read muscle activity.
- **Optical fiber:** Construction of sensor band using optical fibers is shown in Fig. 2.2(c). In this method pressure applied by MCI forces induce attenuation and variations in light intensity being trasmitted through the fiber, which is then mapped back to the applied MCI force [139].

2.3 FSR sensor for FMG

Among all the above mentioned sensors FSR are most commonly used sensors to perform FMG. These sensors have the advantage of simple filtering and amplification interface, moreover, construction of sensor bands is also easy. Comparing to other sensors, like for strain gauge sensors operating temperature has significant effect in its measurements. In case of optical fiber sensors CCD cameras [139] have been commonly used to read light intensity, which is hindrances for real time implementation for exoskeleton control. Recently an embedded amplifier [140] has been reported that brings it close to practical implementation of assistive exoskeleton, but still requires validation. On the other hand FSR are interfaced to basic operational amplifiers, which are readily available, compact and more suitable for real time applications. Moreover, FSR sensors are also not affected by temperature changes. Furthermore, FMG data obtained through FSR is also been validated with

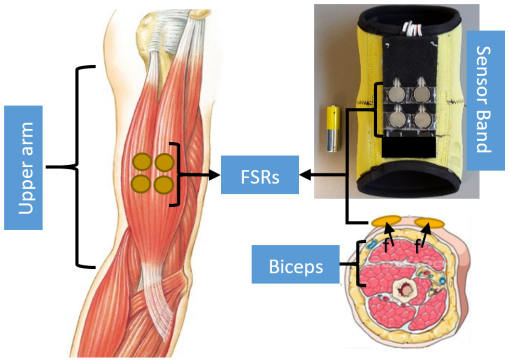

(a)

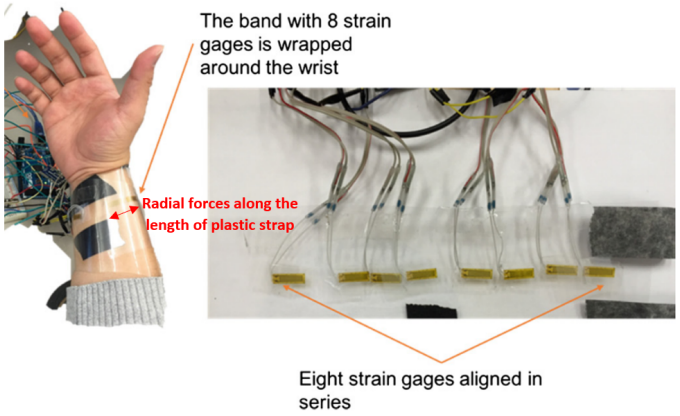

(b)

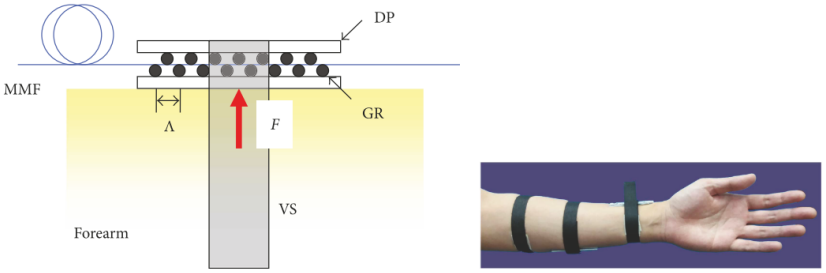

(c)

Figure. 2.2. Sensor band designs using (a) FSR, (b) Strain gauge [138] and (c) Optical fiber [139].

(a) (b)

Figure. 2.3. (a) FSR-402 used for sensor band construction (b) side view of FSR placed inside sensor band.

standard EMG method [141]. Therefore in this thesis FSR sensors are used to detect upper limb activities.

2.3.1 Sensor band construction

FSR is the sensor that can read the forces applied normal to its surface. An array of these sensors are used to construct the sensor band in this thesis. The employed sensors are FSR-402, shown in Fig. 2.3(a), developed by Interlink. FSR-402 can read the forces in the range of 0.1-10N.

The developed sensor band has three layers as shown in Fig. 2.3(b). (1) The inner most layer is the FSR-402 that measures the MCI force, (2) the middle layer is the "FSR base" that is made of soft fabric and is of the same size as of FSR. This layer ensures the proper contact of FSR with the skin of the user. (3) The outermost layer called "Band", which is the strap to be wrapped around the limb of the user.

2.3.2 Signal amplification

FSR sensors works as a variable resistor and it's output is inversely proportional to the applied force. Figure 2.4 show an amplification circuit to interface FSR. Output voltage in this configuration is given by,

$$V_{out} = \frac{R_{ref}}{R_{ref} + R_{fsr}} V_{in} \tag{2.1}$$

here V_{out} is the output voltage, V_{in} is the fixed supply voltage, R_{ref} is the reference resistance and R_{fsr} is the FSR resistance.

In this configuration desired force range of the amplifier can be adjusted by changing reference resistance. In another configuration, shown in Fig. 2.5, a non-inverting amplifier is implemented. In this design, output of the amplifier is given by,

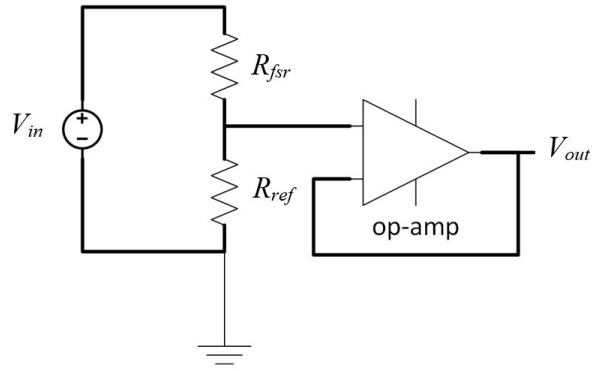

Figure. 2.4. Voltage divider followed by buffer amplifier to process FSR data.

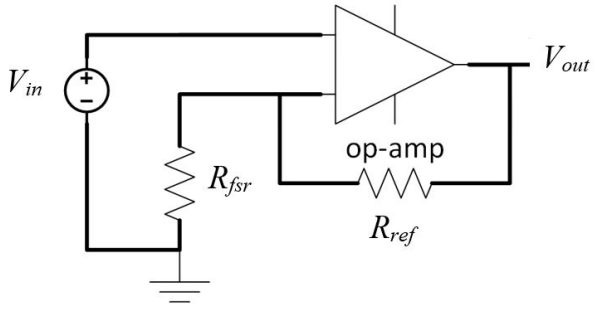

Figure. 2.5. non-inverting amplifier to process FSR data.

$$V_{out} = (1 + \frac{R_{ref}}{R_{fsr}})V_{in} \tag{2.2}$$

here the output of the amplifier can be varied by changing both R_{ref} and V_{in}.

The later configuration, shown in Fig. 2.5, is comparatively more convenient in adjusting the FSR force sensing range during real-time testing. On daily basis it is very challenging to achieve same tightness of the sensor band. In such scenario it is possible that maximum resolution of the amplifier is not achieved for a given set of movements. Using the amplifier shown in Fig. 2.5, V_{in} can be controlled through a DAC channel and by using an API it can be tuned conveniently. In this work the later version of the amplifier was used to obtain FSR data.

2.3.3 Motion detection

Data obtained through FMG has been used to detect limb movements either in form of discrete states using classification approach or in form of continuous trajectory by implementing a regression algorithm.

Regression

In regression the data obtained from FMG is used to generate a continuous output signal. This method has been reported to track finger movements, hand/wrist force/torque, forearm stiffness, grasp intensity and knee joint angle [86, 94, 97, 142, 143]. In these methods data from each FSR was treated as a separate input feature and to predict desired task support vector machine, kernel ridge regression, random forest and NN techniques have been implemented.

Classification

In classification discrete output states are predicted. In FMG, this method has been implemented to classify forearm, wrist and hand gestures [87, 100, 101, 103] and also been used to identify locomotion modes and ankle positions [144–146]. The implementation of classification techniques involves three main steps i.e. windowing, features extraction and classifier training. Windowing in the process of segmenting raw data, either at discrete time stamp or a running window of fixed time interval. It is an important step as the detection accuracy and latency in controlling a machine depends on it. Followed by windowing is features extraction process, in which time and frequency domain information is extracted from the segmented raw data. In FMG, mainly time domain features i.e. mean, root mean square, variance, waveform length, window symmetry and many more, have been reported. With the extracted features, the last step is to train a classifier. Many machine learning techniques have been reported to train a classifier i.e. SVM, LDA, random forests, NN and deep learning. In real-time testing the trained classifier are then used to predict different movements.

2.3.4 Methods used in this thesis

In this thesis work, both regression and classification techniques were used. In **Chapter 3** and **4**, classification approach is implemented to detect forearm and hand motions. Whereas, in **Chapter 5** regression is used to detect the carried payload.

An example of using FMG data in regression and classification is given in forthcoming section.

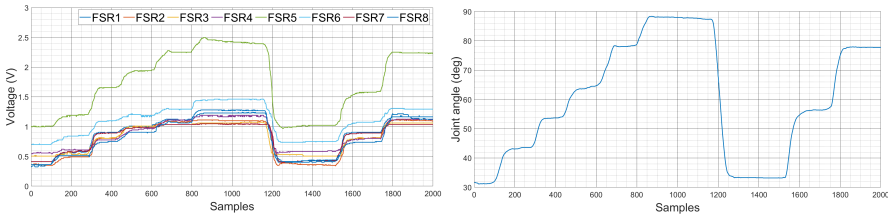

(a) (b)

Figure. 2.6. Dataset of elbow flexion/extension, (a) MCI forces obtained in terms of FSR amplifier output voltage. (b) elbow joint angle.

Dataset

The collected dataset, shown in Fig. 2.6, is for elbow flexion/extension. Two sensors, i.e. FSR array and IMU, are used to collect this dataset. FSR array embedded inside a flexible sensor band is placed in the middle of the upper arm to measure the MCI forces. Whereas, elbow joint angle is measured by placing two IMU sensors, one on upper arm and one on forearm.

The dataset shown in Fig. 2.6 is split into two sets i.e. a) **Data-Samples-A** samples 0-1000 and b) **Data-Samples-B** samples 1300-2000, which are used as training and testing datasets, respectively, for regression and classification.

Regression

In regression MCI data, shown in Fig. 2.6(a), is used to estimate the elbow joint angle, shown in Fig. 2.6(b). To implement this technique each FSR output is treated as input feature and SVM is used as an estimator.

In this implementation **Data-Samples-A** is used as training dataset and **Data-Samples-B** is used as testing dataset. The results of the joint angle estimation using the testing data are shown in Fig. 2.7. It can be seen that the trained model is able to track the actual value quite accurately. An RMSE of 2.53° and standard deviation of 2.33° is obtained.

Classification

In classification same training and testing datasets are used, as for regression. In this implementation the elbow joint angle below 44° is treated as class **1**, between 44° and 66° is treated as class **2** and finally above 66° is labeled as class **3**. Hence, as shown in Fig. 2.8, the samples between 0-280, 281-620 and 621-1000 are labeled as **1**, **2** and **3** respectively.

In this implementation raw FSR data is used as input feature and decision is made on each sample. Furthermore, the classification between different

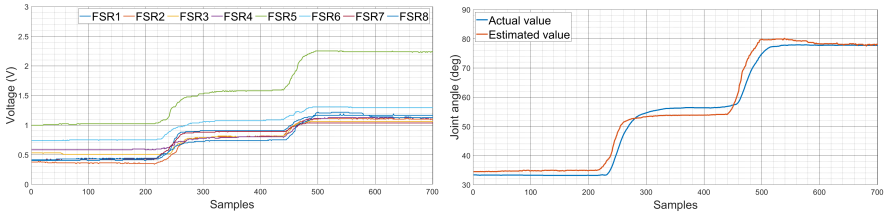

(a) (b)

Figure. 2.7. Results of joint angle estimation, (a) FSR sensors reading, (b) actual and estimated elbow joint angles.

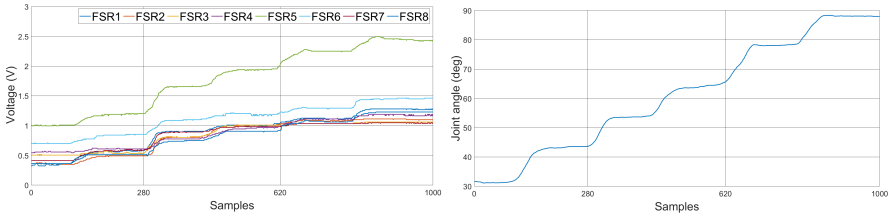

(a) (b)

Figure. 2.8. Training dataset of joint position prediction, (a) FSR sensors reading, (b) elbow joint angle. Samples 0-280, 281-620 and 621-1000 are labeled as class **1**, **2** and **3** respectively.

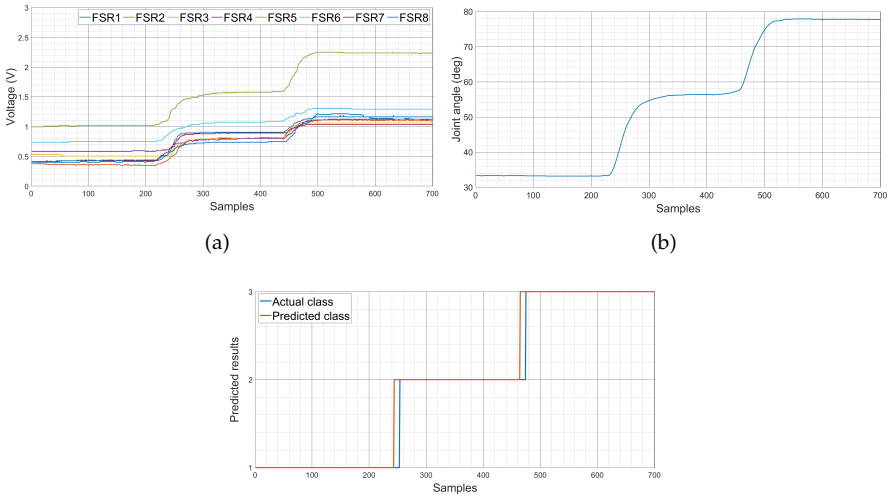

Figure. 2.9. Results of joint position prediction, (a) FSR sensors reading, (b) elbow joint angle and (c) actual and predicted classes.

classes is done using SVM classifier.

Using the testing dataset, shown in Figs. 2.9(a) and 2.9(b), the results obtained are shown in Fig. 2.9(c). It can be seen that during steady state there is no miss classification, each class is predicted accurately. Whereas, during transition there are some miss classifications. Overall an average of 97.15% accuracy is achieved for all classes.

Chapter 3

Paper I

A comparative study of motion detection with FMG and sEMG methods for assistive applications

Muhammad Raza Ul Islam, Asim Waris, Ernest Nlandu Kamavuako and Shaoping Bai

The paper has been published in the
Journal of Rehabilitation and Assistive Technologies Engineering, vol. 7, pp. 1–11, 2020.
doi.org/10.1177/2055668320938588

Original Article

RATE

Journal of Rehabilitation and Assistive Technologies Engineering
Volume 7: 1–11

DOI: 10.1177/2055668320938588
journals.sagepub.com/home/jrt
SAGE

A comparative study of motion detection with FMG and sEMG methods for assistive applications

Muhammad Raza Ul Islam[1], Asim Waris[2], Ernest Nlandu Kamavuako[3] and Shaoping Bai[1]

Abstract

Introduction: While surface-electromyography (sEMG) has been widely used in limb motion detection for the control of exoskeleton, there is an increasing interest to use forcemyography (FMG) method to detect motion. In this paper, we review the applications of two types of motion detection methods. Their performances were experimentally compared in day-to-day classification of forearm motions. The objective is to select a detection method suitable for motion assistance on a daily basis.

Methods: Comparisons of motion detection with FMG and sEMG were carried out considering classification accuracy (CA), repeatability and training scheme. For both methods, classification of motions was achieved through feed-forward neural network. Repeatability was evaluated on the basis of change in CA between days and also training schemes.

Results: The experiments shows that day-to-day CA with FMG can reach 84.9%, compared with a CA of 77.8% with sEMG, when the classifiers were trained only on the first day. Moreover, the CA with FMG can reach to 86.5%, comparable to CA of 84.1% with sEMG, if classifiers were trained daily.

Conclusions: Results suggest that data recorded from FMG is more repeatable in day-to-day testing and therefore FMG-based methods can be more useful than sEMG-based methods for motion detection in applications where exoskeletons are used as needed on a daily basis.

Keywords

Day-to-day performance comparison, forcemyography, human-machine interfaces, neural network, surface-electromyography, assistive exoskeletons

Date received: 29 August 2019; accepted: 2 June 2020

Introduction

Many human activities, either occupational or in daily life, require our muscles having a certain level of strength.[1] Exoskeletons[2] have the capability to overcome the muscle strength limitation by providing power augmentation.[3–6] This can contribute to enhance endurance for workers and to improve motion capability for the elderly and people with motion limitations.

In the control of exoskeletons, human motion detection is critical[7] for appropriate assistance control and human-robot interaction. Many methods have been developed, which are based on either physical or cognitive interfaces. Of them, sEMG is one of the conventional methods to determine upper limb movement activities[8–16] in terms of elbow/shoulder joint angles, hand gestures and task identification. EMG based exoskeleton controls have been reported in literature.[17–22] The effect of training time on sEMG based classification has also been studied earlier.[23–26] The results indicate that performance continuously downgrades as the

[1]Department of Materials and Production, Aalborg University, Aalborg, Denmark
[2]Department of Biomedical Engineering and Sciences, National University of Sciences and Technology, Islamabad, Pakistan
[3]Department of Informatics, King's College, London, UK

Corresponding author:
Muhammad Raza Ul Islam, Department of Materials and Production, Aalborg University, Aalborg, Denmark.
Email: mraza@mp.aau.dk

time difference between training and testing day increases. On the other hand, FMG as an alternative to detect upper and lower limb muscle activities has been used in different applications with healthy subject[27–37] and with stroke/amputated subjects.[38,39]

Given different applications of these methods, comparisons of their performance are necessary for their proper use in applications. Some comparison works have been reported in the literature. In Ravindra and Castellini[40] the performances of using pressure sensing (FMG), sEMG and ultrasound methods for estimating finger force were reported in terms of overall estimation accuracy, change in estimation accuracy with repetition of each task (stability), wearability and cost. It was reported that pressure sensing performed well in term of accuracy and stability. In Jiang et al.,[41] the performances of FMG and sEMG for recognizing hand gestures were compared. Average accuracy was reported as 87.35% for FMG and 81.85% for sEMG. Moreover, FMG performance was also evaluated by increasing the number of force sensing resistor (FSR) sensors and an increase of 5.7% in accuracy was obtained. The performances in elbow, forearm and wrist position classification were reported in Xiao and Menon.[42] The results showed that overall performances with FMG and sEMG were consistent. Study on combining both sEMG and FMG was also reported to achieve better performance.[43]

It is noted that in the aforementioned studies, the performance of FMG and sEMG was compared for classifying static postures and finger force estimation. Moreover, the experiments with FMG were conducted for one-time data testing. Comparisons of day-to-day performances with the two methods are not reported yet.

In this work, we compare day-to-day performances of FMG and sEMG methods for classifying motions, including both static pose and dynamic arm movement. Our interest in this work is to understand the advantages and limitations of the two methods, in order to apply a proper method for motion assistance through exoskeletons that are used on a daily basis.

This paper is organized as follows: Materials and methods for performance testing are explained in the upcoming section. A further section presents the testing results, which is followed by the discussion in next section. The work is concluded in the final section.

Methods

Motion types

The motions studied in this work include forearm flexion, extension, pronation, supination and rest. Except rest state, the other four motion types were classified during the dynamic state. The starting and ending states of each motion are shown in Figure 1. Flexion was performed by moving the forearm from neutral to fully flexed forearm position (Figure 1(a)). Extension was performed by moving the forearm from fully flexed

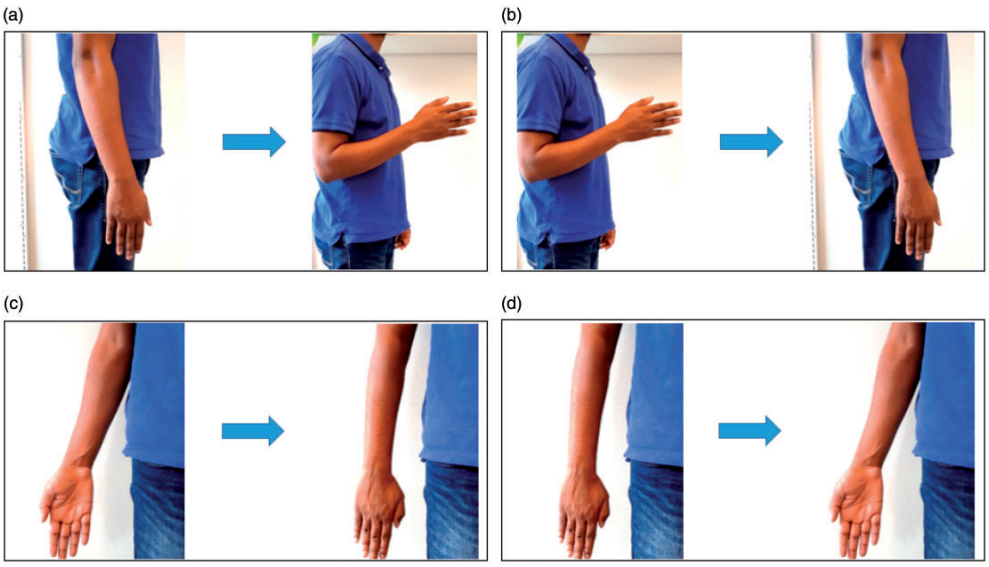

Figure 1. Starting and ending states of (a) flexion, (b) extension, (c) pronation and (d) supination.

to fully extended position (Figure 1(b)). Pronation was performed by rotating the forearm from fully supinated to fully pronated position (Figure 1(c)) and supination was performed by rotating the forearm from fully pronated to fully supinated position (Figure 1(d)).

Sensors and placement

The forearm motions are classified separately using FMG and sEMG based classifiers. With FMG, muscle activity is recorded in terms of lateral force caused during muscle deformation, whereas with sEMG the activity is recorded in terms of electrical signals.

For FMG testing, two sensor bands with embedded FSR, namely, FSR-402 developed by Interlink, were used. One sensor band comprised of six FSR sensors was placed at the middle of the upper arm. The other sensor band also comprised of six FSR sensors was placed at the forearm near the elbow joint. Figure 2 (a) shows the placement of sensor bands.

For sEMG testing, four pairs of EMG electrodes, Neuroline 720 from Ambu, were used. Their placements are shown in Figure 2(b), for detecting muscle activities of biceps brachi, triceps, pronator teres, and supinator, whereas, the reference electrode was placed at the wrist. Before the placement of the electrodes, the skin was shaved and cleaned with alcohol wipes. Conductive gel was also applied to acquire good quality of signals.

Data collection

Figure 3 shows the hardware setup to collect FMG and sEMG data. The FMG was recorded through custom developed non-inverting operational amplifier and sEMG was recorded through commercially available AnEMG12 amplifier from OT Bioelettronica. Both systems were interfaced to Arduino Due. The data from Arduino was further transmitted to a laptop through serial communication, where MATLAB based GUI was designed to record the data at the frequency of 700 Hz. The GUI was designed to display each motion type to be performed in a randomized order during training and testing sessions. Moreover, all subjects were instructed to complete each given motion in four seconds. It was understood that it is less probable that the subjects will exactly start and finish the motion in the given time. Therefore, the initial and last quarter second of the data were not included, only the middle three and a half seconds of data was used for training and testing.

Data was recorded for three consecutive days for each subject, the details are as follow

- Day 1: Training dataset, $\mathbf{T}_{r1}$, 10 repetitions of each motion type. Testing dataset, $\mathbf{T}_{s1}$, 5 repetitions of each motion type.

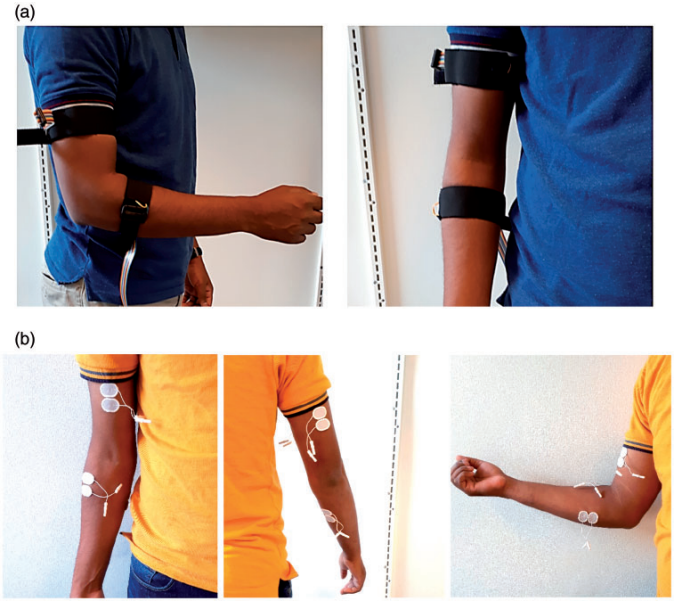

Figure 2. Sensor placements on human arm, (a) FMG and (b) sEMG.

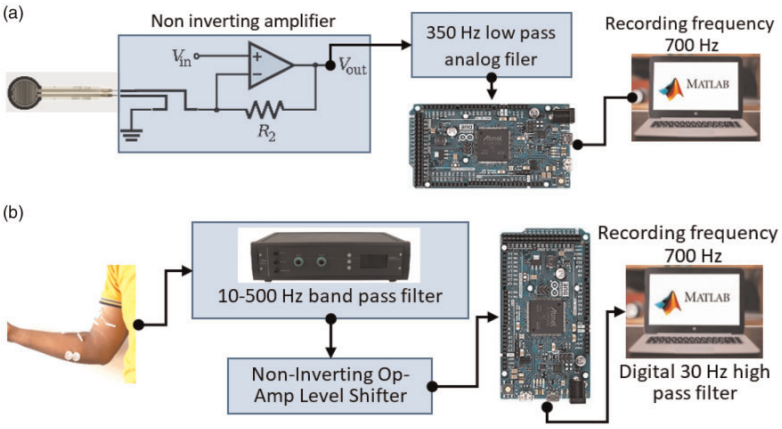

Figure 3. Hardware setup to collect data with (a) FMG, and (b) sEMG.

- Day 2: Training dataset, $\mathbf{T}_{r2}$, 2 repetitions of each motion type. Testing dataset, $\mathbf{T}_{s2}$, 5 repetitions of each motion type.
- Day 3: Training dataset, $\mathbf{T}_{r3}$, 2 repetitions of each motion type. Testing dataset, $\mathbf{T}_{s3}$, 5 repetitions of each motion type.

On each day a new set of electrodes were used and to maintain the consistent places, electrodes placement was marked each day. In the case of FMG, the FSR sensors were not replaced, however, the placement of the sensor bands were marked every day so that they could be placed at the same spot. Markers were also placed on the sensor band in order to achieve similar tightness.

Furthermore, for sEMG signals, a digital high pass filter of 30 Hz was applied to remove the DC offset. Whereas, FMG was passed through a low pass filter of 100 Hz to remove high-frequency noise. FMG data was also calibrated to zero for rest condition each day. The raw data collected for both methods, i.e. FMG and sEMG, is shown in Figure 4.

Signal processing and feature extraction

In further post-processing, five time-domain features were extracted from sEMG i.e. mean absolute value, waveform length, zero crossing, slope sign changes and wilson amplitude. Time domain features have been widely used for their classification performance and low computational complexity.[44] Moreover, these features have been reported in other classification studies[41–43] as well.

In the case of FMG, four time-domain features were extracted i.e. root mean square, slope, mean-mode difference and slope sign count, presented in Table 1. Within these features RMS is a generally used[33,42] feature to obtain the average signal amplitude. Whereas, slope, mean-mode difference and slope sign count are used to compute the direction and change in signal amplitude w.r.t time.

Prior to feature extraction, FSR sensors data from upper arm sensor band was summed together and used as a single input. Similarly, FSRs data from forearm sensor band was also summed together. Furthermore, a window size of 150 ms with an overlapping window of 50 ms was used for feature extraction and Neural Network (NN) was implemented to perform the classification. In the NN setup number of hidden layers and neurons were selected according to the rules defined in Heaton.[45] Single hidden layer with 7 neurons and 10 neurons were used for training FMG and sEMG based classifiers, respectively. Maximum iteration limit in both cases was set to 10000.

Experiments

Five able-bodied male subjects took part in the experiments. All of them were healthy, right-handed and their ages were in the range of 27-35 years. Moreover, all of them were provided written informed consent prior to participation. Ethical approval to conduct these experiments was obtained from ethical committee, Region Nordjylland, Denmark.

Testing scenarios

The primary focus of this study was to investigate FMG and sEMG based NN classifiers for classifying forearm motions. The classifiers were tested on all three testing datasets ($\mathbf{T}_{s1}$, $\mathbf{T}_{s2}$ and $\mathbf{T}_{s3}$) after being trained

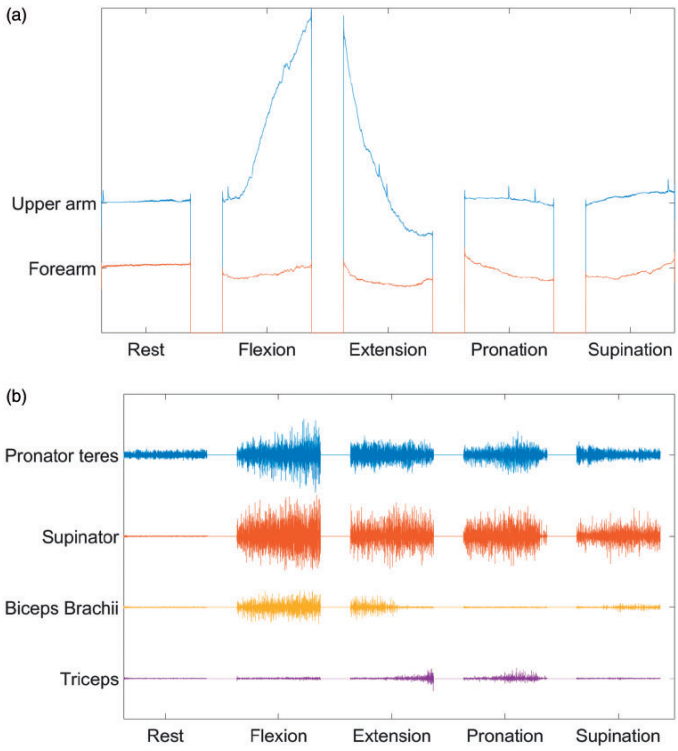

Figure 4. Raw data obtained with (a) FMG and (b) sEMG.

Table 1. Features extracted from FMG raw data. **x** represents the vector containing raw data, t_{win} is the window time for features extraction, N is the number of samples collected in 150 ms window and ϵ is the threshold limit determined by rest state data.

Feature	Expression
Root mean square	$\sqrt{\frac{1}{N}\sum_{i=1}^{N} x_i^2}$
Slope	$\frac{RMS_j - RMS_{j-1}}{t_{win}}$
mean-mode difference	$\frac{1}{N}\sum_{i=1}^{N} x_i - mode(\mathbf{x})$
Slope sign count	$\sum_{i=2} f(x_i - x_{i-1})$
	$f(x) = \begin{cases} 0 & \lvert f(x)\rvert \le \epsilon \\ 1 & f(x) > \epsilon \\ -1 & f(x) < -\epsilon \end{cases}$

with different combinations of training datasets, which leads to two tests. The details on classifier training for each test is described as following,

- Test A: In this test, the classifiers were tested after being trained only with Day 1 training dataset $\mathbf{T}_{r1}$. CA was separately computed for each testing dataset $\mathbf{T}_{s1}$, $\mathbf{T}_{s2}$ and $\mathbf{T}_{s3}$ referring to Day 1, 2 and 3 testing data, respectively. Afterward, statistical analysis were performed to investigate the consistency and repeatability of the classification methods.
- Test B: In this test, the classifiers were further evaluated by training them with multiple training datasets. The classifiers were first trained on training datasets $\mathbf{T}_{r1}$ and $\mathbf{T}_{r2}$ and then on training datasets $\mathbf{T}_{r1}$, $\mathbf{T}_{r2}$ and $\mathbf{T}_{r3}$. In both sessions, the classifiers were tested on testing datasets in the same way as in Test A. The purpose of this study was to investigate the

effect of including training data from additional days on CA.

Furthermore, tests were also performed to compare the CA with different techniques, i.e. support vector machine[35] (SVM), linear discriminant analysis[46] (LDA), k-nearnest neighbor[46] (KNN) and random forest[47] (RF), using training datasets $\mathbf{T}_{r1}$, $\mathbf{T}_{r2}$ and $\mathbf{T}_{r3}$.

Results

The results are displayed according to the tasks defined in the previous section.

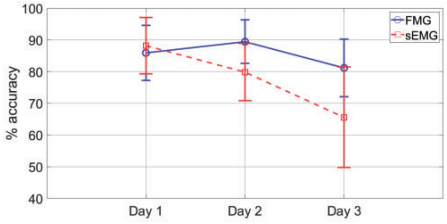

Figure 5. Average CA for training the classifier with $\mathbf{T}_{r1}$.

Test A

For both FMG and sEMG motion detection methods, CA was calculated over three days of testing data with the classifier trained on Day 1. The results of CA w.r.t each day are displayed graphically in Figure 5. An average CA of $85.9 \pm 8.64\%$ was obtained for FMG with the testing dataset $\mathbf{T}_{s1}$, whereas, for sEMG, average CA was $88.2 \pm 8.91\%$. With Day 2 testing dataset, $\mathbf{T}_{s2}$, an average CA of $89.4 \pm 6.87\%$ was obtained for FMG and $79.8 \pm 9.05\%$ for sEMG. With Day 3 testing dataset, $\mathbf{T}_{s3}$, FMG has an average CA of $81.2 \pm 9.07\%$, while sEMG has an CA of $65.6 \pm 15.84\%$. The average CA for each individual subject is shown in Figure 6.

The average CA over all three days was $84.9 \pm 3.36\%$ for FMG and $77.9 \pm 11.06\%$ for sEMG. If we look only at Day 1 performance, sEMG showed better results than FMG. However, it has to be noted that for the next two days the CA with sEMG is reduced by 25,6%. Kruskal-Wallis test also showed that the CA between days was significantly reduced ($p = 0.046$), which indicates that the data acquired was not repeatable. On the contrary, FMG accuracy of Day 1 testing was lower than sEMG, however, the average accuracy

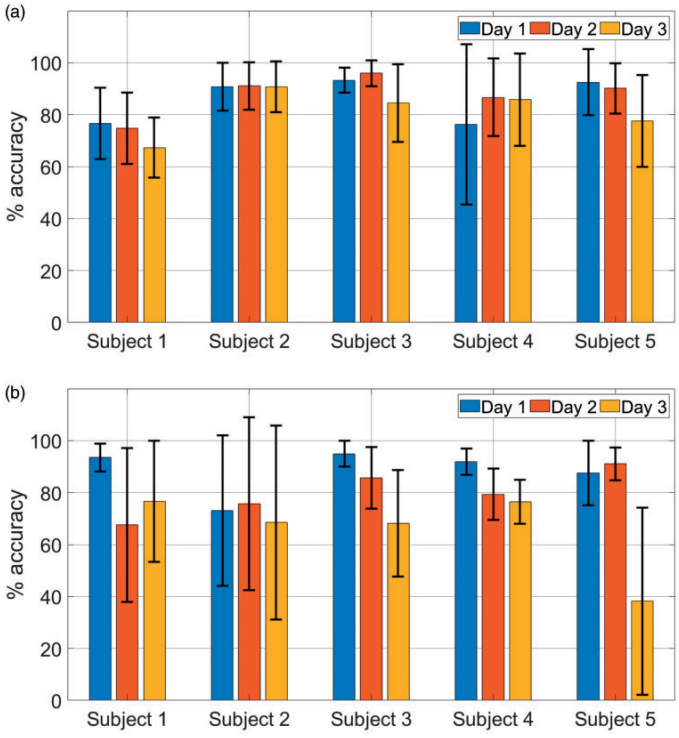

Figure 6. Average CA obtained for individual subjects, (a) with FMG and (b) with sEMG.

is only reduced by 5.5% in the next two days. There was also no significant difference observed between each day average accuracy ($p = 0.403$), which indicates that data acquired through FMG is comparatively more repeatable than sEMG.

Test B

The long-term performances of both FMG and sEMG were further analyzed by testing the datasets $\mathbf{T}_{s1}$, $\mathbf{T}_{s2}$ and $\mathbf{T}_{s3}$ using the classifiers trained with different training schemes. As the tests lasted for three days, we define three training schemes (TS):

1. TS_1: Training the classifiers using dataset $\mathbf{T}_{r1}$, same as Test A.
2. TS_2: Training the classifiers using datasets $\mathbf{T}_{r1}$ and $\mathbf{T}_{r2}$.
3. TS_3: Training the classifiers using datasets $\mathbf{T}_{r1}$, $\mathbf{T}_{r2}$ and $\mathbf{T}_{r3}$.

The results of CA with training scheme TS_2 are shown in Figure 7(b). When comparing the results with TS_1, it can be seen that the CA in the case of FMG was improved for Day 2 by 3.1% and Day 3 by 2.6%. In the case of sEMG, CA only improved for Day 2 by 2.2%. However, the change in CA for both methods, FMG (p-value = 0.917) and sEMG (p-value = 0.917), was not significant.

The results of CA with training scheme TS_3 are shown in Figure 7(c). The results show that the CA obtained through FMG only improved for Day 3 by 1.4% when compared with the results obtained through TS_2. In comparison to TS_1, the CA was increased for Day 2 by 2.2% and Day 3 by 4%. However, the Kruskal-Wallis test indicated that the change in CA occurred between all three training scenarios was not significant (p-value = 0.97). Whereas, in the case of sEMG, the CA was significantly improved. When compared with TS_2 the CA was increased for all three days, Day 1, 2 and 3, by 2.2%, 3.1%, and 17.8%, respectively. Moreover, in comparison to TS_1 the CA for Day 2 and Day 3 were increased by 5.3% and 16%, respectively. The increase in CA was also observed from the Kruskal-Wallis test. The p-value of 0.049 was obtained, which indicates the increase in CA was significant.

The average CA obtained for each training scheme is shown in Figure 8 and summarized in Table 2. It is noted that the repeatability in Table 2 represents the percentage of CA decrease from Day 1 to Day 3 w.r.t Day 1. In the case of FMG, the average CA slightly

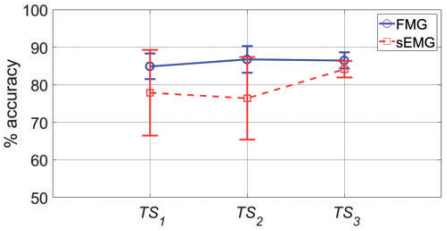

Figure 8. Average CA for three training schemes.

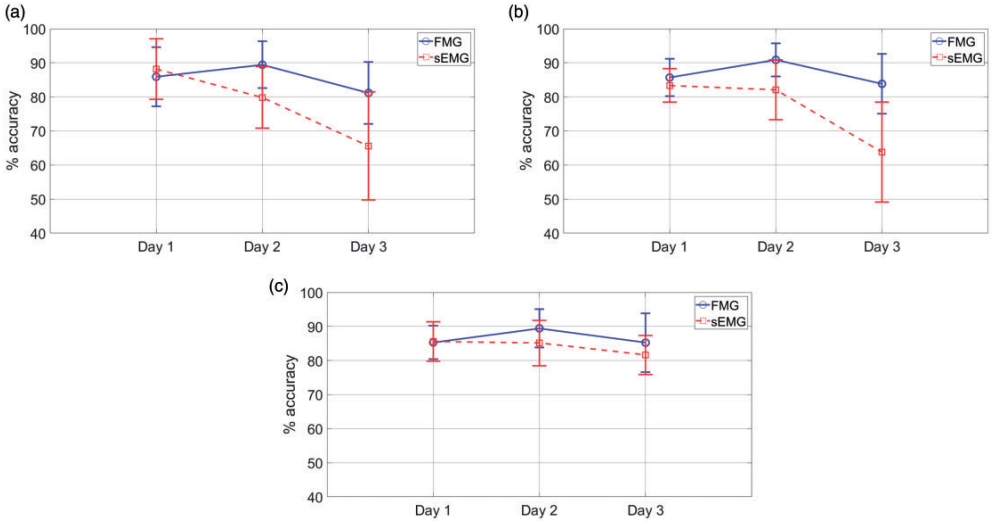

Figure 7. Day-to-Day CA with training schemes (a) TS_1, (b) TS_2, and (c) TS_3.

increases from TS_1 to TS_2 but decrease from TS_2 to TS_3. Whereas, in the case of sEMG, the CA slightly decreases from TS_1 to TS_2, but increased significantly from TS_2 to TS_3 by 7.7%. However, repeatability results showed a similar pattern for both methods. The difference in CA between Day 1 and Day 3 decreased from TS_1 to TS_3. Although both methods showed a similar pattern in repeatability, FMG has a better performance than sEMG in both aspects i.e. CA and repeatability.

Figure 9 shows the results for each individual subject. The CA results obtained with FMG are shown in Figure 9(a). It can be seen that a significant increase in CA was only observed for subject 4, which was 5.07%. However, in the case of sEMG (Figure 9(b)), CA was improved by 3.9%, 10.18%, 5.78% and 11.69% for subjects 1, 2, 3 and 5, respectively.

Table 2. CA and repeatability achieved through FMG and sEMG.

Training scheme	FMG		sEMG	
	% CA	Repeatability	% CA	Repeatability
TS_1	84.9	5.5	77.9	25.6
TS_2	86.8	2.2	76.4	23.5
TS_3	86.5	0.1	84.1	4.7

Classification techniques comparison

In this experiment performances of five different classification techniques were compared i.e. SVM, LDA, KNN, RF and NN. Results of this experiment are shown in Figure 10.

It can be seen that LDA has the lowest performance for both FMG and sEMG. Whereas, highest CA is achieved using NN approach. However, In case of FMG, Figure 10(a), the performances of NN and RF are comparable, accuracy obtained through RF being only 0.3% less than NN.

Discussion

This study was aimed to investigate the accuracy of classifying forearm motions using FMG and sEMG based classifiers. The study addresses the day-to-day performance of both methods. Results have shown that FMG ($84.9 \pm 3.38\%$) performed better than sEMG ($77.9 \pm 11.43\%$). Another noticeable result is that the FMG method is more stable than sEMG. Our results show that the CA with FMG method was nearly the same for all three days for the classifier

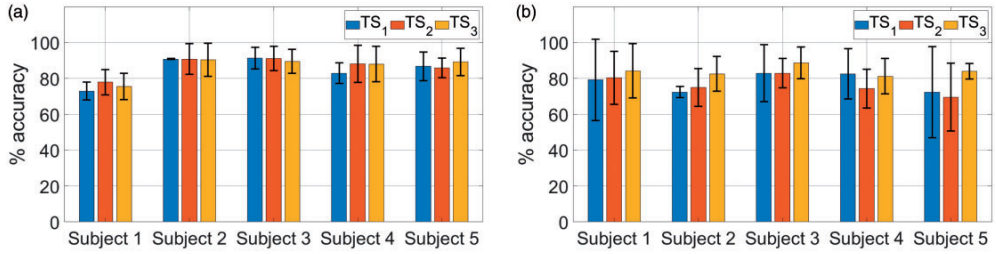

Figure 9. Within days average CA for each training scenario and each individual subject for, (a) FMG, (b) sEMG.

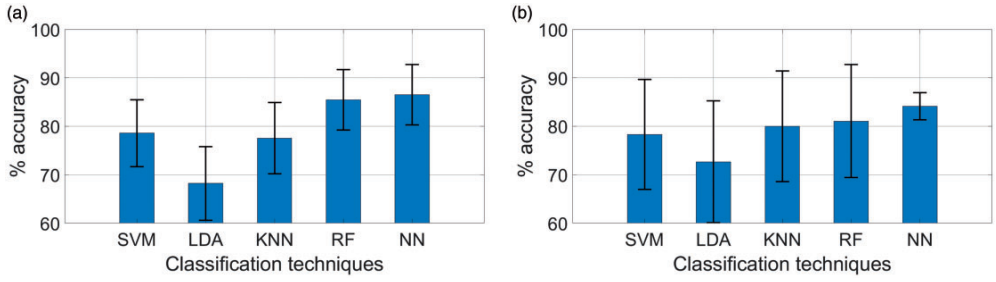

Figure 10. Results of different classification techniques, (a) FMG, (b) sEMG.

trained on the first day. On the other hand, the CA obtained through sEMG was better on the first day, but significantly decreased for the rest of the two days, when the classifier was only trained on the first day.

Our study also showed that retraining the classifier each day didn't cause significant improvement in CA for FMG. On the other hand, a significant increase in CA was observed for sEMG. The performances for both methods (FMG and sEMG) were comparable. FMG yielded the average CA of $86.5 \pm 2.11\%$ and sEMG yielded the CA of $84.1 \pm 2.18\%$. It can be noticed that only 1.6% increase in CA is found for FMG, which again implies that the data recorded through FMG was consistent. Therefore, the inclusion of additional training dataset in retraining the classifier didn't improve the average accuracy for FMG as much as it improved in case of sEMG, which is 7.63%.

The results obtained in this study comply with the studies reported in literature,[40,41] where it was reported that FMG performed better then sEMG for classifying hand gestures and estimating fingers force. It is noted that those studies were carried out for one day only, while day-to-day performances were not considered.

In this study, four FMG features were used to predict the movements. Through experiments it was observed that slope had the highest contribution in the CA, whereas mean-mode difference had the lowest contribution. With the results obtained, CA can be further increased by applying weight to the existing features or introducing more features in the classifier. In future studies, each sensor output will be considered separately. On the other hand, only two repetitions were used to retrain the classifiers. More repetitions can also affect the CA of both methods. Moreover, the performance comparison in this work was conducted on healthy young subjects, so the results are not generally applicable to motion detection of humans of all ages and physical conditions.

Conclusions

In this study, the performances of FMG and sEMG were investigated for classifying forearm flexion, extension, pronation, supination and rest state. CA and repeatability of these methods were analyzed for motion identification testing over a period of three days under different training schemes.

The results show that the accuracy obtained through FMG was less affected by the time difference between training and testing day. The results indicate that the performance was consistent and repeatable. However, CA obtained through sEMG was significantly affected by the time difference. The decrease in CA was gradual and significant. The improvement in CA and repeatability was observed when the classifiers were retrained each day. Whereas, CA with FMG didn't show significant improvement using retraining approach, which indicates that the data obtained through FMG is comparatively more repeatable.

Our testing results on CA and repeatability indicate that FMG is more suited than sEMG for assistive exoskeleton applications, which are designed for ADL activities. As using exoskeletons on a daily basis user might take the exoskeleton on and off several times, a requirement of retraining makes it less acceptable to end-user. Whereas, sEMG requires retraining to achieve repeatable performance and therefore it is more suited for rehabilitation applications, where the primary focus is on acquiring muscle activity for monitoring and analysis purpose.

Acknowledgements

The authors would like to thank participants for the contribution of time to this study.

Declaration of conflicting interests

The author(s) declared no potential conflicts of interest with respect to the research, authorship, and/or publication of this article.

Funding

The author(s) disclosed receipt of the following financial support for the research, authorship, and/or publication of this article: This work was supported by AAL Programme's funding bodies for project AXO-SUIT (http://www.axo-suit.eu/) and Innovation Fund Denmark for project EXO-AIDER (https://www.exo-aider.dk).

Guarantor

MR.

Contributorship

MR and SB defined and developed this research work. MR and AW prepared initial protocol draft, collected data and performed analysis. EN and SB were involved in getting ethical approval and protocol finalization. MR and AW wrote the first draft of the manuscript. All authors reviewed the manuscript and approved the final version.

Research ethics and participants consent

Ethical approval to conduct this study was obtained from ethical committee, Region Nordjylland, Denmark. Also, all participants provided written informed consent prior to experiments.

ORCID iD

Muhammad Raza Ul Islam https://orcid.org/0000-0001-7020-7451

References

1. Cheng S, Yang Y, Cheng F, et al. The changes of muscle strength and functional activities during aging in male and female populations. *Int J Gerontol* 2014; 8: 197–202.
2. Bai S, Christensen S, Islam M, et al. Development and testing of full-body exoskeleton AXO-SUIT for physical assistance of the elderly. In: *International symposium on wearable robotics,* 2018, pp. 180–184, Springer.
3. Lo HS and Xie SQ. Exoskeleton robots for upper-limb rehabilitation: state of the art and future prospects. *Med Eng Phys* 2012; 34: 261–268.
4. Veale AJ and Xie SQ. Towards compliant and wearable robotic orthoses: a review of current and emerging actuator technologies. *Med Eng Phys* 2016; 38: 317–325.
5. Zhou L, Li Y and Bai S. A human-centered design optimization approach for robotic exoskeletons through biomechanical simulation. *Robot Autonom Syst* 2017; 91: 337–347.
6. Viteckova S, Kutilek P and Jirina M. Wearable lower limb robotics: a review. *Biocybernet Biomed Eng* 2013; 33: 96–105.
7. Mukhopadhyay SC. Wearable sensors for human activity monitoring: a review. *IEEE Sensors J* 2015; 15: 1321–1330.
8. Liu HJ and Young KY. Upper-limb EMG-based robot motion governing using empirical mode decomposition and adaptive neural fuzzy inference system. *J Intell Robot Syst* 2012; 68: 275–291.
9. Liu H and Young K. Robot motion governing using upper limb EMG signal based on empirical mode decomposition. In: *IEEE International Conference Systems Man and Cybernetics*, 2010, pp. 441–446. Piscataway, NJ: IEEE.
10. Yang D, Jiang L, Huang Q, et al. Experimental study of an EMG-controlled 5-DOF anthropomorphic prosthetic hand for motion restoration. *J Intell Robot Syst* 2014; 76: 427–441.
11. Wang J and Wichakool W. Artificial elbow joint classification using upper arm based on surface-EMG signal. In: *3rd IEEE International Conference on Engineering Technologies and Social Sciences*, 2017, pp. 1–4. Piscataway, NJ: IEEE.
12. Kundu AS, Mazumder O, Lenka PK, et al. Hand gesture recognition based omnidirectional wheelchair control using IMU and EMG sensors. *J Intell Robot Syst* 2018; 91: 529–541.
13. Zhang Q, Zheng C and Xiong C. EMG-based estimation of shoulder and elbow joint angles for intuitive myoelectric control. In: *International Conference on Cyber Technology in Automation, Control, and Intelligent Systems*, 2015, pp. 1912–1916, IEEE.
14. Liarokapis MV, Artemiadis PK, Katsiaris PT, et al. Learning human reach-to-grasp strategies: towards EMG-based control of robotic arm-hand systems. In: *IEEE International Conference on Robotics and Automation*, 2012, pp. 2287–2292. Piscataway, NJ: IEEE.
15. Jiang S, Lv B, Guo W, et al. Feasibility of wrist-worn, real-time hand, and surface gesture recognition via sEMG and IMU sensing. *IEEE Trans Ind Inf* 2018; 14: 3376–3385.
16. Al-Faiz MZ, Ali AA and Miry AH. A k-nearest neighbor based algorithm for human arm movements recognition using EMG signals. In: *1st International Conference Energy, Power and Control*, 2010, pp. 159–167, IEEE.
17. Leonardis D, Barsotti M, Loconsole C, et al. An EMG-controlled robotic hand exoskeleton for bilateral rehabilitation. *IEEE Trans Haptics* 2015; 8: 140–151.
18. Bouteraa Y, Abdallah IB and Elmogy AM. Training of hand rehabilitation using low cost exoskeleton and vision-based game interface. *J Intell Robot Syst* 2019; 96: 31–47.
19. Kiguchi K and Imada Y. EMG-based control for lower-limb power-assist exoskeletons. In: *IEEE workshop robotic intelligence in informationally structured space,* 2009, pp. 19–24. Piscataway, NJ: IEEE.
20. Chen D, Ning M, Zhang B, et al. Control strategy of the lower-limb exoskeleton based on the EMG signals. In: *IEEE Conference on Robotics and Biomimetics,* 2014, pp. 2416–2420. Piscataway, NJ: IEEE.
21. Kiguchi K, Rahman MH, Sasaki M, et al. Development of a 3DOF mobile exoskeleton robot for human upper-limb motion assist. *Robot Autonom Syst* 2008; 56: 678–691.
22. Lu L, Wu Q, Chen X, et al. Development of a sEMG-based torque estimation control strategy for a soft elbow exoskeleton. *Robot Autonom Syst* 2019; 111: 88–98.
23. He J, Zhang D, Jiang N, et al. User adaptation in long-term, open-loop myoelectric training: implications for EMG pattern recognition in prosthesis control. *J Neural Eng* 2015; 12. DOI:10.1088/1741-2560/12/4/046005.
24. Waris A, Niazi I, Jamil M, et al. The effect of time on EMG classification of hand motions in able-bodied and transradial amputees. *J Electromyogr Kinesiol* 2018; 40: 72–80.
25. Kaufmann P, Englehart K and Platzner M. Fluctuating EMG signals: investigating long-term effects of pattern matching algorithms. *2010 Annual International Conference of the IEEE Engineering in Medicine and Biology, IEEE*, 2010, pp. 6357–6360.
26. Amsuss S, Goebel PM, Jiang N, et al. Self-correcting pattern recognition system of surface EMG signals for upper limb prosthesis control. *IEEE Trans Biomed Eng* 2014; 61: 1167–1176.
27. Islam MRU, Xu K and Bai S. Position sensing and control with FMG sensors for exoskeleton physical assistance. In: *International Symposium on Wearable Robotics,* 2018, pp. 3–7, Springer.
28. Islam MRU and Bai S. Intention detection for dexterous human arm motion with FSR sensor bands. In: *Proceedings of the Companion of the ACM/IEEE*

International Conference on Human-Robot Interaction, 2017, pp. 139–140, ACM.
29. Islam MRU and Bai S. Payload estimation using force-myography sensors for control of upper-body exoskeleton in load carrying assistance. *Model Identif Control* 2019; 40: 189–198.
30. Shull PB, Jiang S, Zhu Y, et al. Hand gesture recognition and finger angle estimation via wrist-worn modified barometric pressure sensing. *IEEE Trans Neural Syst Rehabil Eng* 2019; 27: 724–732.
31. Sakr M and Menon C. Study on the force myography sensors placement for robust hand force estimation. In: *IEEE International Conference on Systems, Man, and Cybernetics*, 2017, pp. 1387–1392. Piscataway, NJ: IEEE.
32. Jiang X, Merhi LK and Menon C. Force exertion affects grasp classification using force myography. *IEEE Trans Human-Mach Syst* 2018; 48: 219–226.
33. Sadarangani GP and Menon C. A preliminary investigation on the utility of temporal features of force myography in the two-class problem of grasp vs. no-grasp in the presence of upper-extremity movements. *Biomed Eng Online* 2017; 16. DOI:10.1186/s12938-017-0349-4.
34. Wininger M, Kim NH and Craelius W. Pressure signature of forearm as predictor of grip force. *J Rehabil Res Dev* 2008; 45: 883–892.
35. Li N, Yang D, Jiang L, et al. Combined use of FSR sensor array and SVM classifier for finger motion recognition based on pressure distribution map. *J Bionic Eng* 2012; 9: 39–47.
36. Castellini C and Ravindra V. A wearable low-cost device based upon force-sensing resistors to detect single-finger forces. In: *IEEE RAS & EMBS International Conference on Biomedical Robotics and Biomechatronics*, 2014, pp. 199–203. Piscataway, NJ: IEEE.
37. Jiang X, Chu HT, Xiao ZG, et al. Ankle positions classification using force myography: an exploratory investigation. In: *IEEE Healthcare Innovation Point-Of-Care Technologies*, 2016, pp. 29–32. Piscataway, NJ: IEEE.
38. Cho E, Chen R, Merhi LK, et al. Force myography to control robotic upper extremity prostheses: a feasibility study. *Front Bioeng Biotechnol* 2016; 4: 18.
39. Sadarangani GP, Jiang X, Simpson LA, et al. Force myography for monitoring grasping in individuals with stroke with mild to moderate upper-extremity impairments: a preliminary investigation in a controlled environment. *Front Bioeng Biotechnol* 2017; 5. DOI:10.3389/fbioe.2017.00042.
40. Ravindra V and Castellini C. A comparative analysis of three non-invasive human-machine interfaces for the disabled. *Front Neurorobot* 2014; 8: 24.
41. Jiang X, Merhi LK, Xiao ZG, et al. Exploration of force myography and surface electromyography in hand gesture classification. *Med Eng Phys* 2017; 41: 63–73.
42. Xiao ZG and Menon C. Performance of forearm FMG and sEMG for estimating elbow, forearm and wrist positions. *J Bionic Eng* 2017; 14: 284–295.
43. Jiang S, Gao Q, Liu H, et al. A novel, co-located EMG-FMG-sensing wearable armband for hand gesture recognition. *Sensor Actuat A Phys* 2020; 301: 111738.
44. Phinyomark A, Franck Q, Sylvie C, et al. EMG feature evaluation for improving myoelectric pattern recognition robustness. *Expert Syst Appl* 2013; 40: 4832–4840.
45. Heaton J. *Introduction to neural networks with java*. Chesterfield, MI: Heaton Research Inc., 2008.
46. Kim KS, Choi HH, Moon CS, et al. Comparison of k-nearest neighbor, quadratic discriminant and linear discriminant analysis in classification of electromyogram signals based on the wrist-motion directions. *Curr Appl Phys* 2011; 11: 740–745.
47. Su R, Chen X, Cao S, et al. Random forest-based recognition of isolated sign language subwords using data from accelerometers and surface electromyographic sensors. *Sensors* 2016; 16. DOI:10.3390/s16010: 100.

Chapter 4

Paper II

Effective multi-mode grasping assistance control of a soft hand exoskeleton using force myography

Muhammad Raza Ul Islam and Shaoping Bai

The paper has been published in the
Frontiers in Robotics and AI, vol. 7, pp. 1–14, 2020.
doi.org/10.3389/frobt.2020.567491

frontiers in Robotics and AI

ORIGINAL RESEARCH
published: 16 November 2020
doi: 10.3389/frobt.2020.567491

Effective Multi-Mode Grasping Assistance Control of a Soft Hand Exoskeleton Using Force Myography

*Muhammad Raza Ul Islam and Shaoping Bai**

Department of Materials and Production, Aalborg University, Aalborg, Denmark

Human intention detection is fundamental to the control of robotic devices in order to assist humans according to their needs. This paper presents a novel approach for detecting hand motion intention, i.e., rest, open, close, and grasp, and grasping force estimation using force myography (FMG). The output is further used to control a soft hand exoskeleton called an SEM Glove. In this method, two sensor bands constructed using force sensing resistor (FSR) sensors are utilized to detect hand motion states and muscle activities. Upon placing both bands on an arm, the sensors can measure normal forces caused by muscle contraction/relaxation. Afterwards, the sensor data is processed, and hand motions are identified through a threshold-based classification method. The developed method has been tested on human subjects for object-grasping tasks. The results show that the developed method can detect hand motions accurately and to provide assistance w.r.t to the task requirement.

Keywords: human intention detection, FSR sensor band, exoskeleton control, grasping assistance, soft hand exoskeletons

OPEN ACCESS

Edited by:
Carlos A. Cifuentes,
Escuela Colombiana de Ingenieria
Julio Garavito, Colombia

Reviewed by:
Dongming Gan,
Purdue University, United States
Chaoyang Song,
Southern University of Science and Technology, China

****Correspondence:***
Shaoping Bai
shb@mp.aau.dk

Specialty section:
This article was submitted to Biomedical Robotics, a section of the journal Frontiers in Robotics and AI

Received: *02 June 2020*
Accepted: *04 September 2020*
Published: *16 November 2020*

Citation:
Islam MRU and Bai S (2020) Effective Multi-Mode Grasping Assistance Control of a Soft Hand Exoskeleton Using Force Myography. Front. Robot. AI 7:567491. doi: 10.3389/frobt.2020.567491

1. INTRODUCTION

Grasping tasks are performed repeatedly in both the home and in workplaces. Studies have shown that a human in a work/home environment performs grasp and transition between different grasps approximately 4,700 times within a 7.45 h window (Zheng et al., 2011; Bullock et al., 2013). Performing these tasks repeatedly over a longer period of time can cause fatigue and injuries. Hand exoskeletons (Gull et al., 2020) have the capability to assist in these tasks, which can reduce human effort and the risk of getting injured/fatigued.

Proper control of the exoskeleton depends mainly on accurate human intention detection. Several methods to determine human intention that are based on electromyography (EMG) (Anam et al., 2017; Meng et al., 2017; Pinzón-Arenas et al., 2019; Qi et al., 2019; Zhang et al., 2019; Asif et al., 2020) and force myography (FMG) (Islam and Bai, 2019; Xiao and Menon, 2019, 2020) have been proposed. Leonardis et al. (2015) used EMG to control a hand exoskeleton for bilateral rehabilitation. Here, a paretic hand was provided with grasping assistance by estimating the grasping force of the non-paretic hand. In another work (Lu et al., 2019), pattern-recognition-based hand exoskeleton control was proposed for spinal cord injury patients. An FMG-based hand gesture classification method was proposed to control a hand prosthetic device in Cho et al. (2016). In total, 10 hand grips were classified using a linear discriminant analysis technique. A high-density force myography-based hand and wrist gesture classification approach was proposed by Radmand et al. (2016). It was shown that for static hand postures 0.33% RMSE is achieved. While variation in upper limb position reduces the accuracy, better performance can be achieved by introducing

limb position variation in training protocol. Several other works on force estimation and pattern-recognition-based hand exoskeleton control have also been reported (Wege and Zimmermann, 2007; Rasouli et al., 2016; Ferigo et al., 2017; Secciani et al., 2019; Arteaga et al., 2020).

In all of the reported works, methods to control a hand exoskeleton are limited to either pattern recognition or force estimation. Furthermore, in these methods machine learning and deep leaning techniques are used that requires large training datasets to achieve good classification/estimation accuracy.

In this work we develop a new sensing method for both pattern recognition and force estimation using FMG. A multi-mode task detection approach, i.e., motion classification and grasp force estimation, is proposed for controlling a hand exoskeleton. In this method, four hand motion states are classified i.e., rest, open, close, and grasp. The classification algorithm is based on threshold approach and requires a small training dataset. Once the grasp is detected, the control mode is switched to grasp assistance. This is achieved by virtue of two sensor bands built with FSRs, which can detect muscle activities conveniently and effectively. In terms of its sensing method, FMG has exhibited a better performance than EMG in classification and estimation tasks considering accuracy, repeatability, and cost (Ravindra and Castellini, 2014; Jiang et al., 2017). Moreover, unlike EMG, FMG is not affected by skin conditions and has a simple electronics interface.

This paper is organized as follows. The design and implementation of the sensor band and exoskeleton control strategy are described in section 2. Section 3 presents the data processing and algorithm design for grasp detection and assistance. Experimental setup and testing results are described in section 4. Discussion on the developed method is presented in section 5. The work is concluded in section 6.

2. MATERIALS AND METHODS

In this section, a methodology to detect hand motions i.e., rest, open, close, and grasp is described. Sensor bands, a hand exoskeleton, and control methods are also presented.

2.1. Methodology

In this work, four hand motion states are classified, i.e., rest, open, close, and grasp. The last three motion states are classified as dynamic states, whereas rest is identified as a static hand state in any posture, e.g., keeping the hand fully opened/closed or holding an object in a fixed posture.

In object grasping, fingers have to be flexed. During flexion, the muscle belly shortens in length and contracts toward the side of the elbow joint, which is referred as isotonic muscle contraction. As the object comes into contact with the hand, muscle shortening stops, and an isometric contraction state is initiated. In this state the muscle belly along the forearm contracts as long as the force applied to hold an object reaches the steady state.

In this work contraction states and the transition between them, i.e., isotonic and isometric, are measured through FMG, using sensor bands built with FSR sensors. In this method, normal forces caused by muscle contraction and applied to the sensor band, hereafter called muscle contraction-induced (MCI) force, are measured. Flexor digitorum profundus and flexor digitorum superficialis are the prime muscles that govern fingers flexion to close the hand. During hand closing movement, the length of these muscle shortens and they contract toward elbow joint. MCI force near the elbow will therefore increase, while it will decrease near the wrist joint. As soon as the object is grasped, muscles stop shortening and isometric contraction takes over. In this case, MCI forces over the muscle belly will increase. This principle can be expanded further to explain hand opening task. In hand opening the object is ungrasped, MCI force on both ends of the forearm will decrease. On the other hand, as the object is released and the fingers are further extended, MCI force measured near the elbow will decrease, while the force measured near wrist will increase. From these changes of MCI force, hand motion states can be determined with certain algorithms.

2.2. Sensor Band

The aforementioned hand motion detection relies on an effective and convenient method to detect MCI forces. To this end, two sensor bands are constructed at Aalborg University exoskeleton lab, as shown in **Figure 1A**.

The sensor bands are designed to be placed on the forearm, as shown in **Figure 1B**. One is placed near the elbow joint. This band, referred to as SB_e, is comprised of eight FSR sensors. The other band is placed near wrist joint, referred to as SB_w, which has an array of four FSR sensors embedded. The placements of FSR sensors inside the sensor bands are shown in **Figure 1A**. All FSR sensors are FSR-402, developed by Interlink electronics, and have the capability of measuring 0.1–10 N. More information on the construction of sensor bands can be found in Islam and Bai (2019).

2.3. SEM Glove

In this work a soft hand exoskeleton SEM Glove (Nilsson et al., 2012; Hashida et al., 2019) is used to provide physical grasping assistance, as shown in **Figure 1B**. The SEM Glove is equipped with FSR sensors placed at the middle and index fingertips and at the thumb. The assistance provided by the exoskeleton can be measured by these sensors. Moreover, in the SEM Glove's own control unit, the assistance level is also controlled using the same sensor data. The tighter the object is grasped the higher the assistance level will be. In this work, the assistance level provided by SEM Glove is controlled through MCI force measured by the sensor band placed near elbow joint instead of using the SEM Glove's own sensors.

2.4. Sensing Data

The sensor bands allow us to collect hand motion data effectively. An example of a dataset of rest, open, close, and grasp, labeled as "R," "O," "C," and "G," respectively, is shown in **Figure 2**. Isotonic contraction during opening and closing of hand can be seen in **Figure 2A**. **Figure 2B** shows the data of an object being grasped

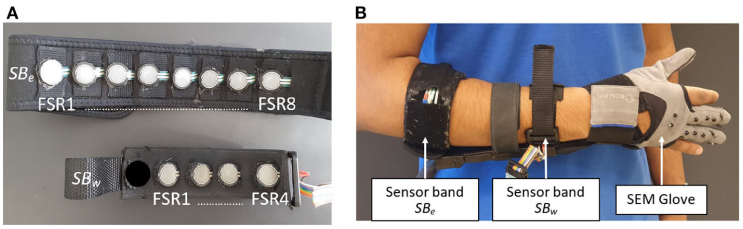

FIGURE 1 | (A) FSR sensors placement inside sensor bands SB_w and SB_e and **(B)** SEM Glove and sensor bands placement on forearm.

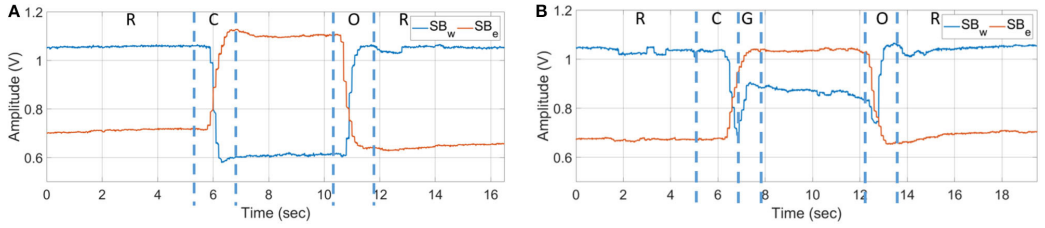

FIGURE 2 | Net output voltage measured from sensor bands for opening and closing of hand **(A)** without grasping and **(B)** grasping an object.

when isometric contraction occurs. The state when the object is grasped is labeled as "G."

In the hand opening task, shown in **Figure 2B**, it can be seen the sensor amplitude first goes down. This muscle activity represents loosening of grip on the object. Afterwards, increase in muscle activity at SB_w and decrease in muscle activity at SB_e are observed, which represents fingers extension to open the hand. In the implementation phase, loosening of grip is treated as a steady state.

2.5. Multi-Mode Control

In this work, a multi-mode control approach is used to assist in grasping, which is shown in **Figure 3**.

The control strategy is divided into two stages i.e., motion classification and grasp force assistance. Motion classification is based on a threshold approach. Out of four actions, i.e., rest, open, close, and grasp, once the algorithm identifies grasp action, the control mode is shifted to grasp force assistance. In this mode a proportional control is implemented, where the assistance force is determined using MCI force measured through SB_e.

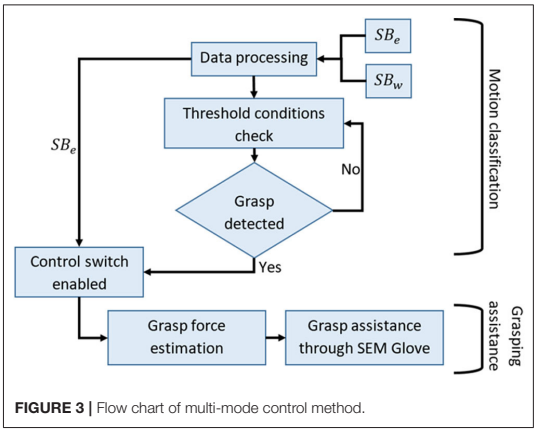

FIGURE 3 | Flow chart of multi-mode control method.

3. DATA PROCESSING

3.1. Sensor Calibration

The FSR sensors in the two sensor bands are interfaced with a non-inverting amplifier. The output voltage of the amplifier is thus given by the following equation:

$$V_{out} = (1 + \frac{R_{ref}}{R_{fsr}})V_{in} \quad (1)$$

Here, V_{out} is the output voltage of the amplifier, V_{in} is the input voltage applied to positive terminal of the amplifier, R_{ref} is the reference resistance, and R_{fsr} represents the FSR resistance, which varies with force applied on it.

With the amplifier designed, it is possible to change the range of force measured by FSR. This is done either by changing the reference resistance R_{ref} or input voltage V_{in}. In our design, the reference resistance is fixed to 100 *kohm*. We therefore adjust the input voltage V_{in} through a DAC port from micro-controller for this purpose, which is a task of sensor calibration.

FIGURE 4 | Gestures used in calibration and training stage. **(A)** open hand gesture to calibrate SB_w, **(B)** close hand gesture to calibrate SB_e, and **(C)** rest state gesture to collect data for threshold determination.

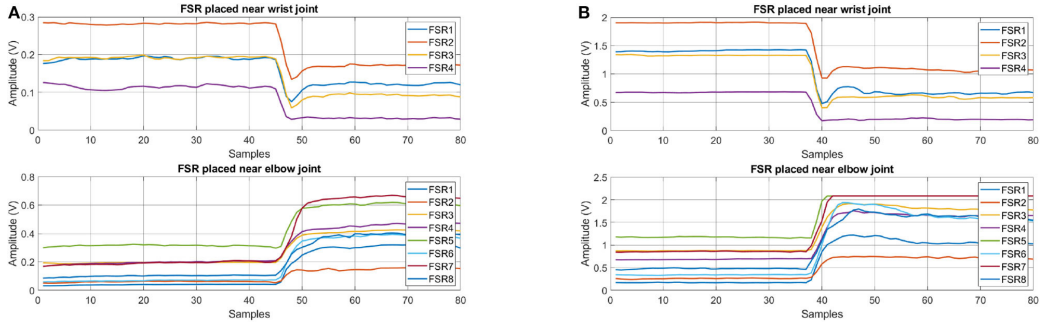

FIGURE 5 | FSR data for hand closing gesture **(A)** before and **(B)** after calibration.

In the calibration stage, input voltage V_{in} is adjusted so that at least three of the FSR sensors from both SB_e and SB_w have reached the maximum voltage limit. In this way, the sensor bands can have high resolution in all detections.

During calibration of SB_w, the subject is asked to keep the hand open, as shown in **Figure 4A**. This posture initiates the calibration procedure. An automated program checks the sensors outputs above threshold level. If the number is less than three, input voltage V_{in} is increased gradually until the condition is fulfilled, i.e., at least three sensors are above threshold limit. Similar procedure is followed for the calibration of SB_e but for the close hand gesture, as shown in **Figure 4B**, to complete the calibration. In the current setup it is set to 1.5 V.

An example dataset of the calibration stage is shown in **Figure 5**. This dataset represents the task of hand closing from fully opened state. **Figure 5A** is the dataset collected before calibration and **Figure 5B** is the dataset collected after calibration.

The improvement in signal resolution, ν, is computed by taking the ratio of change in signal amplitude, from open to close hand gesture, to the standard deviation of signal value during the steady state condition. Mathematically it is given as,

$$\nu = \frac{|\mu(V_O) - \mu(V_C)|}{\max(\sigma(V_O), \sigma(V_C))} \tag{2}$$

Here, V_O and V_C represent the net voltage measured from the sensor bands for open hand and close hand gestures respectively, and μ and σ are the mean and standard deviation respectively. The results obtained through aforementioned equation are provided in **Table 1**. The results clearly show that the resolution of both sensor bands is increased significantly, more than two times, after calibration.

TABLE 1 | Resolution measured before and after calibration.

Sensor band	Resolution ν		% increase
	Without calibration	With calibration	
SB_w	27.88	60.13	221
SB_e	27.94	61.74	222

3.2. Features Selection

While grasping an object, sensor readings highly depend on the shape and weight of the object. Moreover, donning and doffing of the sensor band also affects the sensor response. Developing a threshold- or machine-learning-based task-detection algorithm will require a large amount of data if the signal amplitude or it's RMS value is used as the input feature. It is noted that when a user takes off the sensor band and puts it back on, it is desirable that the sensor band has to be placed exactly at the same place and with the same tightness, but this is very challenging. All these factors will affect the classification performance.

With experiments, it is observed that the feature that gives consistent results with less deviation is slope. This feature

represents the change in signal amplitude w.r.t time. An example dataset of grasping different shape and weight objects is shown in **Figure 6**. A grasping dataset for each object is represented in 3s windows. From time 0 to 3, 3 to 6, and 6 to 9 s objects A, B, and C are grasped sequentially, as shown in **Figure 8**. From 9 to 18 s a dumbbell bar is grasped three times with different weight hanged on the sides of it. The weights of the dumbbells, applied from $t = 9$ to 12, 12 to 15, and 15 to 18 s were 1.2, 2.3, and 3.4 kg, respectively. Data sessions from 0 to 9 and from 9 to 18 s were recorded separately. It can be seen from **Figure 6A** that there is big variation in FSR reading, as it depends on the shape and weight of the object. However, if we look at the slope feature in **Figure 6B**, a similar pattern but with different peaks can be observed. Initially, fingers are flexed therefore we see opposite slopes for the FSR sensors placed near elbow and wrist joint. As soon as an object is grasped, positive slopes for both sensor bands are observed. By carefully selecting the threshold value, grasp action can be detected very effectively. In this work we therefore selected slope feature for detection of hand motion.

3.3. Features Extraction

Two features are extracted from raw sensor data, i.e., root mean square (RMS) and slopes. RMS from raw sensor data is obtained using a 150 ms window in which 100 ms is non-overlapping and 50 ms is overlapping from previous window. After calculating RMS values for each FSR sensor, slopes are obtained using the following equation:

$$\kappa = \frac{R^i - R^{i-1}}{t_{ws}} \tag{3}$$

Here, κ represents the slope feature, R^i represents the newest sample of RMS data, and t_{ws} is the window time to extract features.

3.4. Threshold Determination

In this method each state, i.e., rest, open, close, and grasp, is identified using a threshold-based classification approach. To determine the threshold limits, subject is asked to hold rest state, as shown in **Figure 4C**, for 5 s. Raw data obtained in this task is post processed to obtain slopes, which are further used to determine threshold limits.

After the computation of slope feature, the minimum and maximum slope value for each FSR was computed:

$$\xi_w^{max} = max(\Delta_w),\ \ \xi_w^{min} = min(\Delta_w) \tag{4}$$

$$\xi_e^{max} = max(\Delta_e),\ \ \xi_e^{min} = min(\Delta_e) \tag{5}$$

with

$$\Delta_w = [\kappa_w^1 \ldots \kappa_w^N],\ \ \Delta_e = [\kappa_e^1 \ldots \kappa_e^M] \tag{6}$$

Here, N and M are the numbers of FSR sensors embedded inside the sensor bands SB_w and SB_e, respectively. ξ_w^{min} and ξ_w^{max} are row matrices of order $1 \times N$ and contain minimum and maximum slope values of SB_w sensor band data computed for rest state. ξ_e^{min} and ξ_e^{max} are also row matrices of order $1 \times M$ and contain minimum and maximum slope values of SB_e sensor band data. Δ_w is a $I \times N$ matrix, where I is the number of slope feature samples computed from rest gesture data, and Δ_e is also a matrix but of $I \times M$ dimension.

Using (4) and (5), threshold conditions to detect each task are given as

$$H_R = \Delta_w^r <= k\xi_w^{max}\ \&\ \Delta_e^r <= k\xi_e^{max} \tag{7}$$

$$H_O = \Delta_w^r > k\xi_w^{max}\ \&\ \Delta_e^r < k\xi_e^{min} \tag{8}$$

$$H_C = \Delta_w^r < k\xi_w^{min}\ \&\ \Delta_e^r > k\xi_e^{max} \tag{9}$$

$$H_G = \Delta_w^r > k\xi_w^{max}\ \&\ \Delta_e^r > k\xi_e^{max} \tag{10}$$

Here, H_R, H_O, H_C, and H_G are the thresholds for rest, open, close, and grasp task detection. Δ_w^r and Δ_e^r are row matrices that are computed during real-time testing. The information in these matrices is in same order as in Δ_w and Δ_e.

3.5. Grasp Force Estimation

During the motion classification stage, if grasp action is detected, the control method is switched to grasp assistance. In this mode, we need to determine and control the grasp assistance provided by the SEM Glove. In this work, it is determined using the following equation:

$$u = (SB_e^{rms} - LB_e)K \tag{11}$$

Here, u is the control input relayed to the SEM Glove, K is the proportional gain and SB_e^{rms} is the net FSR output measured from the sensor band SB_e. LB_e is the net FSR output measured at the time of grasp detection and is given by following equation:

$$LB_e = mean(R_e^i, R_e^{i-1}) \tag{12}$$

Here, i is the sample when grasp action was detected, and $i - 1$ represents the sample before.

3.6. Performance Analysis

The performance of the task detection technique is analyzed with a group of four parameters, namely, precision, recall, F1-score, and accuracy (Powers, 2011). Mathematically, these parameters are calculated by

$$P_{\text{pre}} = \frac{N_{\text{TP}}}{N_{\text{TP}} + N_{\text{FP}}} \tag{13}$$

$$P_{\text{rec}} = \frac{N_{\text{TP}}}{N_{\text{TP}} + N_{\text{FN}}} \tag{14}$$

$$P_{\text{F1}} = 2 \cdot \frac{P_{\text{pre}} \cdot P_{\text{rec}}}{P_{\text{pre}} + P_{\text{rec}}} \tag{15}$$

$$P_{\text{acc}} = \frac{N_{\text{TP}} + N_{\text{TN}}}{N_{\text{TP}} + N_{\text{TN}} + N_{\text{FP}} + N_{\text{FN}}} \tag{16}$$

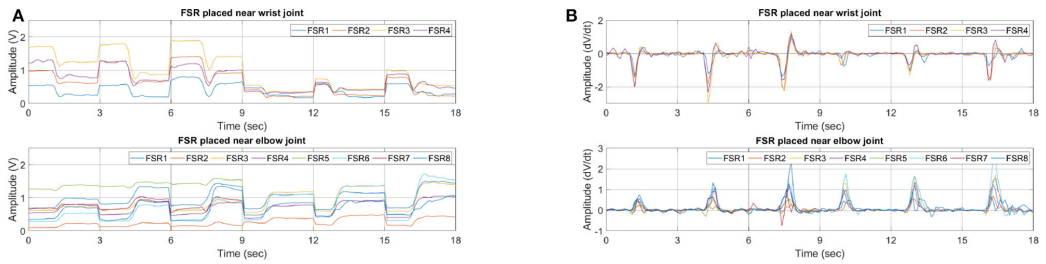

FIGURE 6 | FSR feature dataset for grasping objects of different sizes and weights. **(A)** RMS and **(B)** slope.

Predicted \ Actual	Class A	Other
Class A	TP	FP
Other	FN	TN

FIGURE 7 | Classification of TP, TN, FP, and FN samples.

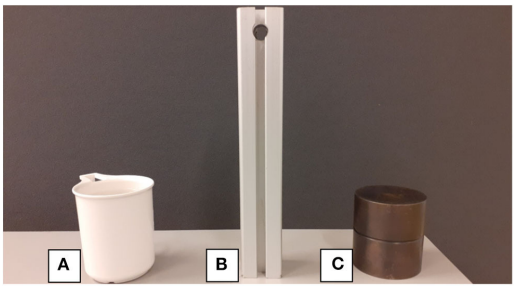

FIGURE 8 | Objects of different shape and weight that are grasped during task identification experiment, **(A)** empty cup, **(B)** aluminum bar, and **(C)** solid metal cylinder.

Here, N_{TP}, N_{TN}, N_{FP}, and N_{FN} represent number of samples that are true positive, true negative, false positive, and false negative, respectively, as illustrated in **Figure 7**. P_{pre}, P_{rec}, P_{F1}, and P_{acc} are the performance measures that represents precision, recall, F1-score, and accuracy, respectively. Of these measures, precision, recall, and F1-score are defined in the range of 0–1, whereas, accuracy is expressed in percentage.

Using these four parameters we can evaluate the classification performance comprehensively and in an unbiased manner. From mathematical representations, we can see that the fundamental difference between accuracy and other parameters is TN samples. In our designed experiment the number of samples in each class is not consistent. In such cases precision and recall can also provide very useful insight into classification performance. Taking the example of rest task, precision calculates from the total number of samples that are classified as rest how many were actually rest. Meanwhile, recall calculates, from the number of times a user was instructed to keep rest state, how many samples were correctly identified as rest state. Finally, the F1-score tells the balance between precision and recall.

4. EXPERIMENTS AND RESULTS

With the developed method, three experiments are performed, i.e., task identification, influence of sensor placement, and grasping assistance. Details and results of each task are provided in forthcoming sections.

4.1. Task Identification

Six subjects participated in this experiment. All of them were healthy, right-handed, and aged between 25 and 35 years. Ethical approval for these experiments was obtained from an ethical committee, Region Nordjylland, Denmark.

In this experiment, performance measures, i.e., precision, recall, F1-score, and accuracy, are computed to evaluate the classification performance. For this purpose, an experiment was designed where a subject performs hand opening and closing, first without any object and afterwards with three objects, as shown in **Figure 8**, of different attributes.

The protocol of the experiment is as follows: the subject is instructed to sit in a chair with their hands resting on the table beside the objects. The first task the subject performs is calibration, as explained in section 3.1, which is followed by a rest state gesture, as shown in **Figure 4C**, which is held for 5 s to determine the threshold limits. Afterwards, real-time testing tasks are performed in which, for open and close tasks, the subject lifts his/her hand from the table and keeps it in open state, as shown in **Figure 4A**. The subject closes his/her hand when the instruction is shown on the screen and opens it up when the instruction to open is shown on the screen again. The subject is instructed that an open hand posture should be maintained throughout the experiment. For the grasp task, hand is lifted from the table and kept open, as shown in **Figure 4A**. When the grasp instruction is shown on the screen, subject grasps the

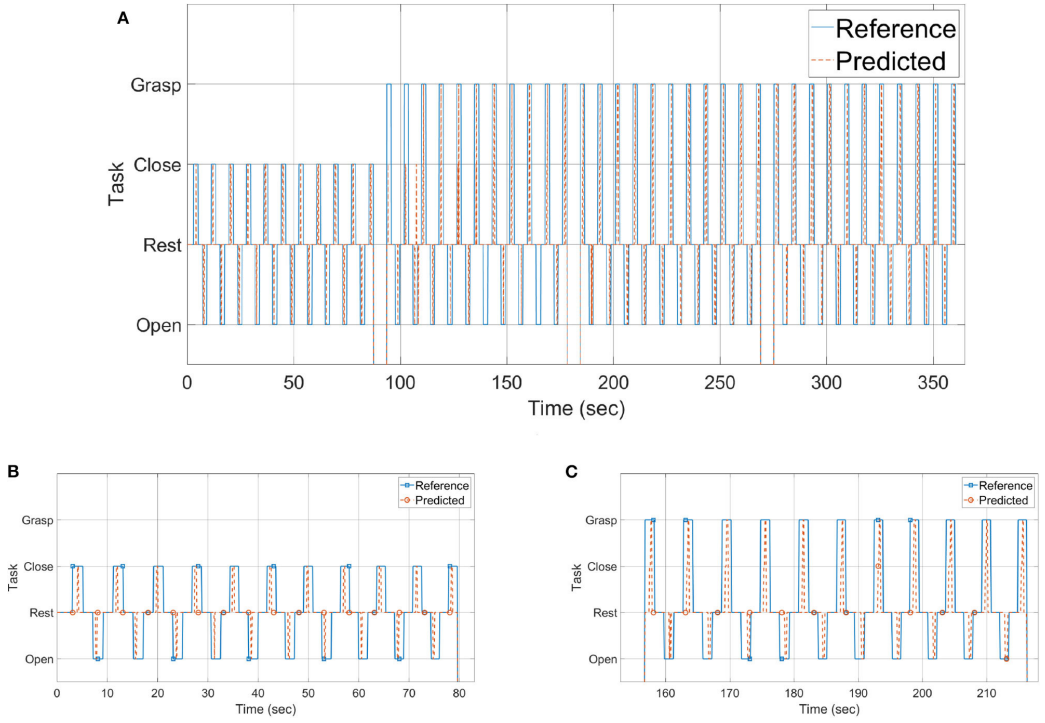

FIGURE 9 | Tasks performed during **(A)** the whole span of time, **(B)** opening and closing of the hand, and **(C)** grasping object B.

object and slightly lifts it from the table with a small clearance of approximately 1.0 cm.

The results of the experiment are shown in **Figures 9–12** and summarized in **Table 2**. **Figure 9** shows the experimental results for one of the subjects. **Figure 9A** shows the reference and predicted tasks. In the first 80 s of the experiment, the subject is instructed to perform the rest, open, and close tasks. From $t = 80$ to 155, $t = 155$ to 220, and $t = 220$ to 285 s, the subject is instructed to grasp objects A, B, and C sequentially. In this figure, the solid blue line shows the task to be performed and the dotted red line the result predicted by a classifier when a subject performs that particular task. A zoomed-in view of open and close tasks is shown in **Figure 9B** and of grasping task for object B is shown in **Figure 9C**.

Single instances of abovementioned tasks are shown in **Figure 10**. **Figure 10A** is the result of an open and close task. The results show that, initially, the hand was in the close state; as the subject opens the hand, a drop in signal amplitude near the elbow and an increase in signal amplitude near the wrist joint is observed. The classifier is able to detect that the hand is opened as the movement is performed. Afterwards, when the hand is closed, the inverse muscle activity pattern can be seen, and, as the movement is performed, the classifier is again able to detect that the hand is closed.

The instances of grasping object A, B, and C are shown in **Figures 10B–D**, respectively. Data is presented in the same order as represented for **Figure 10A**. Initially, the subject is holding the object. As the hand is opened, it is seen from the FSR readings that their associated muscle contraction near the wrist increases, and contraction near elbow is decreased. From the opened hand state when the subject is instructed to grasp the object, it can be seen that classifier first detects that the hand is closing. It can also be seen from the FSR readings that it is increasing near the elbow and decreasing near the wrist, indicating hand closing. As the object is grasped, an increase in readings on both sensor bands is seen, and the classifier correctly detects that an object is being grasped. These results show that the threshold-based classifier is able to distinguish between all four motion states, i.e., rest/steady, open, close, and grasp, accurately.

Results in terms of precision, recall, F1-score, and accuracy are shown in **Figures 11**, **12** and **Table 2**. In the figures, the error bar represents the performance deviation within the tasks, i.e., rest, open, close, and grasp.

The average performance values w.r.t each task are shown in **Figure 12**. Considering the rest state, it can be seen that

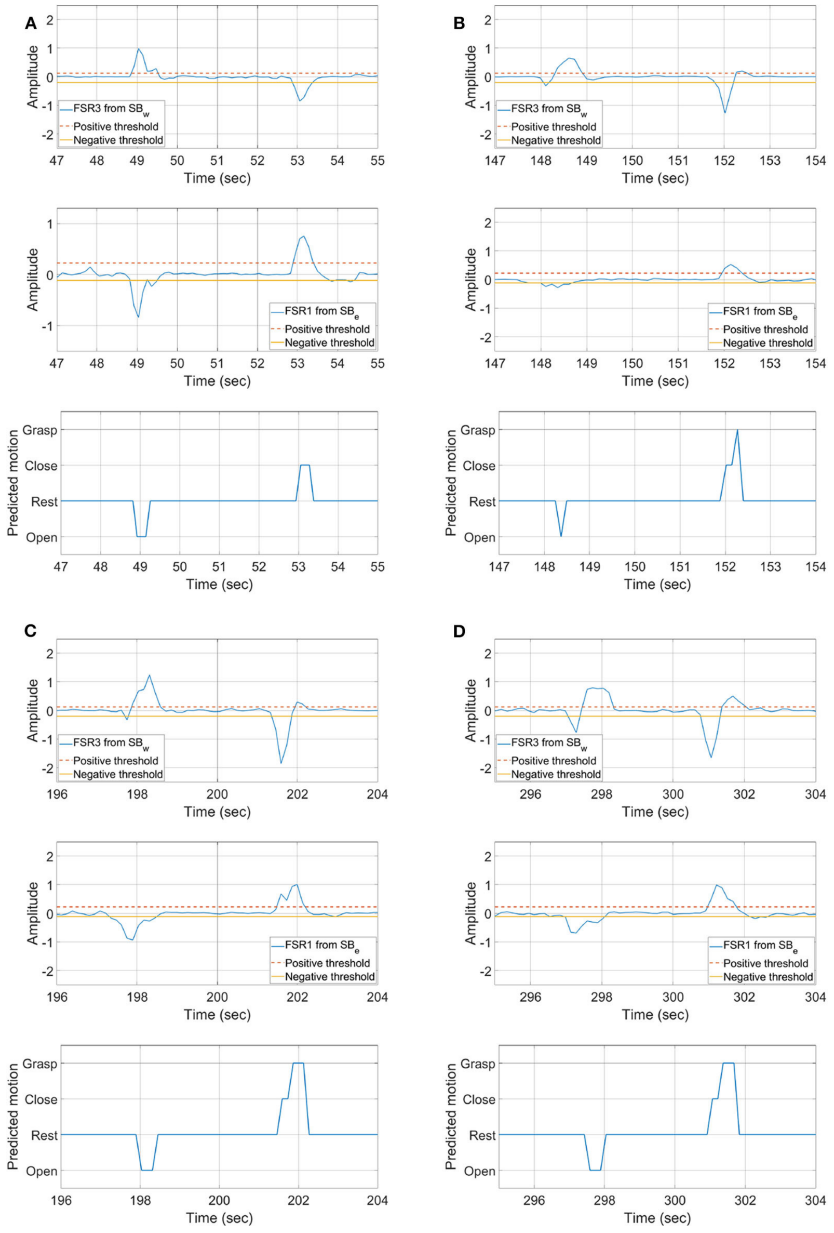

FIGURE 10 | Results of single instances **(A)** open/close, grasping objects **(B)** A, **(C)** B, and **(D)** C, shown in **Figure 8**.

average recall value is 0.98, which reveals that only 2% of the rest states were not detected. It is to be noted that rest state was held in all postures, i.e., open hand, close hand, and grasp. In the context of real-time operation, this result is very critical. Any miss-classification can cause undesirable movement/action, especially if subject is holding an object. The results show that the

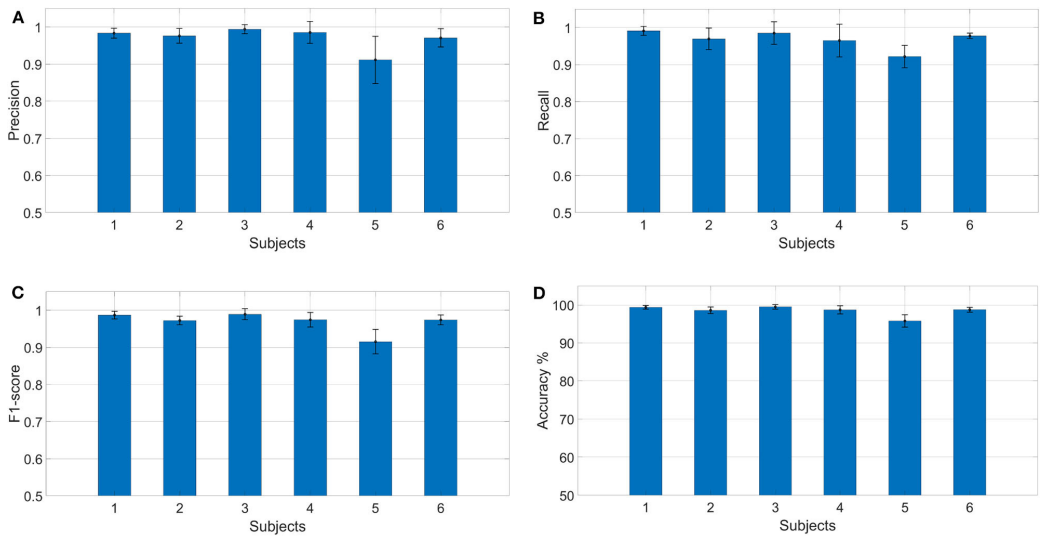

FIGURE 11 | Results calculated for each subject individually **(A)** precision, **(B)** recall, **(C)** F1-score, and **(D)** accuracy.

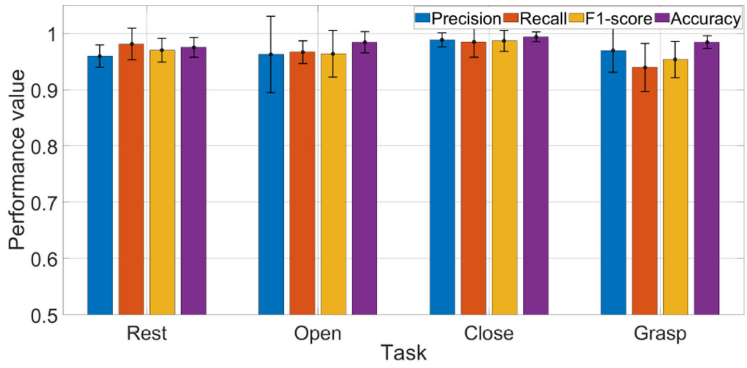

FIGURE 12 | Average results of each performance measure w.r.t each task. Accuracy plot is shown normalized between 0 and 1.

algorithm is highly accurate in detecting the rest state. Precision for detecting rest state is equal to 0.96, which shows that in only few cases where subject was performing another task (open, close, or grasp), classifier detected it as rest state.

For open and close tasks, it can be seen that recall and precision scores are very similar. For grasp, we can see that precision (0.97) is higher than recall (0.94). From precision, we can deduce that, of all the tasks that were classified as grasp, only 3% of them were miss-classifications. Meanwhile, the recall result tells us that 6% of the times when a subject grasped an object, the classifier did not detect it as grasp. To improve precision, the threshold level should be raised, but this will affect the performance of recall. Raising the threshold will have the opposite impact on other performances. It will improve the recall but might reduce the precision. With the current setup, classification performance of the algorithm depends on the trade-off between recall and precision. Depending on the applications, threshold levels can be tuned to get better results. The performance can be improved by incorporating more FSR sensors or by using more features for threshold determination.

4.2. Influence of Sensor Placement

In this experiment, the effect of sensor placement on motion detection is studied. To achieve this objective

sensor bands are placed over the forearm in three different orientations/placements, as shown in **Figure 13**. In placement A, FSR1 from sensor bands SB_e and SB_w is aligned with brachioradialis and near insertion of brachioradialis. In placement B, it is aligned with brachioradialis and flexor carpi ulnaris muscles. Finally, in placement C, it is aligned with palmaris longus and near the insertion of brachioradialis.

Tasks performed for each placement of sensor bands are as follows:

- Open and close of hand without grasping any object
- Grasping object C as shown in **Figure 8**.

Each task is performed 10 times under same conditions as explained in section 4.1. The results of each experiment are shown in **Figure 14**, where **Figures 14A–C** are the results of placement A, B, and C, respectively, by sensor band orientation. In each sub-figure of **Figure 14**, the first figure is the FSR sensors data from the sensor band placed near the wrist, and the second is the data of FSR sensors placed near the elbow, and the third figure displays the reference and predicted tasks.

Even though the raw data is not similar for each sensor placement, the developed method is able to detect all four hand gestures accurately. The performance of task detection is less affected. As seen from predicted results, rest state, hand opening, closing, and grasping achieved the average accuracies of 98.15, 99.24, 100, and 98.16% for all three placements.

4.3. Grasping Assistance

In this work, grasping assistance is provided using SEM Glove where the desired assistance level is regulated by implementing a proportional control scheme. The block diagram of the control scheme is shown in **Figure 15**. Referring to Equation (11), the input of the proportional control is the average MCI force measured by the sensor band placed near the elbow, and the output u is then relayed to the exoskeleton. Moreover, grasping assistance provided by SEM Glove is further validated by measuring the grasping force through force sensors embedded inside SEM Glove exoskeleton.

In this experiment the sensor bands are worn on right forearm and exoskeleton is worn on the left hand. Furthermore, three different payloads, i.e., 1.2, 2.3, and 3.4 kg, applied from $t = 0$ to 20, $t = 20$ to 40, and $t = 40$ to 60 s, respectively, are being grasped for three times each. The results of the experiment are shown in **Figure 16**.

Figure 16A shows the task predicted by the classifier. Net MCI force measured by the SB_e sensor band is shown in **Figure 16B**. The resulting grasping force measured from SEM Glove sensors is shown in **Figure 16C**. Whereas, the single instance of grasp task is shown in **Figure 17**. With the detection of a grasping task and MCI force, assistance is provided by the exoskeleton, which is evident from the sensor reading of the SEM Glove.

If we look closely at **Figures 16B,C**, we can see that the MCI forces are increasing with the payload grasped by the subject. It is also seen that the forces read by the sensors placed at the middle finger and thumb are increasing with the payload. These are the grasping forces that are caused by the physical interaction between fingertips and the object. When assistance provided by the exoskeleton is increased, the exoskeleton will help to grasp the object tightly and in turn grasping force measured the sensors, placed in finger tips, will increase. This validates that with the increase in MCI force, shown in **Figure 16B**, exoskeleton is able to provide the grasping assistance accordingly.

TABLE 2 | Average results of performance measures calculated for each subject.

Performance measures	Precision	Recall	F1-score	Accuracy %
Subject 1	0.98 ± 0.013	0.99 ± 0.012	0.99 ± 0.010	99 ± 0.5
Subject 2	0.98 ± 0.019	0.97 ± 0.029	0.97 ± 0.011	99 ± 0.9
Subject 3	0.99 ± 0.012	0.98 ± 0.030	0.99 ± 0.014	99 ± 0.6
Subject 4	0.99 ± 0.029	0.96 ± 0.044	0.97 ± 0.019	99 ± 1.0
Subject 5	0.91 ± 0.063	0.92 ± 0.030	0.92 ± 0.032	96 ± 1.6
Subject 6	0.97 ± 0.024	0.98 ± 0.007	0.97 ± 0.013	99 ± 0.7
Average	0.97 ± 0.029	0.97 ± 0.024	0.97 ± 0.027	98 ± 1.3

5. DISCUSSION

In this work a novel method is developed for hand motion detection and for the provision of assistance in carrying out an object grasping task. We also addressed the challenge of data collection for training and proposed an alternative solution for it.

The new method is advantageous in reducing the complexity and increasing the usability of the system for a longer period. In an AI-based pattern recognition method, obtaining a correct

FIGURE 13 | Three placements of sensor bands, **(A)** two FSR1 from SBe and SBw are aligned with brachioradialis and near insertion of brachioradialis, **(B)** aligned with brachioradialis and flexor carpi ulnaris, **(C)** aligned with palmaris longus and near insertion of brachioradialis.

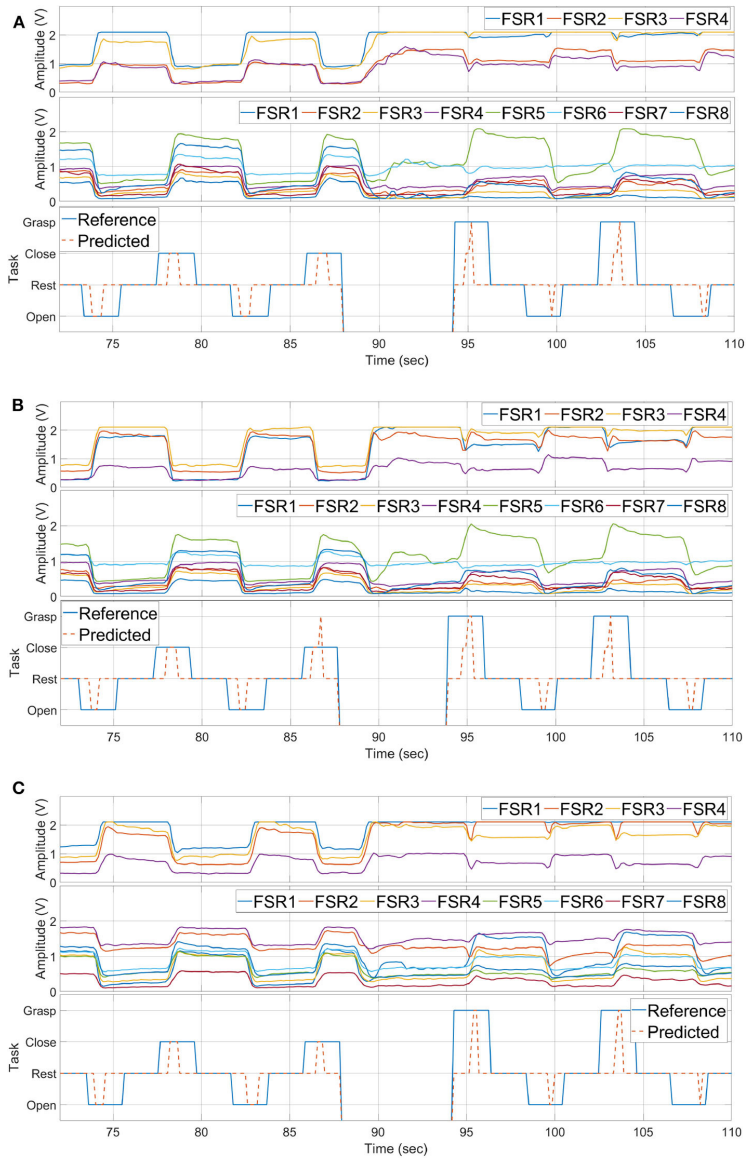

FIGURE 14 | Hand motion detection with three placements of the sensor bands, **(A)** with placement A, **(B)** with placement B, **(C)** with placement C.

and sufficient training dataset is one of the major challenges. Moreover, even if the training data is obtained correctly there still exists another challenge of reusing it from time to time. The reason is due to the placement of sensor at the exact location and change in muscle activity levels. The method proposed in this work effectively addresses these challenges. The method requires sensor calibration and rest state data of the hand. Afterwards, the system can detect the hand motions based on change in activity level. Additionally, the requirement on placing sensor band at exact location is mitigated. Moreover, the calibration procedure

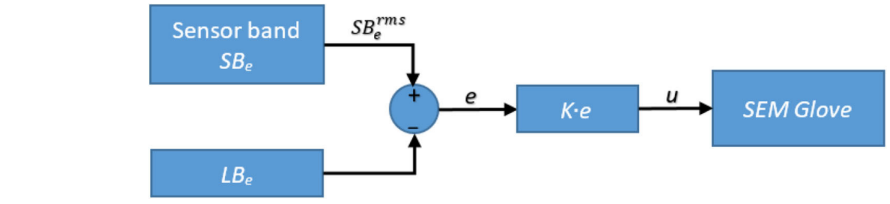

FIGURE 15 | Block diagram of the exoskeleton control.

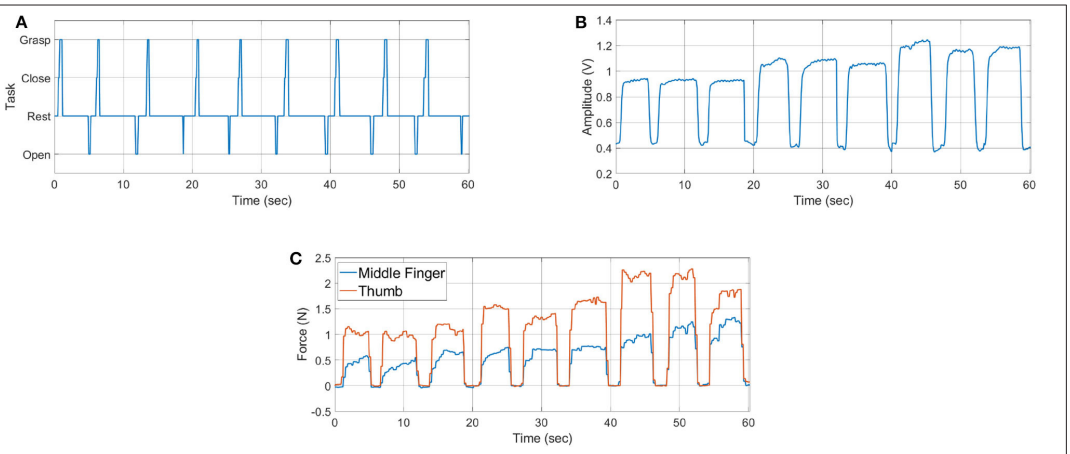

FIGURE 16 | Hand exoskeleton control results: **(A)** task identified, **(B)** MCI force measured from sensor band placed near elbow joint, and **(C)** assistance force provided by SEM Glove.

increases the sensor's sensitivity and solves the problem of sensor resolution if the band tightness is changed from one day to the next.

Another advantage of this method is the dual working modes of the sensor band. Besides motion recognition, the sensor band is also used to control assistance level in grasping an object, which is proportional to the MCI force measured.

The results in this work are significant for physical assistance in workplaces. For a workplace environment, it is critical for any solution that it be accurate, robust, involving less training, and is not sensitive to environmental conditions. With these requirements in mind, comparing our method to other detection methods like sEMG, which is highly prone to noise that is caused by sensor placement, orientation, and skin conditions, our method is less affected by skin condition and can be worn without very exact orientation and placement. Moreover, our developed method has the advantage of using small training datasets. In Arteaga et al. (2020) and Pinzón-Arenas et al. (2019), each gesture was repeated for more than 10 times. Whereas, in our method beside calibration, rest data is recorded for only one time. By this advantage the user can take off the device and put it back on conveniently without worrying about its performance.

This novel method using FSR sensor bands offers a robust and accurate alternative for human-robot interaction. The works presented in this paper and in previous studies (Islam et al., 2018; Islam and Bai, 2019) have shown that FSR-based sensor bands can be applied for control of upper-body assistive exoskeletons in different ways. Beside these, sensor bands can be applied for other types of applications of upper-limb and lower-limb exoskeletons. Moreover, this method can be used to assess the muscle activities for medical purposes and design of control strategies.

Besides these advantages, some limitations of the method are noted. External contact with the sensor band can change the sensor readings, which can result in incorrect motion detection. Hand motion speed is also a factor that can lead to miss-classification. If the motion is performed at slow speed, the algorithm might not be able to detect the task. These challenges can be addressed by either placing the FSR array outside of the sensor band or by implementing robust AI techniques for fault detection. Movement speed challenge can be addressed by increasing the window size during features extraction stage. However, increasing the window size can introduce delay in exoskeleton response.

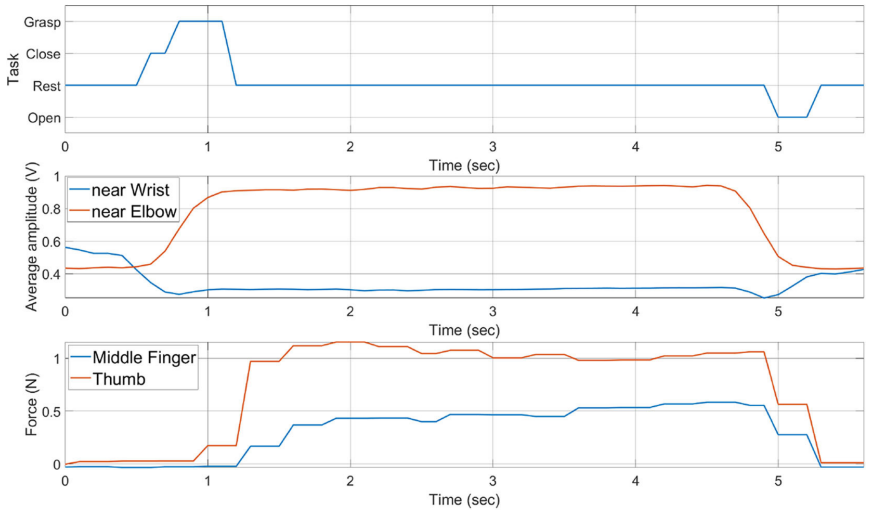

FIGURE 17 | History of task performed, average MCI forces, and grasping forces measured by SEM Glove.

6. CONCLUSIONS

This work is aimed at developing an effective and convenient method to detect hand motions, i.e., rest, open, close, and grasp, using FSR-based sensor bands, which is further used to control hand exoskeleton and provide assistance in grasping task. The objectives are achieved by developing a threshold-based task detection algorithm to determine the hand motion, which is based on the change in MCI forces. Moreover, with the detection of grasping task a proportional force control is also implemented to provide assistance through a soft hand exoskeleton.

The contribution of this work is to experimentally validate whether the sensor bands can be used to detect hand motion and to implement proportional assistance control. Detection of hand motion with the requirement of minimal training data and its validation with testing on multiple subjects are other contributions of this work. The results showed that the developed method can detect each task with high precision, recall, and accuracy. Furthermore, experimental verification of proportional assistance control with SEM Glove in a grasping task is another contribution of this work. The results have shown that the developed method can be used with soft exoskeleton to assist workers in grasping tasks.

In this work, experiments were performed in a controlled environment. In order to test the method for daily routine activities, our future work will focus on sensor fusion techniques to improve robustness against disturbances, which can be caused by other limb movements. Furthermore, the method can be extended to detect other hand gestures and elbow and lower extremity motions.

DATA AVAILABILITY STATEMENT

The raw data supporting the conclusions will be made available by the lead author on reasonable request.

ETHICS STATEMENT

The studies involving human participants were reviewed and approved by ethical committee, Region Nordjylland, Denmark. The participants provided their written informed consent to participate in this study.

AUTHOR CONTRIBUTIONS

MI and SB defined and developed this research work. MI developed the initial protocol draft, collected data, performed the analysis, and wrote the first draft of the manuscript. SB finalized the protocol, reviewed the manuscript, and approved the final version. Both authors contributed to the article and approved the submitted version.

FUNDING

This work was supported by Innovation Fund Denmark for project EXO-AIDER (https://www.exo-aider.dk).

ACKNOWLEDGMENTS

The authors would like to thank participants for their time contributed to this study.

REFERENCES

Anam, K., Rosyadi, A. A., Sujanarko, B., and Al-Jumaily, A. (2017). "Myoelectric control systems for hand rehabilitation device: a review," in *2017 4th International Conference on Electrical Engineering, Computer Science and Informatics (EECSI)*, 1–6. doi: 10.1109/EECSI.2017.8239091

Arteaga, M. V., Castiblanco, J. C., Mondragon, I. F., Colorado, J. D., and Alvarado-Rojas, C. (2020). EMG-driven hand model based on the classification of individual finger movements. *Biomed. Signal Process. Control* 58:101834. doi: 10.1016/j.bspc.2019.101834

Asif, A. R., Waris, A., Gilani, S. O., Jamil, M., Ashraf, H., Shafique, M., et al. (2020). Performance evaluation of convolutional neural network for hand gesture recognition using EMG. *Sensors* 20:1642. doi: 10.3390/s20061642

Bullock, I. M., Zheng, J. Z., De La Rosa, S., Guertler, C., and Dollar, A. M. (2013). Grasp frequency and usage in daily household and machine shop tasks. *IEEE Trans. Hapt*. 6, 296–308. doi: 10.1109/TOH.2013.6

Cho, E., Chen, R., Merhi, L.-K., Xiao, Z., Pousett, B., and Menon, C. (2016). Force myography to control robotic upper extremity prostheses: a feasibility study. *Front. Bioeng. Biotechnol*. 4:18. doi: 10.3389/fbioe.2016.00018

Ferigo, D., Merhi, L.-K., Pousett, B., Xiao, Z. G., and Menon, C. (2017). A case study of a force-myography controlled bionic hand mitigating limb position effect. *J. Bion. Eng*. 14, 692–705. doi: 10.1016/S1672-6529(16)60435-3

Gull, M. A., Bai, S., and Bak, T. (2020). A review on design of upper limb exoskeletons. *Robotics* 9:16. doi: 10.3390/robotics9010016

Hashida, R., Matsuse, H., Bekki, M., Omoto, M., Morimoto, S., Hino, T., et al. (2019). Evaluation of motor-assisted gloves (SEM Glove) for patients with functional finger disorders: a clinical pilot study. *Kurume Med. J*. 64, 1–18. doi: 10.2739/kurumemedj.MS652007

Islam, M. R., Xu, K., and Bai, S. (2018). "Position sensing and control with FMG sensors for exoskeleton physical assistance," in *International Symposium on Wearable Robotics* (Pisa: Springer), 3–7. doi: 10.1007/978-3-030-01887-0_1

Islam, M. R. U., and Bai, S. (2019). Payload estimation using forcemyography sensors for control of upper-body exoskeleton in load carrying assistance. *Model. Identif. Control* 40, 189–198. doi: 10.4173/mic.2019.4.1

Jiang, X., Merhi, L.-K., Xiao, Z. G., and Menon, C. (2017). Exploration of force myography and surface electromyography in hand gesture classification. *Med. Eng. Phys*. 41, 63–73. doi: 10.1016/j.medengphy.2017.01.015

Leonardis, D., Barsotti, M., Loconsole, C., Solazzi, M., Troncossi, M., Mazzotti, C., et al. (2015). An EMG-controlled robotic hand exoskeleton for bilateral rehabilitation. *IEEE Trans. Hapt*. 8, 140–151. doi: 10.1109/TOH.2015.2417570

Lu, Z., Stampas, A., Francisco, G. E., and Zhou, P. (2019). Offline and online myoelectric pattern recognition analysis and real-time control of a robotic hand after spinal cord injury. *J. Neural Eng*. 16:036018. doi: 10.1088/1741-2552/ab0cf0

Meng, Q., Meng, Q., Yu, H., and Wei, X. (2017). "A survey on sEMG control strategies of wearable hand exoskeleton for rehabilitation," in *2017 2nd Asia-Pacific Conference on Intelligent Robot Systems (ACIRS)* (Wuhan), 165–169. doi: 10.1109/ACIRS.2017.7986086

Nilsson, M., Ingvast, J., Wikander, J., and von Holst, H. (2012). "The soft extra muscle system for improving the grasping capability in neurological rehabilitation," in *2012 IEEE-EMBS Conference on Biomedical Engineering and Sciences* (Langkawi), 412–417. doi: 10.1109/IECBES.2012.6498090

Pinzón-Arenas, J. O., Jiménez-Moreno, R., and Herrera-Benavides, J. E. (2019). "Convolutional neural network for hand gesture recognition using 8 different EMG signals," in *2019 XXII Symposium on Image, Signal Processing and Artificial Vision (STSIVA)* (Bucaramanga), 1–5. doi: 10.1109/STSIVA.2019.8730272

Powers, D. M. (2011). Evaluation: from precision, recall and F-measure to ROC, informedness, markedness and correlation. *J. Mach. Learn*. 2, 37–63.

Qi, J., Jiang, G., Li, G., Sun, Y., and Tao, B. (2019). Intelligent human-computer interaction based on surface EMG gesture recognition. *IEEE Access* 7, 61378–61387. doi: 10.1109/ACCESS.2019.2914728

Radmand, A., Scheme, E., and Englehart, K. (2016). High-density force myography: a possible alternative for upper-limb prosthetic control. *J. Rehabil. Res. Dev*. 53, 443–456. doi: 10.1682/JRRD.2015.03.0041

Rasouli, M., Chellamuthu, K., Cabibihan, J.-J., and Kukreja, S. L. (2016). "Towards enhanced control of upper prosthetic limbs: a force-myographic approach," in *2016 6th IEEE International Conference on Biomedical Robotics and Biomechatronics (BioRob)* (University Town), 232–236. doi: 10.1109/BIOROB.2016.7523629

Ravindra, V., and Castellini, C. (2014). A comparative analysis of three non-invasive human-machine interfaces for the disabled. *Front. Neurorobot*. 8:24. doi: 10.3389/fnbot.2014.00024

Secciani, N., Bianchi, M., Meli, E., Volpe, Y., and Ridolfi, A. (2019). A novel application of a surface electromyography-based control strategy for a hand exoskeleton system: a single-case study. *Int. J. Adv. Robot. Syst*. 16, 1–13. doi: 10.1177/1729881419828197

Wege, A., and Zimmermann, A. (2007). "Electromyography sensor based control for a hand exoskeleton," in *2007 IEEE International Conference on Robotics and Biomimetics (ROBIO)* (Sanya), 1470–1475. doi: 10.1109/ROBIO.2007.4522381

Xiao, Z. G., and Menon, C. (2019). A review of force myography research and development. *Sensors* 19:4557. doi: 10.3390/s19204557

Xiao, Z. G., and Menon, C. (2020). Towards the investigation on the effect of the forearm rotation on the wrist FMG signal pattern using a high-density FMG sensing matrix. *Cogent Eng*. 7:1795051. doi: 10.1080/23311916.2020.1795051

Zhang, Z., Yang, K., Qian, J., and Zhang, L. (2019). Real-time surface EMG pattern recognition for hand gestures based on an artificial neural network. *Sensors* 19:3170. doi: 10.3390/s19143170

Zheng, J. Z., De La Rosa, S., and Dollar, A. M. (2011). "An investigation of grasp type and frequency in daily household and machine shop tasks," in *2011 IEEE International Conference on Robotics and Automation* (Shanghai), 4169–4175. doi: 10.1109/ICRA.2011.5980366

Conflict of Interest: The authors declare that the research was conducted in the absence of any commercial or financial relationships that could be construed as a potential conflict of interest.

Chapter 5

Paper III

Payload estimation using forcemyography sensors for control of upper-body exoskeleton in load carrying assistance

Muhammad Raza Ul Islam and Shaoping Bai

The paper has been published in the
Modeling, Identification and Control, vol. 40, no.4, pp. 189–198, 2019.
doi.org/10.4173/mic.2019.4.1

Modeling, Identification and Control, Vol. 40, No. 4, 2019, pp. 189–198, ISSN 1890–1328

Payload estimation using forcemyography sensors for control of upper-body exoskeleton in load carrying assistance

Muhammad R. U. Islam [1] Shaoping Bai [1]

[1] *Department of Materials and Production, Aalborg University, Aalborg, Denmark. E-mail: (mraza,shb)@mp.aau.dk*

Abstract

In robotic assistive devices, the determination of required assistance is vital for proper functioning of assistive control. This paper presents a novel solution to measure conveniently and accurately carried payload in order to estimate the required assistance level. The payload is estimated using upper arm forcemyography (FMG) through a sensor band made of force sensitive resistors. The sensor band is worn on the upper arm and is able to measure the change of normal force applied due to muscle contraction. The readings of the sensor band are processed using support vector machine (SVM) regression technique to estimate the payload. The developed method was tested on human subjects, carrying a payload. Experiments were further conducted on an upper-body exoskeleton to provide the required assistance. The results show that the developed method is able to estimate the load carrying status, which can be used in exoskeleton control to provide effectively physical assistance needed.

Keywords: Forcemyography, payload estimation, assistive exoskeleton, physical human-robot interaction.

1 Introduction

With the advancement in robot technology, exoskeletons are being developed for medical, industrial and service applications. Based on the applications, exoskeletons are categorized in three types i.e. rehabilitation, assistance and power augmentation exoskeletons Fan and Yin (2013); Hsieh et al. (2017); Cui et al. (2016); Keller et al. (2016); Huang et al. (2015); Castro et al. (2019); Christensen and Bai (2018); Gunasekara et al. (2012); Zhou et al. (2015). Rehabilitation and power augmentation exoskeletons are mainly focused on serving humans to regain their mobility and helping the users with extra power to enhance their capability, respectively Bai et al. (2018). In this work, our interest is to use exoskeletons to assist users, which can be either factory workers, elderly or person weak muscle strength, in load carrying tasks.

For physical assistance exoskeletons, the determination of required assistance level is one of primary concerns. In load carrying tasks, one method to determine required assistance level is by knowing the payload value and joint configuration. In existing upper body exoskeleton systems, payload information is acquired by integrating force sensors at the end-effector, where the weight is hanged on to the exoskeleton and not carried by the human Rosen et al. (2001); Lee et al. (2014). This method is useful in specific applications, particularly heavy-load carrying tasks. The implementation of this method for daily routine activities or factory tasks is not feasible, where the user carries objects of different attributes. To overcome this challenge, Electromyography (EMG) based estimation methods are used instead to determine joint torques and provide assistance through exoskeletons McDonald et al. (2017); Mangukiya et al. (2017); Leonardis et al. (2015); Abdallah et al. (2017); Mghames et al. (2017); Tang et al. (2014); Rahman et al. (2015); Li et al. (2013); Kiguchi

doi:10.4173/mic.2019.4.1

and Hayashi (2012). In these methods the assistance to each joint is provided by analyzing the muscle activities of its prime mover muscle group. In upper body multi DOF exoskeleton, this approach brings computational complexity, as large number of EMG electrodes need to be processed. Moreover, for daily usage placement of EMG electrodes to right place, proper skin preparation, low S/N ratio and convenience are other challenges to be addressed.

In this work, we proposed FMG based method to estimate the payload level. This method requires no load cell to be attached at the end-effector and only requires an Force Sensitive Resistor (FSR) sensor band to perceive upper arm muscles activity and joint configuration in estimating payload level. Compared with other methods like EMG sensors, the new method requires simple electronics. S/N ratio is also better and is not affected by skin condition.

In literature, there are some reported works on using FMG to detect upper body and lower body movements Cho et al. (2016); Kadkhodayan et al. (2016); Xiao and Menon (2017); Sadarangani and Menon (2017); Islam and Bai (2017); Jiang et al. (2016); Xiao et al. (2014); Islam et al. (2018). However, this approach has not been used yet for payload estimation to control upper-body exoskeleton in load carrying tasks. In this work, we developed an FSR sensor band, which measures the normal force applied by the muscles as they contract. The required assistance level is then estimated from the sensor readings, processed by machine learning, in terms of carried payload. The new method provides convenient and accurate estimates of payload carried by a person.

This paper is organized as follow: Design and implementation of the sensor band is described in Section 2. Section 3 presents the algorithm design of payload estimation. Experimental setup for sensor testing and its results are described in Section 4. In Section 5, we include briefly exoskeleton control with the developed sensor band to demonstrate the application. Discussion on the developed method is presented in Section 6 and the work is concluded in Section 7.

2 Sensor band design

Figure 1 shows an FSR sensor band developed. When the sensor band is worn on an upper arm, it measures the normal force applied due to muscle contraction, called muscle contraction-induced (MCI) force. FSR sensors register this applied force in terms of varying resistance. An amplifier is used to read the resistance change and output a smooth and amplified voltage signal. The output voltage signal is passed to a computer for post processing. In post processing, the voltage signal is converted to respective force measured by the FSRs. Moreover, machine learning is implemented to interpret the force signal in terms of payload. The details of all major components are described presently.

2.1 FSR distribution

The sensor band is comprised of an array of FSRs embedded inside a flexible strap. In the current setup, four FSR sensors of model FSR-402 are utilized, which are able to measure applied force in the range of 0.1-10N.

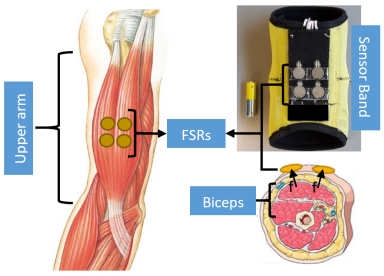

Figure 1: Sensor band working principle and it's placement on the upper arm.

FSRs distribution over the sensor band and its placement on arm are shown in Fig. 1. The sensors are distributed in a way that they can cover some areas of muscles, specially, where they can read the maximum normal force. The flexibility of strap ensures a good contact between FSRs and arm muscles, which allows the FSRs to sense the normal force exerted by the muscles on them. Moreover, the design of sensor band allows it to apply same pressure over the muscles every time the user puts it on.

2.2 FSR-amplifier coupling

The FSR responds to the applied force by varying its resistance. Therefore, a non-inverting amplifier is interfaced with the FSRs according to Fig. 2.

The output of the amplifier is given by the following equation,

$$V_{out} = (1 + \frac{R_{ref}}{R_{fsr}})V_{in} \tag{1}$$

where V_{out} is the output voltage of the amplifier, V_{in} is the input voltage to the positive terminal of the amplifier, R_{ref} is the reference resistance and R_{fsr} represents the resistance of FSR. The output of the amplifier can be changed by varying V_{in} and R_{ref}. In the implementation V_{in} was fixed and R_{ref} was varied to read

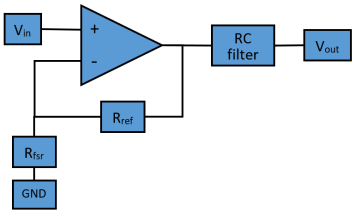

Figure 2: FSR amplification circuitry.

the desired force range of the FSR. R_{ref} was finally selected, so that the full range of amplifier output is utilized and maximum resolution is obtained. In the circuit a low pass filter is also included to filter out high frequency noises.

3 Estimation algorithm

The algorithm of payload estimation is based on MCI force and joint orientation. In this method two MCI force profiles are modeled for carrying two different payloads across human arm range of motion in sagittal plane. The profiles are obtained using SVM based regression technique, in which MCI force is treated as output parameter and elbow and shoulder joint angles as input parameters. In the real-time testing the given MCI force is compared with the developed MCI profiles to estimate the payload.

3.1 System setup

The data for training SVM regression models is acquired through an instrumented passive exoskeleton. As shown in Fig. 3, the passive exoskeleton has an absolute encoder, Novotechnik RFD-4021, at elbow joint and an accelerometer ADXL 335 to monitor the upper arm movement. The output of RFD-4021 encoder determines the elbow joint angle, whereas the output of accelerometer is calibrated and mapped to shoulder joint (flexion/extension) angle as,

$$\theta_s = -154.93V_a^2 + 217.33V_a + 18.53 \qquad (2)$$

here V_a represents the x-axis output voltage of the accelerometer.

3.2 Datasets

Two datasets are recorded in the training session, namely, $\mathbf{D_1}$ and $\mathbf{D_2}$ to train the regression models for payload estimation. The contents of these datasets are as follows.

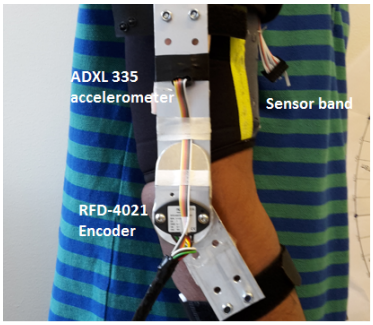

Figure 3: An instrumented passive arm exoskeleton to collect the data for SVM training.

3.2.1 $\mathbf{D_1}$

This dataset is comprised of net MCI force f_a measured by the sensor band in carrying a payload ρ_a. In collecting the data subject lifts the payload in several elbow and shoulder joint angle configurations.

3.2.2 $\mathbf{D_2}$

This dataset is comprised of net MCI force f_a measured by the sensor band in carrying a payload ρ_b. Arm configuration used for $\mathbf{D_1}$ is followed in collecting this dataset.

After collecting these datasets two regression models are trained, whose details are given in forthcoming section.

3.3 Regression models

Both datasets, explained earlier, are used to train two regression models i.e. $\mathbf{R_1}$ and $\mathbf{R_2}$.

Taking $\mathbf{R_1}$ as an example. Dataset $\mathbf{D_1}$ is used to train this regression model with joint angles θ_e and θ_s as predictor and net MCI force f_a, sum of forces measured by FSR sensors embedded inside the sensor band, as response variable. Hence, during the real-time testing, the regression model uses the joint angles θ_e and θ_s to estimate the force, f_1, that muscle generated if a person lifts or carries payload ρ_a. Similarly, model $\mathbf{R_2}$ is trained with dataset $\mathbf{D_2}$. The inputs and outputs of both regression models are illustrated in Fig. 4.

3.4 Real-time estimation model

During real-time estimation, the algorithm first computes forces f_1 and f_2 using regression models $\mathbf{R_1}$ and $\mathbf{R_2}$, respectively.

After all forces are obtained, payload is determined by following equation,

$$\rho = (\rho_b - \rho_a)(f_a - f_1)/(f_2 - f_1) \quad (3)$$

where ρ represent the estimated payload.

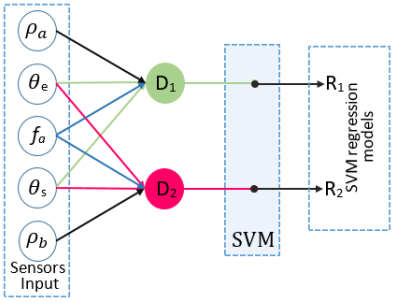

(a)

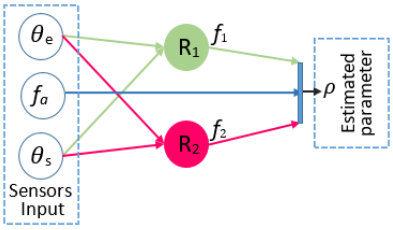

(b)

Figure 4: Flow diagram of algorithm design, (a) SVM training session to compute regression models, (b) real-time estimation of payload.

A 3D surface plot illustrating the MCI variation with respect to θ_e and θ_s is shown in Fig. 5.

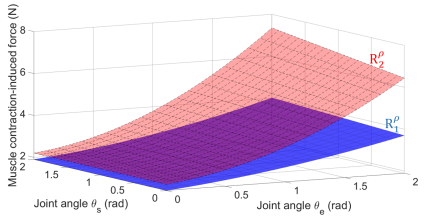

Figure 5: Illustration of payload estimation when two payloads are used for training the regression models.

4 Payload estimation

Experiments were carried out to test the performance of the developed payload determination method. The experiments of payload estimation first include training of SVM regression models, which is followed by real-time testing of the developed estimation method.

4.1 Data collection protocol

A MATLAB based GUI is developed to collect the data, which is comprised of MCI force readings from sensor band, elbow joint and shoulder joint angles. The GUI allows the data to be collected at a frequency of 200 Hz and sorting out the necessary information for training session.

The protocol of data collection involves a set of static postures, shown in Fig. 6, that the user maintains for a few seconds. The detailed description of protocol is as follow.

- Subject wears the sensor band and passive exoskeleton as shown in Fig. 3.
- Subject is free of payload, i.e. $\rho_a = 0$ kg, and keeps the elbow and shoulder angles according to Fig. 6(a) for 10 s.
- Subject rests for 20 s and raises his/her arm to the next configuration as shown in Fig. 6(b) and maintains the pose for 10 s.
- Subject repeats the task for all the positions shown in Fig. 6, with a rest for 20 s in between each position.
- After completing all positions subject rests for 10 minutes and repeats the whole process for payload $\rho_b = 2.5$ kg.

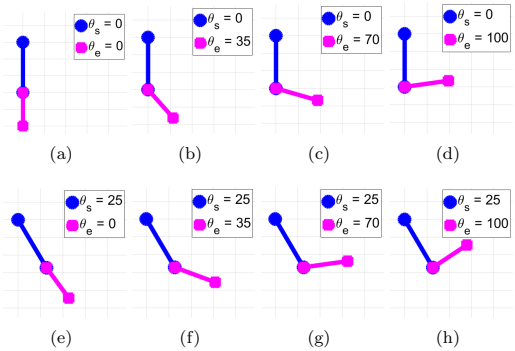

Figure 6: Joint configurations selected for collecting sensors data.

The data collected in these experiments is divided into two sets i.e. $\mathbf{D_1}$ and $\mathbf{D_2}$, which is followed by the training of regression models $\mathbf{R_1}$ and $\mathbf{R_2}$, respectively.

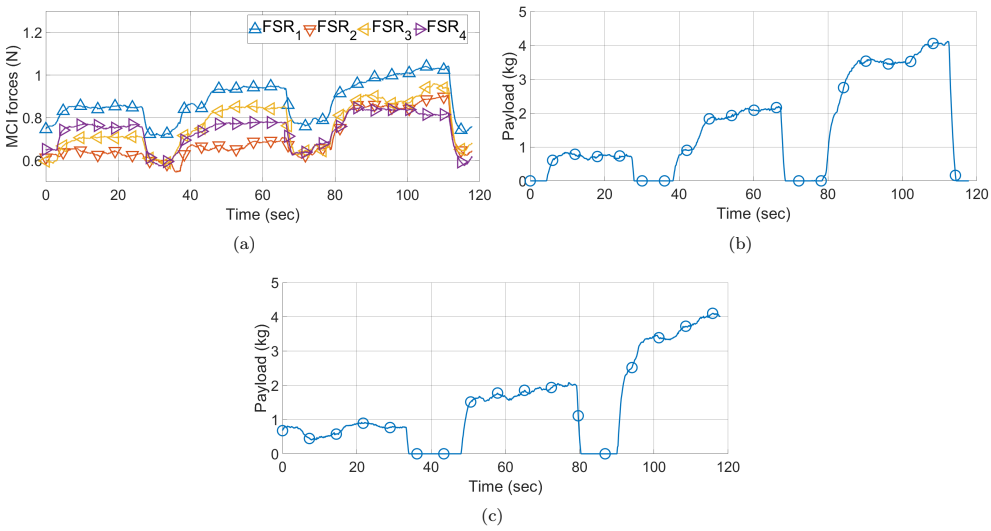

Figure 7: Payload estimation testing results, (a) MCI forces measured by sensor band for a configuration of $\theta_e = 76°$ and $\theta_s = 34°$, (b) payload estimated for case (a), and (c) payload estimated for a configuration of $\theta_e = 76°$ and $\theta_s = 52°$.

4.2 Results of real-time testing

Five healthy subjects, aged between 20-30, participated in this experiment. Subjects were provided with written consent forms prior to the experiments. Moreover, experiments were performed with ethical approval obtained from ethical committee, Region Nordjylland, Denmark.

In this testing the regression models for payload estimation were trained and tested for each subject separately. After training the regression models, real-time testing was carried out with the passive exoskeleton, in which three different payloads in the range of 0 kg to 5 kg were lifted by the subjects.

Figure 7 shows the test results with three payloads $\rho_1 = 0.8$ kg, $\rho_2 = 2.5$ kg and $\rho_3 = 4$ kg, which were held by Subject 1 at his hand sequentially.

The testing is static, which means that the elbow and shoulder joint angles remain fixed. Figure 7(a) displayed raw data of FSR readings measured for angles $\theta_e = 76°$ and $\theta_s = 34°$. Figure 7(b) shows the estimated payload. Another result of payload estimation is shown in Fig. 7(c), with the arm configuration slightly changed i.e. $\theta_e = 76°$ and $\theta_s = 52°$.

The testing shows that the developed method can determine the payload level correctly and close to real values for varying configurations. It is also noticed in Figs. 7(b) and 7(c) that even though the SVM models were trained for up to 2.5 kg payload, the sensor can even estimate correctly the payload level higher than the top level used in the training.

The results of all the other subjects are shown in Fig. 8, displaying errors in payload estimation. The error in estimated payload is computed for all the tasks performed in saggital plane, as the training condition in payload estimation included arm configurations for different shoulder and elbow joint angles.

Figures 8(a) and 8(b) show absolute and relative error of estimation, respectively. Absolute error is computed as the difference between actual and estimated payload value, whereas, relative error is obtained by normalizing the error w.r.t the maximum payload. It can be seen in Fig. 8(a) that the mean value of absolute error varies from 0.14 kg to 0.37 kg. In Fig. 8(b) mean value of relative error varies from 0.07 to 0.17 for the five subjects.

5 Exoskeleton control

With the developed sensor for payload determination, we conducted further experiments of physical assistance control on a 4-DOF upper-body exoskeleton (see Fig. 9), developed at AAU, Aalborg, Denmark Bai et al. (2017). The exoskeleton has 3 ac-

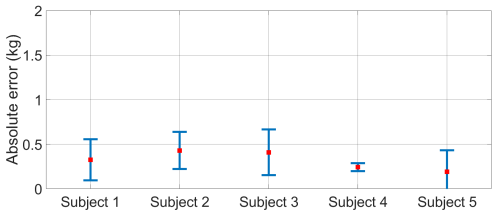

(a)

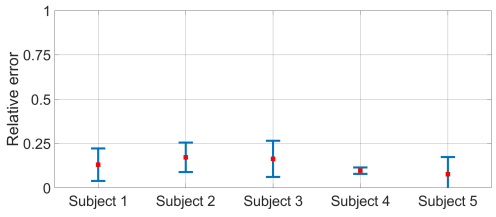

(b)

Figure 8: Errors of estimation, (a) absolute error, and (b) relative error, where red dot refers to the mean values.

tive joints (i.e. elbow flexion/extension, shoulder flexion/extension and shoulder abduction/adduction) and 1 passive joint (shoulder internal/external rotation). In these experiments shoulder abduction/adduction and internal/external rotation motions are restricted and only elbow/shoulder flexion/extension motors are actuated.

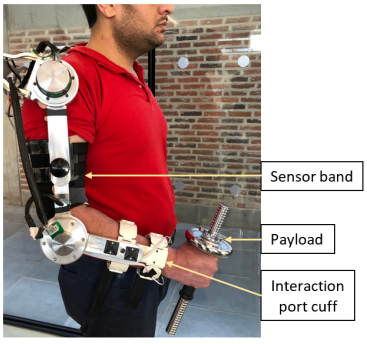

Figure 9: Upper-body exoskeleton for physical assistance testing.

The exoskeleton adapts admittance control and gravity compensation. Admittance control is implemented to control the elbow actuator motion, whereas, gravity compensation is implemented to provide support at shoulder joint. The block diagram of the control algorithm is presented in Fig. 10.

The control input u relayed to exoskeleton is,

$$u = [\tau_e \quad \tau_s] \tag{4}$$

where τ_e represents the elbow actuator control input and τ_s the shoulder actuator control input.

The elbow torque is dependent on interaction torque τ_{int} at attachment cuff and assistance torque τ_a associated to the payload ρ, which are computed by

$$\tau_{int} = f_p \cdot r \tag{5}$$

$$\tau_a = k_{AL}\ \rho g l_p \sin(\theta_e + \theta_s) \tag{6}$$

where f_p is the interaction port force that is measured from the port cuff in Fig. 9, r is the distance from the middle point of the interaction port cuff to elbow joint, g is the gravity acceleration, l_p is the distance from elbow joint to the center of palm and k_{AL} is assistance coefficient, which is computed through

$$k_{AL} = \frac{A}{1 - A} \tag{7}$$

where $A \in [0,\ 1)$, defines the percentage of assistance provided by the exoskeleton. Eq. 7 ensures the equilibrium between human effort and exoskeleton's assistance for a desired value of A, in order to perform the task jointly.

After determining the interaction and assistive force, the corresponding joint torque is computed, which is followed by the admittance filter (Y(s)) to obtain the desired velocity. Both are mathematically represented as,

$$\tau_{net} = \tau_{int} \quad + \quad \tau_a \tag{8}$$

$$Y(s) = \frac{\omega_d(s)}{\tau_{net}(s)} = \frac{1}{Bs + D + \frac{K}{s}} \tag{9}$$

where τ_{net} is the required joint torque, ω_d is the desired velocity and B, D and K represent the inertia, damping and stiffness parameters of the admittance filter. Furthermore, the desired joint velocity is tracked through a PI controller which outputs the control input τ_e given by,

$$\tau_e = k_p\ \omega_e + k_i \int \omega_e dt \tag{10}$$

where k_p and k_i are the proportional and integral gains, respectively. ω_e is the error signal and is given by,

$$\omega_e = \omega_d - \omega_a \tag{11}$$

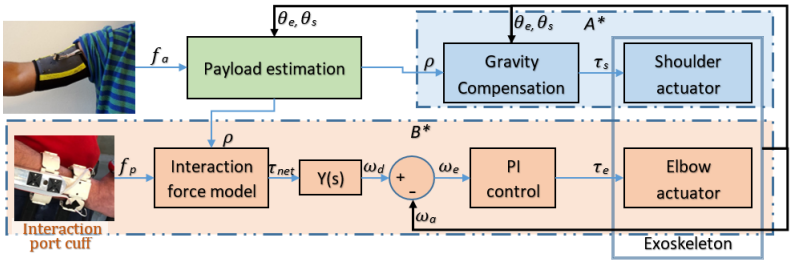

Figure 10: Exoskeleton control block diagram, where A* and B* are two blocks for control of shoulder and elbow joint, respectively.

Table 1: Exoskeleton and control parameters

Parameter	Value	Parameter	Value
m_e	1.39 kg	A	0.5
m_s	0.307 kg	k_s	50
l_e	0.165 m	B	0.05 kgm^2
l_s	0.15 m	D	0.105 Nsm^{-1}
l_{se}	0.33 m	K	0 Nm^{-1}
r	0.27 m	k_p	1
r_{fr}	0.30 m	k_i	0.0067

where ω_a represents the actual joint angular velocity.

The shoulder actuation is controlled with gravity compensation. The shoulder joint control input τ_s is computed by,

$$\tau_s = m_s g l_s \sin\theta_s + (m_e + \rho k_{AL}) g (l_e \sin(\theta_e + \theta_s) + l_{se} \sin\theta_s) \quad (12)$$

where m_e and m_s represent the forearm and upper arm link mass, l_e is the distance from elbow joint to the center of mass of forearm link, l_s is the distance from shoulder joint to the center of mass of upper arm link and l_{se} is the distance from shoulder joint to elbow joint. The values of the exoskeleton and control parameters are provided in Table 1.

The results of the estimated payload and physical assistance provided by exoskeleton are shown in Fig. 11. Figure 11(a) shows the results of subject holding a payload of 2.5 kg without wearing the active exoskeleton, in an arm configuration i.e. $\theta_e = 88°$ and $\theta_s = 24°$ approximately. It can be seen that the estimated payload value is close to the actual payload value i.e. 2.5 kg.

Figures 11(b) and 11(c) show the result of payload estimation and joint torques, respectively, for subject carrying the same payload while wearing the exoskeleton, in arm configuration similar to the payload carrying task without exoskeleton. In this test, the exoskele-

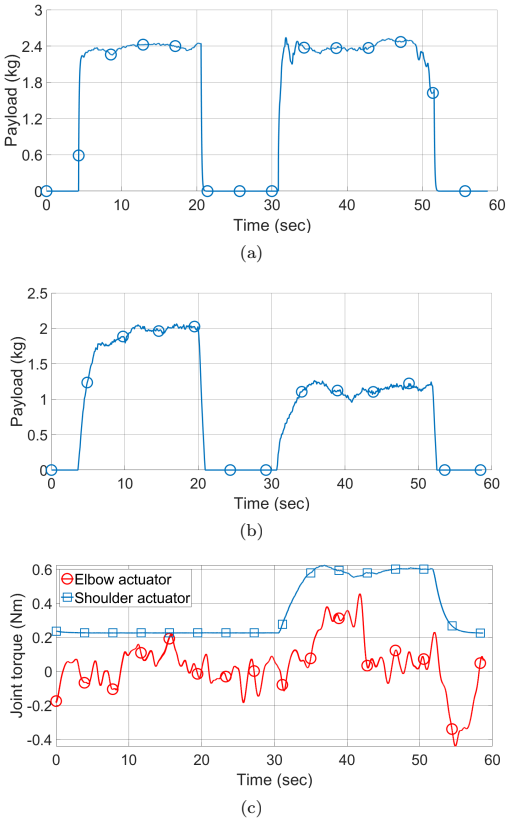

Figure 11: Exoskeleton control results, (a) estimated payload without exoskeleton, (b) estimated payload with exoskeleton and (c) torques provided by exoskeleton at each joint, first in transparent mode (3-21 s) and then in assistive mode (31-52 s).

ton worked in transparent mode for t=3-21 s and then in assistive mode for t=31-52 s.

It can be seen that in transparent mode the estimated payload is approximately 2 kg, which is slightly less than the estimated payload without exoskeleton that was nearly 2.4 kg. This can be justified as in transparent mode the exoskeleton provides slight assistance and therefore, effort exerted by upper arm muscles will decrease. The decrease in muscle effort results in decrease of MCI force. Since our method of payload estimation is based on upper arm MCI force, therefore with the decease in MCI force the algorithm will estimate reduced payload.

Comparing the results of payload carrying task without exoskeleton and payload carrying task with exoskeleton in assistive mode, it can be seen that the estimated payload value decreased from 2.4 kg to 1.2 kg, respectively. The decrease in payload value justifies that the exoskeleton is providing assistance in load carrying task. As explained earlier, the payload estimation algorithm is based on MCI force of upper arm muscles. With assistance from exoskeleton, the upper arm muscles activity will decrease. The decrease in muscle activity causes the MCI force to decrease. Therefore, it is seen that in assistive exoskeleton control the 2.5 kg payload is estimated, or in other words, felt as 1.2 kg payload carried by the subject.

6 Discussion

In this work, we developed a novel method for the estimation of payload. The developed method shows some advantages for exoskeleton assistance control.

The new method is advantageous in reducing complexity in upper arm exoskeleton control. Conventionally, in order to provide assistance at elbow and shoulder joint, activities of muscles that govern the elbow and shoulder joint movement need to be observed. This makes the system physically and computationally complex. In this work only biceps muscle readings along with elbow and shoulder joint encoder are used to estimate the payload. The method has significantly reduced the complexity not only in real-time operations but also in training sessions. Additionally, the sensor band can be readily and conveniently put on human arms and used when needed. Moreover, unlike EMG based solutions FSR output is not affected by the skin condition and slight displacement from optimum position does not affect the sensor output.

It is noticed that the developed method has some limitations. One limitation is that the sensor band readings can be affected by external interference. Sensor band primarily measures the contact force that can result from external contact, which can be cuffs to hold the exoskeleton. Therefore, the design of the cuffs needs to be in a way to not come in contact with the FSRs. Possible saturation of FSR sensor output is another limitation. The amplifier is thus required to be properly tuned in order to avoid saturation. These limitations need further improvements in future research.

7 Conclusion

The paper presents a novel method of estimating payload using an FSR based sensor band. The sensor band is able to measure the muscle contraction-induced forces. Machine learning is used to process and interpret the readings of the sensor, which yields the payload estimated. The method has been tested and validated in a series of testing and then applied to the assistive control of an upper-body exoskeleton to provide required assistance.

The main contribution of the presented work lies in the convenient and accurate estimation of payload using an FSR based sensor band, which makes it simple and effective for practical use. In this work, the accuracy of payload determination is tested through experiments. This method also makes it possible for exoskeletons to control physical assistance with a simple setup such as the FSR based sensor band. The experimental work on the exoskeleton control for load carrying assistance justifies this possibility, which is another contribution of this work.

In the presented work sensor band is applied for upper-body exoskeleton control. The sensor technology can also be used in other systems, for example, soft/rigid hand exoskeleton or lower limb exoskeleton to detect the load level. The future work will focus on more comprehensive testing of the payload estimation and extending the current work to full upper-body exoskeleton control. Moreover, comparative study of different regression algorithms for the estimation of payload will be considered. The developed sensor technology with various control strategies will also be considered.

Acknowledgment

The authors would like to thank EU AAL Programme's funding bodies to support the project AXO-SUIT (http://www.axo-suit.eu/) and Innovation Fund Denmark's support to EXO-AIDER (https://www.exo-aider.dk/).

References

Abdallah, I. B., Bouteraa, Y., and Rekik, C. Design and development of 3D printed myoelectric robotic exoskeleton for hand rehabilitation. *International Journal on Smart Sensing & Intelligent Systems*, 2017. 10(2). doi:10.21307/ijssis-2017-215.

Bai, S., Christensen, S., and Islam, M. R. U. An upper-body exoskeleton with a novel shoulder mechanism for assistive applications. In *2017 IEEE International Conference on Advanced Intelligent Mechatronics (AIM)*. pages 1041–1046, 2017. doi:10.1109/AIM.2017.8014156.

Bai, S., Virk, G. S., and Sugar, T. *Wearable Exoskeleton Systems: Design, Control and Applications*. Institution of Engineering and Technology, 2018. doi:10.1049/PBCE108E.

Castro, M. N., Rasmussen, J., Andersen, M. S., and Bai, S. A compact 3-DOF shoulder mechanism constructed with scissors linkages for exoskeleton applications. *Mechanism and Machine Theory*, 2019. 132:264–278. doi:10.1016/j.mechmachtheory.2018.11.007.

Cho, E., Chen, R., Merhi, L.-K., Xiao, Z., Pousett, B., and Menon, C. Force myography to control robotic upper extremity prostheses: a feasibility study. *Frontiers in Bioengineering and Biotechnology*, 2016. 4:18. doi:10.3389/fbioe.2016.00018.

Christensen, S. and Bai, S. Kinematic analysis and design of a novel shoulder exoskeleton using a double parallelogram linkage. *Journal of Mechanisms and Robotics*, 2018. 10(4):041008. doi:10.1115/1.4040132.

Cui, X., Chen, W., Jin, X., and Agrawal, S. K. Design of a 7-DOF cable-driven arm exoskeleton (CAREX-7) and a controller for dexterous motion training or assistance. *IEEE/ASME Transactions on Mechatronics*, 2016. 22(1):161–172. doi:10.1109/TMECH.2016.2618888.

Fan, Y. and Yin, Y. Active and progressive exoskeleton rehabilitation using multisource information fusion from EMG and force-position epp. *IEEE Transactions on Biomedical Engineering*, 2013. 60(12):3314–3321. doi:10.1109/TBME.2013.2267741.

Gunasekara, J., Gopura, R., Jayawardane, T., and Lalitharathne, S. Control methodologies for upper limb exoskeleton robots. In *2012 IEEE/SICE International Symposium on System Integration (SII)*. pages 19–24, 2012. doi:10.1109/SII.2012.6427387.

Hsieh, H.-C., Chen, D.-F., Chien, L., and Lan, C.-C. Design of a parallel actuated exoskeleton for adaptive and safe robotic shoulder rehabilitation. *IEEE/ASME Transactions on Mechatronics*, 2017. 22(5):2034–2045. doi:10.1109/TMECH.2017.2717874.

Huang, J., Huo, W., Xu, W., Mohammed, S., and Amirat, Y. Control of upper-limb power-assist exoskeleton using a human-robot interface based on motion intention recognition. *IEEE Transactions on Automation Science and Engineering*, 2015. 12(4):1257–1270. doi:10.1109/TASE.2015.2466634.

Islam, M. R., Xu, K., and Bai, S. Position sensing and control with FMG sensors for exoskeleton physical assistance. In *International Symposium on Wearable Robotics*. pages 3–7, 2018. doi:10.1007/978-3-030-01887-0_1.

Islam, M. R. U. and Bai, S. Intention detection for dexterous human arm motion with FSR sensor bands. In *Proceedings of the Companion of the 2017 ACM/IEEE International Conference on Human-Robot Interaction*. pages 139–140, 2017. doi:10.1145/3029798.3038377.

Jiang, X., Chu, H. T., Xiao, Z. G., Merhi, L.-K., and Menon, C. Ankle positions classification using force myography: An exploratory investigation. In *2016 IEEE Healthcare Innovation Point-Of-Care Technologies Conference (HI-POCT)*. pages 29–32, 2016. doi:10.1109/HIC.2016.7797689.

Kadkhodayan, A., Jiang, X., and Menon, C. Continuous prediction of finger movements using force myography. *Journal of Medical and Biological Engineering*, 2016. 36(4):594–604. doi:10.1007/s40846-016-0151-y.

Keller, U., van Hedel, H. J., Klamroth-Marganska, V., and Riener, R. ChARMin:The first actuated exoskeleton robot for pediatric arm rehabilitation. *IEEE/ASME Transactions on Mechatronics*, 2016. 21(5):2201–2213. doi:10.1109/TMECH.2016.2559799.

Kiguchi, K. and Hayashi, Y. An EMG-based control for an upper-limb power-assist exoskeleton robot. *IEEE Transactions on Systems, Man, and Cybernetics*, 2012. 42(4):1064–1071. doi:10.1109/TSMCB.2012.2185843.

Lee, H.-D., Lee, B.-K., Kim, W.-S., Han, J.-S., Shin, K.-S., and Han, C.-S. Human–robot cooperation control based on a dynamic model of

an upper limb exoskeleton for human power amplification. *Mechatronics*, 2014. 24(2):168–176. doi:10.1016/j.mechatronics.2014.01.007.

Leonardis, D., Barsotti, M., Loconsole, C., Solazzi, M., Troncossi, M., Mazzotti, C., Castelli, V. P., Procopio, C., Lamola, G., Chisari, C., et al. An EMG-controlled robotic hand exoskeleton for bilateral rehabilitation. *IEEE Transactions on Haptics*, 2015. 8(2):140–151. doi:10.1109/TOH.2015.2417570.

Li, Z., Wang, B., Sun, F., Yang, C., Xie, Q., and Zhang, W. sEMG-based joint force control for an upper-limb power-assist exoskeleton robot. *IEEE Journal of Biomedical and Health Informatics*, 2013. 18(3):1043–1050. doi:10.1109/JBHI.2013.2286455.

Mangukiya, Y., Purohit, B., and George, K. Electromyography EMG sensor controlled assistive orthotic robotic arm for forearm movement. In *2017 IEEE Sensors Applications Symposium (SAS)*. pages 1–4, 2017. doi:10.1109/SAS.2017.7894065.

McDonald, C. G., Dennis, T. A., and O'Malley, M. K. Characterization of surface electromyography patterns of healthy and incomplete spinal cord injury subjects interacting with an upper-extremity exoskeleton. In *2017 International Conference on Rehabilitation Robotics (ICORR)*. pages 164–169, 2017. doi:10.1109/ICORR.2017.8009240.

Mghames, S., Laghi, M., Della Santina, C., Garabini, M., Catalano, M., Grioli, G., and Bicchi, A. Design, control and validation of the variable stiffness exoskeleton FLEXO. In *2017 International Conference on Rehabilitation Robotics (ICORR)*. pages 539–546, 2017. doi:10.1109/ICORR.2017.8009304.

Rahman, M. H., Ochoa-Luna, C., Saad, M., and Archambault, P. EMG based control of a robotic exoskeleton for shoulder and elbow motion assist. *Journal of Automation and Control Engineering*, 2015. 3(4). doi:10.12720/joace.3.4.270-276.

Rosen, J., Brand, M., Fuchs, M. B., and Arcan, M. A myosignal-based powered exoskeleton system. *IEEE Transactions on Systems, Man, and Cybernetics-part A: Systems and humans*, 2001. 31(3):210–222. doi:10.1109/3468.925661.

Sadarangani, G. P. and Menon, C. A preliminary investigation on the utility of temporal features of force myography in the two-class problem of grasp vs. no-grasp in the presence of upper-extremity movements. *Biomedical Engineering online*, 2017. 16(1):59. doi:10.1186/s12938-017-0349-4.

Tang, Z., Zhang, K., Sun, S., Gao, Z., Zhang, L., and Yang, Z. An upper-limb power-assist exoskeleton using proportional myoelectric control. *Sensors*, 2014. 14(4):6677–6694. doi:10.3390/s140406677.

Xiao, Z. G., Elnady, A. M., and Menon, C. Control an exoskeleton for forearm rotation using FMG. In *5th IEEE RAS/EMBS International Conference on Biomedical Robotics and Biomechatronics*. pages 591–596, 2014. doi:10.1109/BIOROB.2014.6913842.

Xiao, Z. G. and Menon, C. Counting grasping action using force myography: an exploratory study with healthy individuals. *JMIR Rehabilitation and Assistive technologies*, 2017. 4(1):e5. doi:10.2196/rehab.6901.

Zhou, L., Bai, S., Andersen, M. S., and Rasmussen, J. Modeling and design of a spring-loaded, cable-driven, wearable exoskeleton for the upper extremity. *Modeling, Identification and Control*, 2015. 36(3):167–177. doi:10.4173/mic.2015.3.4.

Chapter 6

Conclusions

The main objective of this work is to develop motion intention detection methods for assistive exoskeleton control. Performance analysis, upper limb motion detection methods and control of exoskeletons are covered in this work. The performance analysis is performed by comparing FMG with sEMG in terms of accuracy and repeatability. With FMG selected, hand gestures detection and payload estimation methods are developed and tested with healthy subjects. Upon validation, the methods are further tested for the control of upper limb assistive exoskeletons.

6.1 Summary of articles

Paper I

In paper I performance of FMG and sEMG is compared classifying upper limb movements. In this work forearm motions i.e. flexion, extension, pronation, supination and rest state are classified by using NN technique and result of the NN are further compared with four other classification schemes. The study is focused on determining the performance of FMG and sEMG in terms of long term accuracy and repeatability.

In order to determine long term accuracy and data repeatability, forearm motion data is collected for three days. Each day the data is divided into a training and testing dataset. Using the datasets, the results of accuracy and repeatability are first calculated by training NN with 1st day training dataset and then testing it with all three testing datasets. Afterwards, day 2 training data is also included for training NN and performance is computed by testing it again on all three testing datasets. Finally NN is trained with each day training dataset for testing purpose. It is observed that for training and testing datasets collected on same day, sEMG performed better then

FMG. However, for the other days testing datasets FMG showed better results and quite similar to the ones obtained from testing dataset for the given day. Whereas, sEMG performance declined as difference between training and testing dataset day increased.

Overall, results showed that FMG has better performance in repeatability than sEMG, which is very critical for the usability and implementation of assistive exoskeletons in real life tasks.

Paper II

In paper II, forearm FMG data is studied to detect dynamic hand motions, i.e. opening, closing, grasping and steady state, and to determine assistance level when grasping task is detected. In this method two sensor bands are placed on forearm, one near elbow joint and other near wrist. Hand motions are classified by detecting threshold levels, where slope feature extracted from raw FMG data is used to determine these threshold values.

In our daily routine tasks, human grasp objects of different shapes and weight. FMG data obtained varies with the attributes of the grasped object. For such tasks large dataset is required for training a machine learning algorithm. In this study the aforementioned challenge is addressed by proposing a threshold based classifier. The proposed method reduces the need of training data significantly. Moreover, with the detection of grasping task, required grasping assistance is also computed which is proportional to the weight of the object. The method is verified experimentally by testing on human subjects.

The results showed that the hand motions can be classified with very high accuracy, precision and recall. Moreover, the method is also tested to control hand exoskeleton for providing assistance in grasping tasks. Experiment showed that the required assistance level is determined correctly and provided effectively by the exoskeleton to hold the object.

Paper III

In **Paper III**, FMG is used to estimate the carried payload. A sensor band is placed on the upper arm, where four FSR sensors are distributed across the biceps muscle belly. By this way, assistive torques for elbow and shoulder joints that is to be provided using an active exoskeleton are determined.

The method is comprised of training SVM based two regression models in order to map the joint orientation to sensor band readings. One regression model output the sensor band readings in case of free payload and the second outputs the readings for a defined payload. Afterwards, using linear interpolation payload is estimated for the given real-time sensor readings.

The method is validated by testing on healthy subjects. Furthermore, a control strategy is also implemented to provide assistance through an active exoskeleton i.e. active elbow and shoulder joints. The assistance to elbow joint is provided using admittance control and assistance to shoulder is provided by implementing gravity compensation. The results showed that the developed method is able to detect the carried payload and thus assistance provided by exoskeleton helps in reducing the human effort in load carrying task.

6.2 Contributions

Novelty of work presented in this thesis lies in knowledge creation in the field of cHRI based exoskeleton control.

In this thesis a novel method of motion intention detection i.e. FMG, is studied. The studies included performance comparison with sEMG, where long term accuracy and repeatability of both methods is analyzed. FMG based classification and regression techniques for detecting upper limb movements and estimating assistance levels are also developed. The methods are tested with upper limb exoskeletons in order to provide support in load carrying tasks.

Within this PhD thesis, the following contributions are made in reference to the research questions addressed in Sec. 1.4.

- **Rq1:** What muscle activity detection method is suitable for the applications of daily use?

  This research question is addressed in **Paper I**. In this work long term performance comparison analysis of FMG and sEMG is analyzed for classifying dynamic forearm movements. The work showed that of the two methods FMG has better overall accuracy and data repeatability.

- **Rq2:** How can the usability of FMG based classification/regression methods be improved for detecting upper arm movement intent?

  Usability of FMG based motion detection methods is improved by addressing three challenges in **Paper II** and **Paper III**, i.e. requirement of large training dataset, performance degradation caused by donning/doffing and number of sensor for detecting desired movement.

  In **Paper II** threshold based classification approach is implemented to detect hand motions. In this work FMG sensor placement and data was analyzed for object grasping task. Based on the analysis sensor distribution is proposed and slope feature is selected that has shown similar pattern across objects of different attributes. With the proposed

method, requirement of training data is minimized significantly without compromising the motion detection accuracy.

Literature has shown that motion detection performance is degraded by donning/doffing of sensors. In **Paper II** it is demonstrated that the proposed motion detection strategy is not effected by donning/doffing.

In **Paper III** regression approach is used to estimate the carried payload. The proposed method presented the solution for dealing with sensors requirement where only biceps data and arm orientation is required to determine payload. The estimated payload can then be used to control multi-DOF exoskeleton assistance level.

- **Rq3:** How can FMG based motion detection methods be integrated into exoskeletons for intelligent physical assistance in load carrying tasks?

  Methods to control upper body assistive exoskeletons i.e. hand and elbow/shoulder are demonstrated in **Paper II** and **III**, respectively. In **Paper II** with the detection of grasping task, FMG data is further processed to implement proportional force control technique. In **Paper III** the estimated payload information is used to determine assistive torque, which is further regulated using admittance control strategy for elbow joint support. Whereas, assistance to shoulder joint is provided by adapting gravity model to the estimated payload.

  In **Paper II** the increase in grasping force, measured through force sensors at fingertips, was used to realize the physical assistance. Whereas, in **Paper III** the results of physical assistance were verified by observing the reduction in muscle activity.

From the findings and contributions of this thesis, it can be concluded that the hypothesis "FMG can effectively and efficiently detect upper limb motion intention in order to control upper limb exoskeleton for providing physical assistance in load carrying tasks" is experimentally confirmed.

6.3 Limitations and future work

In the previous section, contributions made in this thesis were presented. The studies have shown promising results of using FMG for upper limb motion detection and assistive exoskeleton control by addressing the challenges identified in Sec. 1.3. However, the FMG sensing method still requires validations from many other perspectives in order to apply it in real environment. For that purpose, following are the limitations of this work identified and based on that future works are recommended:

- In **Paper I**, comparison of FMG and sEMG is presented.

  - The pronation/supination movement was only performed at fully extended elbow position Furthermore, fingers were also kept in extended position all the time. Further investigation is needed by extending the data collection protocol i.e. including more elbow positions for pronation/supination, varying movement speed and keeping hand in rest state.
  - Average output of FSR sensors was used for FMG features extraction. The approach makes the classification algorithm computationally less expensive but using each FSR as a separate input can improve the performance furthermore.

- In **Paper II**, hand motion detection and grasping assistance method is developed. Some limitations and future work related to this study are presented here.

  - In the experiments of grasping assistance sensor bands and hand exoskeleton were not worn on the same hand. It was hypothesized that the hand exoskeleton is of soft nature and it will not affect the dynamics of the muscle activity when worn on the same hand as FMG sensors. However, the performance validation of the hand motion detection and grasping assistance by wearing the exoskeleton on the same hand requires more testing.
  - In this work hand motions i.e. opening, closing, grasping and rest state are detected by applying threshold based classification method. These threshold levels can be registered for other hand/ wrist movements i.e. wrist flexion/extension, wrist rotation and forearm pronation/supination etc. In order to apply the developed method in actual environment advanced algorithms are required that can distinguish between all these motions. With advanced algorithms, requirement of training data will increase and in turn it will affect the usability of developed method in work environment. On the other hand, sensor fusion techniques, combining FMG and IMU, can be the most suitable approach to tackle this problem. IMU placed at back of the palm can register all of the motions performed by wrist and forearm. Developing a generalized machine learning algorithm using IMU is thus possible with high intra and inter-subject repeatability.

- In **Paper III**, a method for payload estimation is presented. Limitation and future work directions of this study are as follows.

  - In this work experiments were performed for static load handling tasks. Muscle activities caused by dynamic movements and co-contractions can cause estimation errors. A classification algorithm

that can detect aforementioned muscle activities are required. Based on the detected activity, parameters of estimation model can be modified to obtain correct results.

- The experiments of payload assistance were carried out with one subject. The experiment was performed to validate that with correct payload estimation, assistance can be provided with the help of exoskeleton. However, in this experiment weight of the exoskeleton was supported by stand, not carried by the human. When exoskeleton is worn by human subject, muscle dynamics will change and modification in payload estimation algorithm will be required. Therefore, validation of correct payload estimation while wearing exoskeleton needs testing with more subjects.
- Payload estimation algorithm requires weight lifting task at multiple joint angles. Performing these tasks properly is physically challenging. Therefore, few positions were considered for collecting training data. Including training data from more joint angles can improve the results but it comes with the expense of increased physical effort and fatigue. Furthermore, fatigue can cause collection of incorrect training data and in turn poor estimation. Advanced calibration and estimation algorithms are thus required to improve payload estimation accuracy without the need of increasing physical effort in collection of training data.

- Lastly, related to overall thesis work following future works are proposed.

  - Performance analysis were carried out with healthy subjects. Furthermore, the tasks were performed in controlled environment. When the technology is implemented at actual work places people can have different muscle volumes and attributes. Moreover, age factor can also have influence on the performance. Therefore, further investigation is required considering such conditions. The results can provide more insight to make robust and stable detection using FMG.
  - FMG is relatively a new domain to detect limb movements. It's performance can be influenced by varying the size and number of sensors. Therefore, studies on optimizing number and size of sensors can facilitate AI with more information in order to improve convenience and applicability in actual environment.

Bibliography

[1] S. Bai, S. Christensen, M. Islam, S. Rafique, N. Masud, P. Mattsson, L. O'Sullivan, and V. Power, "Development and testing of full-body exoskeleton AXO-SUIT for physical assistance of the elderly," in *International Symposium on Wearable Robotics*, 2018, pp. 180–184.

[2] J. C. Perry, J. Rosen and S. Burns, "Upper-limb powered exoskeleton design," *IEEE/ASME Transactions on Mechatronics*, vol. 12, no. 4, pp. 408–417, 2007.

[3] G. Chen, C. K. Chan, Z. Guo and H. Yu, "A review of lower extremity assistive robotic exoskeletons in rehabilitation therapy," *Critical Review in Biomedical Engineering*, vol. 41, no. 4–5, 2013.

[4] N. Rehmat, J. Zuo, W. Meng, Q. Liu, S. Q. Xie and H. Liang, "Upper limb rehabilitation using robotic exoskeleton systems: a systematic review," *International Journal of Intelligent Robotics and Applications*, vol. 2, no. 3, pp. 283–295, 2018.

[5] R. Bogue, "Exoskeletons–a review of industrial applications, "*Industrial Robot: An International Journal*, vol. 45, no. 5, pp. 585–590, 2018.

[6] K. Kong and D. Jeon, "Design and control of an exoskeleton for the elderly and patients," *IEEE/ASME Transactions on Mechatronics*, vol. 11, no. 4, pp. 428–432, 2006.

[7] T. Bosch, J. V. Eck, K. Knitel, and M. de Looze, "The effects of a passive exoskeleton on muscle activity, discomfort and endurance time in forward bending work," *Applied Ergonomics*, vol. 54, pp. 212–217, 2016.

[8] J. L. Pons, "Wearable robots: biomechatronic exoskeletons," *John Wiley and Sons*, 2008.

[9] M. A. Gull, S. Bai, and T. Bak, "A review on design of upper limb exoskeletons," *Robotics*, vol. 9, no. 1, pp. 16, 2020.

[10] S. Kim, M. A. Nussbaum, M. I. M. Esfahani, M. M. Alemi, B. Jia, and E. Rashedi, "Assessing the influence of a passive, upper extremity exoskeletal vest for tasks requiring arm elevation: part II–"unexpected" effects on shoulder motion, balance, and spine loading," *Applied Ergonomics*, vol. 70, pp. 323–330, 2018.

[11] I. Pacifico, A. Scano, E. Guanziroli, M. Moise, L. Morelli, A. Chiavenna, D. Romo, S. Spada, G. Colombina, F. Molteni *et al.*, "An experimental evaluation of the Proto-MATE: a novel ergonomic upper-limb exoskeleton to reduce workers' physical strain," *IEEE Robotics & Automation Magazine*, vol. 27, no. 1, pp. 54–65, 2020.

[12] I. de Looij, "Modeling and altering the force profile of a spring-based upper body exoskeleton with design adjustments," *Master thesis, Delft University of Technology*, 2017.

[13] T. Rahman, W. Sample, S. Jayakumar, M. M. King *et al.*, "Passive exoskeletons for assisting limb movement," *Journal of Rehabilitation Research and Development*, vol. 43, no. 5, p. 583, 2006.

[14] C. Lambelet, M Lyu, D. Woolley, R. Gassert, and N. Wenderoth, "The eWrist—A wearable wrist exoskeleton with sEMG-based force control for stroke rehabilitation," in *Proceedings of International Conference on Rehabilitation Robotics*, 2017, pp. 726–733.

[15] M. Nilsson, J. Ingvast, J. Wikander, and H. von Holst, "The soft extra muscle system for improving the grasping capability in neurological rehabilitation," in *IEEE-EMBS Conference on Biomedical Engineering and Sciences*, 2012, pp. 412–417.

[16] A. Ebrahimi, D. Gröninger, R. Singer, and U. Schneider, "Control parameter optimization of the actively powered upper-body exoskeleton using subjective feedbacks," in *IEEE International Conference on Control, Automation and Robotics*, 2017, pp. 432–437.

[17] J. C. Perry, J. Rosen, and S. Burns, "Upper-limb powered exoskeleton design," *IEEE/ASME Transactions on Mechatronics*, vol. 12, no. 4, pp. 408–417, 2007.

[18] R. A. R. C. Gopura, K. Kiguchi, and Y. Li, "Sueful-7: A 7dof upper-limb exoskeleton robot with muscle-model-oriented EMG-based control," in *IEEE/RSJ International Conference on Intelligent Robots and Systems*, 2009, pp. 1126–1131.

[19] M. A. Gull, M. Thoegersen, S. H. Bengtson, M. Mohammadi *et al.*, "A 4-DOF upper limb exoskeleton for physical assistance: design,

modeling, control and performance evaluation," *Applied Sciences*, vol. 11, no. 13, pp. 5865, 2021.

[20] F. Xiao, Y. Gao, Y. Wang, Y. Zhu, and J. Zhao, "Design of a wearable cable-driven upper limb exoskeleton based on epicyclic gear trains structure," *Technology and Health Care*, vol. 25, no. S1, pp. 3–11, 2017.

[21] M. Gunasekara, R. Gopura, and S. Jayawardena, "6-REXOS: upper limb exoskeleton robot with improved pHRI," *International Journal of Advanced Robotic Systems*, vol. 12, no. 4, pp. 47, 2015.

[22] J. A. French, C. G. Rose, and M. K. O'malley, "System characterization of MAHI EXO-II: A robotic exoskeleton for upper extremity rehabilitation," in *Dynamic Systems and Control Conference*, 2014.

[23] A. Toth, G. Fazekas, G. Arz, M. Jurak, and M. Horvath, "Passive robotic movement therapy of the spastic hemiparetic arm with REHAROB: report of the first clinical test and the follow-up system improvement," in *IEEE International Conference on Rehabilitation Robotics*, 2005, pp. 127–130.

[24] L. Pignolo, L. L. Lucca, G. Basta, S. Serra, M. E. Pugliese, W. G. Sannita, and G. Dolce, "A new treatment in the rehabilitation of the paretic upper limb after stroke: the ARAMIS prototype and treatment protocol," *Annali Dell'Istituto Superiore Di Sanita*, vol. 52, no. 2, pp. 301–308, 2016.

[25] A. Otten, C. Voort, A. Stienen, R. Aarts, E. Van Asseldonk, and H. van der Kooij, "LIMPACT: a hydraulically powered self-aligning upper limb exoskeleton," *IEEE/ASME Transactions on Mechatronics*, vol. 20, no. 5, pp. 2285–2298, 2015.

[26] H. S. Park, Y. Ren, and L. Q. Zhang, "IntelliArm: An exoskeleton for diagnosis and treatment of patients with neurological impairments," in *IEEE RAS & EMBS International Conference on Biomedical Robotics and Biomechatronics*, 2008, pp. 109–114.

[27] E. Rocon, J.B. Lois, A. Ruiz, M. Manto, J. C. Moreno, and J. L. Pons, "Design and validation of a rehabilitation robotic exoskeleton for tremor assessment and suppression," *IEEE Transactions on Neural Systems and Rehabilitation Engineering*, vol. 15, no. 3, pp. 367–378, 2007.

[28] S. H. Chen, W. M. Lien, W. W. Wang, G. D. Lee, L. C. Hsu, K. W. Lee, S. Y. Lin, C. H. Lin, L. C. Fu, J. S. Lai *et al.*, "Assistive control system for upper limb rehabilitation robot," *IEEE Transactions on Neural Systems and Rehabilitation Engineering*, vol. 24, no. 11, pp. 1199–1209, 2016.

[29] S. J. Housman, V. Le, T. Rahman, R. J. Sanchez, and D. J. Reinkensmeyer, "Arm-training with T-WREX after chronic stroke: preliminary results of a randomized controlled trial," in *IEEE International Conference on Rehabilitation Robotics*, 2007, pp. 562–568.

[30] T. Nef, M. Guidali, and R. Riener, "ARMin III–arm therapy exoskeleton with an ergonomic shoulder actuation," *Applied Bionics and Biomechanics*, vol. 6, no. 2, pp. 127–142, 2009.

[31] R. Wei, S. Balasubramanian, L. Xu, and J. He, "Adaptive iterative learning control design for RUPERT IV," in *IEEE RAS & EMBS International Conference on Biomedical Robotics and Biomechatronics*, 2008, pp. 647–652.

[32] J. Huang, W. Huo, W. Xu, S. Mohammed, and Y. Amirat, "Control of upper-limb power-assist exoskeleton using a human-robot interface based on motion intention recognition," *IEEE Transactions on Automation Science and Engineering*, vol. 12, no. 4, pp. 1257–1270, 2015.

[33] M. Baklouti, P. A. Guyot, E. Monacelli, and S. Couvet, "Force controlled upper-limb powered exoskeleton for rehabilitation," in *IEEE/RSJ International Conference on Intelligent Robots and Systems*, pp. 78140, 2008.

[34] W. Huo, J. Huang, Y. Wang, J. Wu, and L. Cheng, "Control of upper-limb power-assist exoskeleton based on motion intention recognition," in *Proceedings IEEE International Conference on Robotics and Automation*, 2011, pp. 2243–2248.

[35] K. Abbruzzese, D. Lee, A. Swedberg, H. Talasan, and M. Paliwal, "An innovative design for an assistive arm orthosis for stroke and muscle dystrophy," in *IEEE Annual Northeast Bioengineering Conference*, 2011, pp. 1–2.

[36] H. D. Lee, B. K. Lee, W. S. Kim, J. S. Han, K. S. Shin, and C. S. Han, "Human-robot cooperation control based on a dynamic model of an upper limb exoskeleton for human power amplification," *Mechatronics*, vol. 24, no. 2, pp. 168–176, 2014.

[37] X. Cui, W. Chen, X. Jin, and S. K. Agrawal, "Design of a 7-DOF cable-driven arm exoskeleton (CAREX-7) and a controller for dexterous motion training or assistance," *IEEE/ASME Transactions on Mechatronics*, vol.22, no.1, pp. 161–172, 2016.

[38] L. M. Miller, and J. Rosen, "Comparison of multi-sensor admittance control in joint space and task space for a seven degree of freedom

upper limb exoskeleton," in *IEEE RAS and EMBS International Conference on Biomedical Robotics and Biomechatronics*, 2010, pp. 70–75.

[39] Z. Li, and S. Bai, "A novel revolute joint of variable stiffness with reconfigurability," *Mechanism and Machine Theory*, vol. 133, pp. 720–736, 2019.

[40] Z. Li, S. Bai, O. Madsen, W. Chen, and J. Zhang, "Design, modeling and testing of a compact variable stiffness mechanism for exoskeletons," *Mechanism and Machine Theory*, vol. 151, pp. 103905, 2020.

[41] B. G. Mendoza, G. S. Ante, and J. M. Antelis, "Detecting the intention to move upper limbs from electroencephalographic brain signals." *Computational and Mathematical Methods in Medicine*, vol. 2016, pp. 3195373, 2016.

[42] E. Lew, R. Chavarriaga, S. Silvoni, and J. D. R. Millán, "Detection of self-paced reaching movement intention from EEG signals," *Frontiers in Neuroengineering*, vol. 5, p. 13, 2012.

[43] K. Li, X. Zhang, and Y. Du, "A SVM based classification of EEG for predicting the movement intent of human body," in *International Conference on Ubiquitous Robots and Ambient Intelligence*, 2013, pp. 402–406.

[44] Y. Wang and S. Makeig, "Predicting intended movement direction using EEG from human posterior parietal cortex." in *International Conference on Foundations of Augmented Cognition*, 2009, pp. 437–446.

[45] D. S. V. Bandara, J. Arata, and K. Kigichi, "Task based motion intention prediction with EEG signals," in *IEEE International Symposium on Robotics and Intelligent Sensors*, 2016, pp. 57–60.

[46] Y. Hayashi, "Estimation of upper-limb motion in sagittal plane based on EEG signals," in *International Conference on Soft Computing and Intelligent Systems and International Symposium on Advanced Intelligent Systems*, 2014, pp. 1229–1232.

[47] K. Nojiri and F. Iwane, "Motion direction estimation of walking base on EEG signal," in *IEEE/ASME International Conference on Advanced Intelligent Mechatronics*, 2014, pp. 542–547.

[48] D. Planelles, E. Hortal, A. Costa, A. Ubeda, E. Iáez, and J. M. Azorín, "Evaluating classifiers to detect arm movement intention from EEG signals." *Sensors*, vol. 14, no. 10, pp. 172–186, 2014.

[49] X. Chen, X. Zhang, Z. Y. Zhao, J. H. Yang, V. Lantz, and K. Q. Wang, "Multiple hand gesture recognition based on surface EMG signal," in *International Conference on Bioinformatics and Biomedical Engineering*, 2007, pp. 506–509.

[50] C. Sapsanis, G. Georgoulas, and A. Tzes, "EMG based classification of basic hand movements based on time frequency features," in *Mediterranean Conference on Control and Automation*, 2013, pp. 716–722.

[51] Y. Fang, H. Liu, G. Li, and X. Zhu, "A multichannel surface EMG system for hand motion recognition," *International Journal of Humanoid Robotics*, vol. 12, no. 2, pp. 1–13, 2015.

[52] W. Geng, Y. Du, W. Jin, W. Wei, Y. Hu, and J. Li, "Gesture recognition by instantaneous surface EMG images," *Scientific Reports*, vol. 6, pp. 6–13, 2016.

[53] A. Boyali, N. Hashimoto, and O. Matsumoto, "Hand posture and gesture recognition using MYO armband and spectral collaborative representation based classification," in *IEEE Global Conference on Consumer Electronics*, 2016, pp. 200–201.

[54] G. Pomboza-Junez and J. Holgado-Terriza, "Hand gesture recognition based on EMG signals using ANN," *International Journal of Computer Application*, vol. 2, no. 3, pp. 31–39, 2016.

[55] Y. Du, Y. Wong, W. Jin, W. Wei, Y. Hu, M. Kankanhalli, and W. Geng, "Semi-supervised learning for surface EMG-based gesture recognition," in *International Joint Conference on Artificial Intelligence*, 2017, pp. 1624–1630.

[56] M. Tavakoli, C. Benussi, P. A. Lopes, L. B. Osorio, and A. T. de Almeida, "Robust hand gesture recognition with a double channel surface EMG wearable armband and SVM classifier," *Biomedical Signal Processing and Control*, vol. 46, pp. 121–130, 2018.

[57] P. Tsinganos, B. Cornelis, J. Cornelis, B. Jansen, and A. Skodras, "Deep learning in EMG-based gesture recognition," in *Proceedings of the International Conference on Physiological Computing Systems*, 2018, pp. 107–114.

[58] E. Noce, A. D. Bellingegni, A. L. Ciancio, R. Sacchetti, A. Davalli, E. Guglielmelli, and L. Zollo, "EMG and ENG-envelope pattern recognition for prosthetic hand control," *Journal of Neuroscience Methods*, vol. 311, pp. 38–46, 2019.

[59] J. Qi, G. Jiang, G. Li, Y. Sun, and B. Tao, "Intelligent human-computer interaction based on surface EMG gesture recognition," *IEEE Access*, vol. 7, pp. 378–387, 2019.

[60] H. Namazi, "Decoding of hand gestures by fractal analysis of electromyography (EMG) signal," *Fractals*, vol. 27, no. 3, 2019.

[61] Y. Mangukiya, B. Purohit, and K. George, "Electromyography(EMG) sensor controlled assistive orthotic robotic arm for forearm movement," in *IEEE Proceedings Sensors Applications Symposium*, 2017, pp. 1–4.

[62] A. Accogli, L. Grazi, S. Crea, A. Panarese, J. Carpaneto, N. Vitiello, and S. Micera, "EMG-based detection of user's intentions for human-machine shared control of an assistive upper-limb exoskeleton," in *Wearable Robotics: Challenges and Trends*,2017, pp. 181–185.

[63] J. Camargo and A. Young, "Feature selection and non-Linear classifiers: effects on simultaneous motion recognition in upper limb," *IEEE Transactions on Neural Systems and Rehabilitation Engineering*, vol. 27, no. 4, pp. 743–750, 2019.

[64] A. Ameri, M. A. Akhaee, E. Scheme, and K. Englehart, "Regression convolutional neural network for improved simultaneous EMG control," *Journal of Neural Engineering*, vol. 16, no. 3, 2019.

[65] J. G. Ngeo, T. Tamei, and T. Shibata, "Continuous and simultaneous estimation of finger kinematics using inputs from an EMG-to-muscle activation model," *Journal of NeuroEngineering and Rehabilitation*, vol. 11, no. 1, pp. 122, 2014.

[66] L. H. Smith and L. J. Hargrove, "Comparison of surface and intramuscular EMG pattern recognition for simultaneous wrist/hand motion classification," in *Proceedings of the Annual International Conference of the IEEE Engineering in Medicine and Biology Society*, 2013, pp. 4223–4226.

[67] L. H. Smith, T. A. Kuiken, and L. J. Hargrove, "Real-time simultaneous and proportional myoelectric control using intramuscular EMG," *Journal of Neural Engineering*, vol. 11, no. 6, 2014.

[68] A. J. Young, S. Member, L. H. Smith, E. J. Rouse, and L. J. Hargrove, "Surface EMG pattern recognition," *IEEE Transactions on Biomedical Engineering*, vol. 60, no. 5, pp. 1250–1258, 2013.

[69] J. O. Pinzón-Arenas, R. Jiménez-Moreno, and J. E. Herrera-Benavides, "Convolutional neural network for hand gesture recognition using 8 different EMG signals," in *Symposium on Image, Signal Processing and Artificial Vision*, 2019.

[70] S. Rawat, S. Vats, and P. Kumar, "Evaluating and exploring the MYO ARMBAND," in *IEEE International conference system modeling and advancement in research trends*, 2016, pp. 115–120.

[71] M. A. Abu, S. Rosleesham, M. Z. Suboh, M. S. M. Yid, Z. Kornain, and N. F. Jamaluddin, "Classification of EMG signal for multiple hand gestures based on neural network," *Indonesian Journal of Electrical Engineering and Computer Science*, vol. 17, no. 1, pp. 256–263, 2019.

[72] I. Batzianoulis, S. El-Khoury, E. Pirondini, M. Coscia, S. Micera, and A. Billard, "EMG-based decoding of grasp gestures in reaching-to-grasping motions," *Robotics and Autonomous Systems*, vol. 91, pp. 59–70, 2017.

[73] D. Leonardis, M. Barsotti, C. Loconsole, M. Solazzi, M. Troncossi, C. Mazzotti, V. P. Castelli, C. Procopio, G. Lamola, C. Chisari, M. Bergamasco, and A. Frisoli, "An EMG-controlled robotic hand exoskeleton for bilateral rehabilitation," *IEEE Transactions on Haptics*, vol. 8, no. 2, pp. 140–151, 2015.

[74] P. K. Artemiadis and K. J. Kyriakopoulos, "Estimating arm motion and force using EMG signals: on the control of exoskeletons," in *EEE/RSJ International Conference on Intelligent Robots and Systems*, 2008, pp. 22–26.

[75] J. B. Ullauri, L. Peternel, B. Ugurlu, Y. Yamada, and J. Morimoto, "On the EMG-based torque estimation for humans coupled with a force-controlled elbow exoskeleton," in *Proceedings of International Conference on Advanced Robotics*, 2015, pp. 302–307.

[76] M. H. Rahman, C. Ochoa-luna, M. Saad, and P. Archambault, "EMG based control of a robotic exoskeleton for shoulder and elbow motion assist," *Engineering and Technology Publishing*, vol. 3, no. 4, pp. 270–276, 2015.

[77] Z. Li, B. Wang, F. Sun, C. Yang, Q. Xie, and W. Zhang, "sEMG-based joint force control for an upper-limb power-assist exoskeleton robot," *IEEE Journal of Biomedical and Health Informatics*, vol. 18, no. 3, pp. 1043–1050, 2014.

[78] A. Samadani, "Gated recurrent neural networks for EMG-based hand gesture classification. A comparative study," in *Proceedings of the Annual International Conference of the IEEE Engineering in Medicine and Biology Society*, 2018, pp. 1–4.

[79] M. V. Arteaga, J. C. Castiblanco, I. F. Mondragon, J. D. Colorado, and C. Alvarado-Rojas, "EMG-driven hand model based on the classification of individual finger movements," *Biomedical Signal Processing and Control*, vol. 58, pp. 101834, 2020.

[80] X. Chen and Z. J. Wang, "Pattern recognition of number gestures based on a wireless surface EMG system," *Biomedical Signal Processing and Control*, vol. 8, no. 2, pp. 184–192, 2013.

[81] A. S. Kundu, O. Mazumder, P. K. Lenka, and S. Bhaumik, "Hand gesture recognition based omnidirectional wheelchair control using IMU and EMG sensors," *Journal of Intelligent and Robotic Systems: Theory and Applications*, vol. 91, no. 3-4, pp. 529–541, 2018.

[82] J. Wu, Z. Tian, L. Sun, L. Estevez, and R. Jafari, "Real-time american sign language recognition using wrist-worn motion and surface EMG sensors," in *IEEE International Conference on Wearable and Implantable Body Sensor Networks*, 2015, pp. 1–6.

[83] X. Chen, X. Zhang, Z. Y. Zhao, J. H. Yang, V. Lantz, and K. Q. Wang, "Hand gesture recognition research based on surface EMG sensors and 2D-accelerometers," *Proceedings of International Symposium on Wearable Computers*, 2007, pp. 11–14.

[84] M. Sakr and C. Menon, "Exploratory evaluation of the force myography (FMG) signals usage for admittance control of a linear actuator," in *Proceedings of the IEEE RAS and EMBS International Conference on Biomedical Robotics and Biomechatronics*, 2018, pp. 903–908.

[85] Z. G. Xiao and C. Menon, "Does force myography recorded at the wrist correlate to resistance load levels during bicep curls?" *Journal of Biomechanics*, vol. 83, pp. 310–314, 2019.

[86] M. Sakr, X. Jiang, and C. Menon, "Estimation of user-applied isometric force/torque using upper extremity force myography," *Frontiers in Robotics and AI*, vol. 6, pp. 1–15, 2019.

[87] D. Yang, N. Chhatre, F. Campi, and C. Menon, "Feasibility of support vector machine gesture classification on a wearable embedded device," in *Canadian Conference on Electrical and Computer Engineering*, 2016, pp. 1–4.

[88] Z. G. Xiao and C. Menon, "Performance of forearm FMG and sEMG for estimating elbow, forearm and wrist positions," *Journal of Bionic Engineering*, vol. 14, no. 2, pp. 284–295, 2017.

[89] M. L. Delva, M. Sakr, R. S. Chegani, M. Khoshnam, and C. Menon, "Investigation into the potential to create a force myography-based smart-home controller for aging populations," in *IEEE International Conference on Biomedical Robotics and Biomechatronics* , 2018, pp. 770–775.

[90] N. Ha, G. P. Withanachchi, and Y. Yihun, "Performance of forearm FMG for estimating hand gestures and prosthetic hand control," *Journal of Bionic Engineering*, vol. 16, no. 1, pp. 88–98, 2019.

[91] C. Ahmadizadeh, B. Pousett, and C. Menon, "Investigation of channel selection for gesture classification for prosthesis control using force myography: a case study," *Frontiers in Bioengineering and Biotechnology*, vol. 7, pp. 1–15, 2019.

[92] A. T. Belyea, K. B. Englehart, and E. J. Scheme, "A proportional control scheme for high density force myography," *Journal of Neural Engineering*, vol. 15, no. 4, 2018.

[93] X. Jiang, L. K. Merhi, and C. Menon, "Force exertion affects grasp classification using force myography," *IEEE Transactions on Human-Machine Systems*, vol. 48, no. 2, pp. 219–226, 2018.

[94] M. Wininger, N. H. Kim, and W. Craelius, "Pressure signature of forearm as predictor of grip force," *Journal of Rehabilitation Research and Development*, vol. 45, no. 6, pp. 883–892, 2008.

[95] M. Sakr and C. Menon, "Regressing force-myographic signals collected by an armband to estimate torque exerted by the wrist: A preliminary investigation," in *Canadian Conference on Electrical and Computer Engineering*, 2016, pp. 1–4.

[96] M. Sakr and C. Menon, "On the estimation of isometric wrist / forearm torque about three axes using force myography," in *IEEE International Conference on Biomedical Robotics and Biomechatronics*, 2016, pp. 827–832.

[97] M. Sakr and C. Menon, "Study on the force myography sensors placement for robust hand force estimation," in *IEEE International Conference on Systems, Man, and Cybernetics*, 2017, pp. 1387–1392.

[98] R. Chengani, M. L. Delva, M. Sakr, and C. Menon, "Pilot study on strategies in sensor placement for robust hand/wrist gesture classification based on movement related changes in forearm volume," in *IEEE Healthcare Innovation Point-of-Care Technologies Conference*, 2016, pp. 46–49.

[99] E. Cho, R. Chen, L. K. Merhi, Z. Xiao, B. Pousett, and C. Menon, "Force myography to control robotic upper extremity prostheses: A feasibility study," *Frontiers in Bioengineering and Biotechnology*, vol. 4, pp. 1–12, 2016.

[100] Z. G. Xiao and C. Menon, "Counting grasping action using force myography: an exploratory study with healthy individuals," *JMIR Rehabilitation and Assistive Technologies*, vol. 4, no. 1, 2017.

[101] M. Anvaripour and M. Saif, "Hand gesture recognition using force myography of the forearm activities and optimized features," in *Proceedings of the IEEE International Conference on Industrial Technology*, 2018, pp. 187–192.

[102] G. P. Sadarangani and C. Menon, "A preliminary investigation on the utility of temporal features of force myography in the two-class problem of grasp vs. no-grasp in the presence of upper-extremity movements," *BioMedical Engineering OnLine*, vol. 16, no. 1, p. 59, 2017.

[103] X. Jiang, Z. G. Xiao, and C. Menon, "Virtual grasps recognition using fusion of leap motion and force myography," *Virtual Reality*, vol. 22, no. 4, pp. 297–308, 2018.

[104] A. Radmand, E. Scheme, and K. Englehart, "High-density force myography: A possible alternative for upper-limb prosthetic control," *Journal of Rehabilitation Research and Development*, vol. 53, no. 4, pp. 443–456, 2016.

[105] D. Ferigo, L. K. Merhi, B. Pousett, Z. G. Xiao, and C. Menon, "A case study of a Force-myography controlled bionic hand mitigating limb position effect," *Journal of Bionic Engineering*, vol. 14, no. 4, pp. 692–705, 2017.

[106] Z. G. Xiao and C. Menon, "A review of force myography research and development," *Sensors*, vol. 19, no. 20, 2019.

[107] R. Singh, S. Chatterji, and A. Kumar, "Trends and challenges in EMG based control scheme of exoskeleton robots-a review," *Int J Sci Eng Res*, vol. 3, no. 9, pp. 933–40, 2012.

[108] Z. G. Xiao and C. Menon, "Performance of forearm FMG and sEMG for estimating elbow , forearm and wrist Positions," *Journal of Bionic Engineering*, vol. 14, no. 2, pp. 284–295, 2017.

[109] X. Jiang, L. K. Merhi, Z. G. Xiao, and C. Menon, "Exploration of force myography and surface electromyography in hand gesture classification," *Medical Engineering and Physics*, vol. 41, pp. 63–73, 2017.

[110] V. Ravindra and C. Castellini, "A comparative analysis of three non-invasive human-machine interfaces for the disabled," *Frontiers in Neurorobotics*, vol. 8, pp. 1–10, 2014.

[111] M. Connan, E. R. Ramírez, B. Vodermayer, and C. Castellini, "Assessment of a wearable force- and electromyography device and comparison of the related signals for myocontrol," vol. 10, pp. 1–13, 2016.

[112] J. Sanford, R. Patterson, and D. O. Popa, "Concurrent surface electromyography and force myography classification during times of prosthetic socket shift and user fatigue," *Journal of Rehabilitation and Assistive Technologies*, vol. 4, pp. 1–13, 2017.

[113] M. Nowak, T. Eiband, and C. Castellini, "Multi-modal myocontrol : testing combined force- and electromyography," in *International Conference on Rehabilitation Robotics* , 2017, pp. 1364–1368.

[114] D. Tkach, H. Huang, and T. A. Kuiken, "Study of stability of time-domain features for electromyographic pattern recognition," *Journal of NeuroEngineering and Rehabilitation*, vol. 7, no. 1, pp. 1–13, 2010.

[115] G. Sadarangani, X. Jiang, L. Simpson, J. Eng, and C. Menon, "Force myography for monitoring grasping in individuals with stroke with mild to moderate upper-extremity impairments: a preliminary investigation in a controlled environment," *Frontiers in Bioengineering and Biotechnology*, vol. 5, pp. 1–11, 2017.

[116] E. Scheme, A. Fougner, Stavdahl, A. D. Chan, and K. Englehart, "Examining the adverse effects of limb position on pattern recognition based myoelectric control," in *Annual International Conference of the IEEE Engineering in Medicine and Biology Society*, 2010, pp. 6337–6340.

[117] L. Chen, Y. Geng, and G. Li, "Effect of upper-limb positions on motion pattern recognition using electromyography," in *Proceedings of International Congress on Image and Signal Processing*, 2011, pp. 139–142.

[118] R. N. Khushaba, A. Al-Timemy, S. Kodagoda, and K. Nazarpour, "Combined influence of forearm orientation and muscular contraction on EMG pattern recognition," *Expert Systems with Applications*, vol. 61, pp. 154–161, 2016.

[119] A. Fougner, E. Scheme, A. D. Chan, K. Englehart, and Ø. Stavdahl, "Resolving the limb position effect in myoelectric pattern recognition," *IEEE Transactions on Neural Systems and Rehabilitation Engineering*, vol. 19, no. 6, pp. 644–651, 2011.

[120] P. Kaufmann, K. Englehart, and M. Platzner, "Fluctuating EMG signals: investigating long-term effects of pattern matching algorithms," in *Annual International Conference of the IEEE Engineering in Medicine and Biology Society*, 2010, pp. 6357–6360.

[121] J. He, D. Zhang, X. Sheng, and X. Zhu, "Effects of long-term myoelectric signals on pattern recognition," *Lecture Notes in Computer Science*, vol. 8102, pp. 396–404, 2013.

[122] S. Amsuss, L. P. Paredes, N. Rudigkeit, B. Graimann, M. J. Herrmann, and D. Farina, "Long term stability of surface EMG pattern classification for prosthetic control," in *Proceedings of the Annual International Conference of the IEEE Engineering in Medicine and Biology Society*, 2013, pp. 3622–3625.

[123] A. Waris, I. K. Niazi, M. Jamil, O. Gilani, K. Englehart, W. Jensen, M. Shafique, and E. N. Kamavuako, "The effect of time on EMG classification of hand motions in able-bodied and transradial amputees," *Journal of Electromyography and Kinesiology*, vol. 40, pp. 72–80, 2018.

[124] S. Amsuss, P. M. Goebel, N. Jiang, B. Graimann, L. Paredes, and D. Farina, "Self-correcting pattern recognition system of surface EMG signals for upper limb prosthesis control," *IEEE Transactions on Biomedical Engineering*, vol. 61, no. 4, pp. 1167–1176, 2014.

[125] A. Phinyomark, F. Quaine, S. Charbonnier, C. Serviere, F. T. Bernard, and Y. Laurillau, "EMG feature evaluation for improving myoelectric pattern recognition robustness," *Expert Systems with Applications*, vol. 40, no. 12, pp. 4832–4840, 2013.

[126] K. Kiguchi and Y. Hayashi, "An EMG-based control for an upper-limb power-assist exoskeleton robot," *IEEE Transactions on Systems, Man, and Cybernetics, Part B: Cybernetics*, vol. 42, no. 4, pp. 1064–1071, 2012.

[127] Z. Li, B. Wang, F. Sun, C. Yang, Q. Xie, and W. Zhang, "sEMG-based joint force control for an upper-limb power-assist exoskeleton robot," *IEEE Journal of Biomedical and Health Informatics*, vol. 18, no. 3, pp. 1043–1050, 2014.

[128] Z. Tang, K. Zhang, S. Sun, Z. Gao, L. Zhang, Z. Yang, Z. Tang, K. Zhang, S. Sun, Z. Gao, L. Zhang, and Z. Yang, "An upper-limb power-assist exoskeleton using proportional myoelectric control," *Sensors*, vol. 14, no. 4, pp. 6677–6694, 2014.

[129] L. Peternel, T. Noda, T. Petrič, A. Ude, J. Morimoto, and J. Babič, "Adaptive control of exoskeleton robots for periodic assistive behaviours based on EMG feedback minimisation," *PLoS ONE*, vol. 11, no. 2, pp. 1–26, 2016.

[130] G. C. Luh, J. J. Cai, and Y. S. Lee, "Estimation of elbow motion intension under varing weight in lifting movement using an EMG-Angle neural network model," in *Proceedings of 2017 International Conference on Machine Learning and Cybernetics, ICMLC 2017*, vol. 2, pp. 640–645, 2017.

[131] Z. Li, Z. Huang, W. He, and C. Y. Su, "Adaptive impedance control for an upper limb robotic exoskeleton using biological signals," *IEEE Transactions on Industrial Electronics*, vol. 64, no. 2, pp. 1664–1674, 2017.

[132] S. Mghames, M. Laghi, C. D. Santina, M. Garabini, M. Catalano, G. Grioli, and A. Bicchi, "Design, control and validation of the variable stiffness exoskeleton FLExo," in *International Conference on Rehabilitation Robotics*, 2017, pp. 539–546.

[133] L. Lu, Q. Wu, X. Chen, Z. Shao, B. Chen, and H. Wu, "Development of a sEMG-based torque estimation control strategy for a soft elbow exoskeleton," *Robotics and Autonomous Systems*, vol. 111, pp. 88–98, 2019.

[134] A. M. Khan, D. W. Yun, M. A. Ali, J. Han, K. Shin, and C. Han, "Adaptive impedance control for upper limb assist exoskeleton," in *Proceedings of IEEE International Conference on Robotics and Automation*, 2015, pp. 4359–4366.

[135] T. Issa, and P. Isaias, "Usability and human computer interaction (HCI)," in *Sustainable design*, Springer, 2015. 19–36.

[136] K. Peffers, T. Tuunanen, M. A. Rothenberger and S. Chatterjee, "A design science research methodology for information systems research," in *Journal of Management Information Systems*, 2007, pp. 45–77

[137] G. Sadarangani, and C. Menon, "A wearable sensor system for rehabilitation apllications," in *IEEE International Conference on Rehabilitation Robotics*, 2015, pp. 672–677.

[138] H. W. Ng, X. Jiang, L. K. Merhi, and C. Menon, "Investigation of the feasibility of strain gauges as pressure sensors for force myography," in *International Conference on Bioinformatics and Biomedical Engineering*, 2017, pp. 261–270.

[139] E. Fujiwara, and C. K. Suzuki, "Optical fiber force myography sensor for identification of hand postures," *Journal of Sensors*, 2018.

[140] Y. T. Wu, M. K. Gomes, W. H. da Silva, P. M. Lazari, and E. Fujiwara, "Integrated optical fiber force myography sensor as pervasive predictor of hand postures," *Biomedical Engineering and Computational Biology*, vol. 11, pp. 1–7, 2020.

[141] A. Prakash, N. Sharma, and S. Sharma, "Novel force myography sensor to measure muscle contractions for controlling hand prostheses," *Instrumentation Science and Technology*, vol. 48, no. 1, pp. 43–62, 2020.

[142] M. Anvaripour, and M. Saif, "Controlling robot gripper force by transferring human forearm stiffness using force myography," in *IEEE International Midwest Symposium on Circuits and Systems*, 2018, pp. 672–675.

[143] A. Kumar, A. K. Godiyal, and D. Joshi, "Force Myography based continuous estimation of knee joint angle using artificial neural network," in *IEEE International Conference for Convergence in Technology*, 2019, pp. 1–3.

[144] X. Jiang, H. T. Chu, Z. G. Xiao, L. K. Merhi, and C. Menon, "Ankle positions classification using force myography: An exploratory investigation," in *IEEE Healthcare Innovation Point-Of-Care Technologies Conference*, 2016, pp. 29–32.

[145] A. K. Godiyal, S. Pandit, A. K. Vimal, U. Singh, S. Anand, and D. Joshi, "Locomotion mode classification using force myography," in *IEEE Life Sciences Conference*, 2017, pp. 121–124.

[146] A. K. Godiyal, U. Singh, S. Anand, and D. Joshi, "Analysis of force myography based locomotion patterns," *Measurement*, vol. 140, pp. 497–50, 2019.

ISSN (online): 2446-1636
ISBN (online): 978-87-7210-871-1 AALBORG UNIVERSITY PRESS